NOVA SCHOOL OF SCIENCE & TECHNOLOGY

DEPARTAMENT OF
Electrical and Computer Engineering

Daniel Filipe Condeça Morais
Bachelor in Electrical and Computer Engineering

Optimization Techniques for Wireless Power Transfer using Resonant Coupled Coils

MASTER IN Electrotecnical and Computer Engineering
NOVA School of Science and Technology – FCT NOVA
September, 2023

DEPARTAMENT OF
Electrical and Computer Engineering

Optimization Techniques for Wireless Power Transfer using Resonant Coupled Coils

Daniel Filipe Condeça Morais

Bachelor in Electrical and Computer Engineering

Advisor: Stanimir Stoyanov Valchev
Tenured Professor, NOVA School of Science and Technology | FCT NOVA

Examination Committee:

Chair: Paulo José Carrilho de Sousa Gil
Tenured Professor, NOVA School of Science and Technology | FCTNOVA

Adviser: Stanimir Stoyanov Valchev
Tenured Professor, NOVA School of Science and Technology | FCT NOVA

Members: Luís Filipe Figueira Brito Palma
Tenured Professor, NOVA School of Science and Technology | FCT NOVA

MASTER IN Electrical and Computer Engineering
NOVA School of Science and Technology – FCT NOVA
September, 2023

Optimization Techniques for Wireless Power Transfer using Resonating Coupled Coils

To my grandparents

ACKNOWLEDGMENTS

I would like to express my deepest gratitude to my advisor Stanimir Stoyanov Valchev for giving me the opportunity to search for new methods to optimize a technology that can enhance quality of life to its users in the future and for his patience and feedback.

I am also grateful to Professors that helped me with their feedback and to NOVA School of Science and Technology - University of Lisbon for creating a good environment for studying.

Lastly, I want to thank my family, especially my parents that paid my course and my grandparents that had already passed away but in life they always fought for giving his grandson a more educated life than they had.

"Necessity makes the invention."

ABSTRACT

The construction of a wireless power transfer system that guarantees an output power for a determined range is needed for manufacturing in large quantities and for the fulfillment of specifications that bring quality of service and other advantages like predicting what will be the manufacturing costs, occupied space and the overall performance, even taking into account that differences in coil construction, even with standardized production, can still not compromise the system and obtain a good performance.

The challenges are the determination of work frequency, coil inductance and parasitic capacitance to know what coils should be build and how they should be build when taking into account the number of turns, height and radius of the coils and creating a model that shows the behavior of the system while distance changes.

The proposed solution consists in creating mathematical models to calculate inductance, parasitic capacity and frequency of the coils and to study the behavior of the coupling coefficient, k, the mutual inductance, M, the power, or in this case, secondary voltage, V_2, that arrives at the receiver, and the rate of transferred energy, RoTE, and global efficiency to predict what coils should be dimensioned and for what range the system guarantees a given output power. A prototype was built to validate the models created and simulations were made to improve prototype blocks before primary.

Keywords: Wireless Power Transfer, Magnetic Resonating Coupled Coils, Mutual Inductance, Inductively Coupled Wireless Power, Efficiency Maximization of Magnetic Coupling.

RESUMO

A construção de um sistema de transferência de energia sem fios que garanta uma potência de saída para um determinado alcance é necessária para a fabricação em grandes quantidades destes dispositivos e para o atendimento de especificações que tragam qualidade de serviço e outras vantagens como prever quais serão os custos de fabricação, espaço ocupado e o desempenho geral, mesmo tendo em consideração que diferenças na construção das bobinas, mesmo com produção em série, conseguem ainda assim não comprometer o sistema e obter um bom desempenho.

Os desafios são a determinação da frequência de trabalho, indutância da bobina e capacitância parasita para saber que bobinas devem ser construídas e como devem ser construídas considerando o número de espiras, altura e raio das bobinas e criando um modelo que mostre o comportamento do sistema enquanto a distância muda.

A solução proposta consiste em criar modelos matemáticos para calcular a indutância, capacidade parasita e frequência das bobinas e estudar o comportamento do coeficiente de acoplamento, k, a indutância mútua, M, a potência, ou neste caso, tensão do secundário, V_2, que chega ao receptor, a taxa de energia transferida, RoTE e eficiência global para prever que bobinas devem ser dimensionadas e para que alcance o sistema garante uma determinada potência de saída. Um protótipo foi construído para validar os modelos criados e foram feitas simulações para melhorar os blocos do protótipo antes do primário.

Palavras-chave: Transferência de Potência Sem Fios, Bobinas Acopladas por Ressonância Magnética, Indutância Mútua, Potência Sem Fios Acoplada Indutivamente, Maximização da Eficiência do Acoplamento Magnético.

SUBJECT INDEX

FIGURE INDEX

TABLE INDEX

List of Acronyms

IRC	Identical Resonating Coils.
MCR	Magnetic Controlled Reactor.
MEET	Maximum Energy Efficiency Transfer.
NIRC	Non Identical Resonating Coils.
PP	Parallel-Parallel.
PS	Parallel-Series.
RoTE	Rate of Transferred Energy.
SP	Series-Parallel.
SS	Series-Series.
WPT	Wireless Power Transfer.

LIST OF SYMBOLS

a	Wire radius
A	Area
A_p	Area of a plate
A_v	Voltage Gain
B	Density of Magnetic Flux
c	Speed of Light in Vacuum
c	Ratio between heights of primary and secondary
C	Capacity
$C_{crossed}$	Capacity created by nonadjacent or crossed turns of the extremity of the coil
$C_{cylinder}$	Capacity of a cylindrical capacitor
C_d	Distributed or Parasitic Capacity of a coil
C_{int}	Total Internal Capacity of one given turn created by itself and all other turns
$C_{interLayerTotal}$	Capacity between layers of turns
$C_{internal}$	Total Internal Capacity of the coil
C_L	Capacity of a coil using Medhurst`s or modified Medhurst`s formulas
C_{layer}	Capacity of one given layer of turns
$C_{middlecrossed}$	Capacity created by nonadjacent or crossed turns of the middle of the coil
Ct	Capacity of each turn
$C_{tmiddle}$	Middle turn`s capacity of one given layer of turns
d	Distance
D	Diameter
f	Frequency
g	Ratio between radius of primary and secondary coils
h	Inductor`s height
h(t)	Impulse Response of WPT transfer function
H(s)	Laplace Transform of h(t)
I_1, I_p	Primary Current
I_2, I_s	Secondary Current
k	Coupling Coefficient
k_C	Constant used in Modified Medhurst`s formula
K_L	Nagaoka`s Constant
L_1, L_2	Self inductance of coils 1 and 2, respectively
L_{12}	Primary inductance created by the secondary
L_{21}	Secondary inductance created by the primary
Leq	Equivalent Inductance
L_t	Inductance of each turn
m	Ratio between number of turns of primary and secondary

M	Mutual Inductance
nLayer	Number of Layers
N_1, N_2	Number of turns of coils 1 and 2, respectively
NperLayer	Number of turns per layer
p	Pitch, distance between two adjacent turns
q	Ratio between Nagaoka`s Coefficients of primary and secondary
Q_1, Q_2	Quality factor of coils 1 and 2, respectively
r_1, r_2	Radius of coils 1 and 2, respectively
R_1, R_{L1}	Electrical Resistance of primary coil
R_2, R_{L2}	Electrical Resistance of secondary coil
R_L	Load Impedance
RoTE	Rate of Transferred Energy
s_1, s_2	Area of coils 1 and 2, respectively
t	Wire coating thickness
V_1, V_p, U_1	Primary Voltage
V_2, V_s, U_2	Secondary Voltage
X_C	Capacitive Reactance
X_L	Inductive Reactance
Z_0	Characteristic Impedance
η	Efficiency
η_{max}	Point where Efficiency is Maximum
ε_r	Relative Dielectric Constant
ε_0	Dielectric Constant of the Air
φ	Angle between Current and Voltage
ϕ_1, ϕ_2	Magnetic Flux of coils 1 and 2, respectively
λ	Wavelength
ψ	Constant used in Modified Medhurst`s formula
ρ	Electrical Resistivity
ω	Angular Frequency
μ_0	Vacuum Magnetic Permeability

1

INTRODUCTION

1.1 Motivations

It is of great interest in the modern day world to have wireless devices that give comfort and mobility where classical wired technology cannot. Wireless technology used on routers, mobile phones, car keys, and more, soon started evolving and making scientists all over the world put more and more effort into the development of such systems, which leads us to Wireless Power Transfer, also known as WPT.

WPT systems are based on channels where electrical energy can flow through without using any wires. It can be as simple as a transformer without the iron core, or a laser pointed at a solar cell.

WPT can be achieved by different methods, such as magnetic resonance, radiowaves, lasers or others due to the fact that each one is more suited for its own application, depending on power, distance, frequency, mobility between transmitter and receiver, etc.

1.2 Main Goals and Contributions

This work is about optimizing the mutual inductance of two magnetic coupled coils and understanding how to combine techniques to obtain an acceptable distance with acceptable efficiency, which is mandatory for the future use of this technology because low efficiency in power transfer means that most energy is lost, which compromises the main goal of using WPT devices, and a too short range would make the device useless. This optimization will further be used to implement a functional prototype of a wireless power transfer device using resonant coupled coils to validate the mathematical models created. The final objective is to optimize the construction method of WPT systems for low power, short range, and high frequency, using resonant coupled coils. For each application, and depending on projects specifications, building methods will be chosen using the proposed optimization techniques to build the WPT system to achieve high performance and other relevant factors, such as size or price in an optimal or at least sub-optimal way, due to conflicting specifications.

1.3 Dissertation Layout

There is still much research needed in order to enhance the wireless power transfer in order to achieve better performance, that is, better efficiency at larger distances, improvements in the charging speed, smaller sizes, and even the quality factor of coils, which commonly increases size as the quality factor increases, and to minimize this, it can be difficult or expensive, for example, bathing copper wire in gold. Increasing the number of coils can also be useful to increase performance, even though it also increases system size.

Thus, further research will contribute to optimizing wireless power transfer system construction to achieve all the goals described.

It is also important to guarantee that the system can dynamically stay efficient as distance varies, so good impedance matching will be important to further development in wireless power transfer in order to avoid too complex control systems, which may be implemented using the help of telecommunications systems. If good impedance matching is achieved just with a control block in primary or secondary, without the need for telecommunications, wireless power transfer promises to be efficient as well as simple.

Even though this work is not about the optimization of a control system, the WPT system will use a controller to dynamically adjust itself to peak performance as distance varies. A control system used to achieve best performance for each distance will also be taken into account for the optimal building method.

Finally, models for predicting system performance, techniques to construct coils with better characteristics and building methods than can enhance WPT systems using resonating coupled coils overall performance are also desirable aspects that will be studied with detail in this dissertation.

2

STATE OF THE ART

With the evolution and development of wireless power transfer, many technologies have been studied, each with its own advantages and disadvantages depending on distance, frequency, efficiency, size, health issues that may be caused, charging speed, and others.

In a first approach, this chapter will be used to gather all information possible about transmission of energy wirelessly. As more and more knowledge is gathered the simpler will be to select the information considered more relevant to apply and explain later, in further chapters.

Considering each technology involved, there will be a description in this chapter on how each one works, as some results that have already been obtained, so the state of the art on this theme has some theoretical concepts that can be understood, and then it will be possible to elaborate a plan to study the behavior of the coupling coefficient, k, and other relevant physical quantities as well, as functions of distances in order to make performance prediction. Furthermore, the mathematical models will be used to compare the model behavior with a functional prototype of a wireless power transfer system for low power, short range, and high frequency behavior.

2.1 An Overview on Wireless Power Transfer Technology

In a world where green economies are growing, WPT systems can potentially help with climate change and reduce pollution and give the comfort of charging equipment without the need for wires as well. For example, there have been studied ways to put solar panels on the moon or satellites [1], where the lack of atmosphere contributes to non-filtering the received radiation by the solar cells, which increases efficiency by increasing the total electromagnetic spectrum used, thus increasing the output power for the same solar panel. Wireless power transfer can help transmission between the moon and Earth because there is no need for using wires, which would not be an acceptable solution.

WPT is already on demand in some uses, for example in the charging of electrical vehicles [2] where weather conditions slowly compromise charging cables, autonomous underwater vehicles capable of searching the seas and doing rescue missions [3], making robot arms more flexible [4], and so on.

The use of lasers with high focus beam and very high frequencies, such as microwaves locked on solar cells, has proved to be a reliable way to transfer energy at long distances [1], but there are human exposure issues when using too much power at those frequencies [4], which leads us to lower the frequency when transferring high power or having a safe distance between human presence and the WPT system.

Furthermore, there has been research on non radiative WPT based on magnetic coupling, which uses mutual inductance between the transmitter and receiving coils to transfer energy [5]. Even though this technology can only be used in short or mid-range applications, it has high efficiency at short distances and the potential to overcome some human exposure issues due to the narrow band in which energy flows.

Due to the fact that there were several attempts to make energy flow, depending on the application and objectives needed to be reached, there are several methods to achieve these goals, and each technology used is best suited for each scenario. [6]

Many methods have been tested since Nikola Tesla's first successful attempt to light a bulb in 1891, using induction to wirelessly charge it.

Induction: It consists of the same working principle as a transformer but without an iron core. This way, the main flux that passes through the iron core is used to pass through the air, producing an induced electromotive force in the secondary coil produced by the magnetic field of the primary coil. [1]

Transmission with lasers: Due to the fact that light can be focused on solar cells to move charges through photodiodes, which create an electrical current, it is possible to beam energy through the air and receive it in a solar cell, even at large distances.

Micro-waves and radio-waves: similar to the working principle of many telecommunications systems, using radio waves or micro-waves in a transmitting antenna and a rectenna in reception, which is an antenna with rectification in order to obtain a DC signal, can be used to transfer energy wirelessly. Directional antennas can transmit rays over a long range, but this technology is susceptible to causing health issues due to high power and frequency combined. So it would be destined, for example, to supply airplanes or helicopters or to transfer energy to a locality far from human beings.

There are many ways to transfer power wirelessly, all with their own pros and cons.

According to the method under study, which consists of the use of the phenomenon of mutual inductance between two resonant coupled coils, the primary or transmitter and secondary or receiver, there were many attempts to improve the system performance, making physical quantities vary in order to obtain families of curves for the efficiency. [2]

In [2], it is described:

$$Q = \frac{X_L}{R} = \frac{\omega L}{R} \tag{2.1.1}$$

With Q, the quality factor of a coil.

X_L is coil reactance.

R and L are the resistance and inductance of the coil, respectively.

ω is the angular frequency.

The coupling coefficient k is:

$$k = \frac{M}{\sqrt{L_1 L_2}} \tag{2.1.2}$$

$M=L_{12}=L_{21}$ is the mutual induction coefficient.

L_1 and L_2 are the self-inductance of coils 1 and 2, respectively.

The maximum efficiency, η_{max} is:

$$\eta_{max} = \frac{k^2 Q_1 Q_2}{\left(1+\sqrt{k^2 Q_1 Q_2}\right)^2} \tag{2.1.3}$$

With Q_1, Q_2 the quality factor of coils 1 and 2, respectively

k, the coupling coefficient.

Assuming two equal coils, operating at same frequency, $Q_1=Q_2=Q$, and deriving the expression (2.1.3):

$$\frac{d\eta_{max}}{dQ} = 0 \tag{2.1.4}$$

Formula (2.1.4) comes from the derivation of equation (2.1.1) as a way to understand its behavior. Figures 2.1.1 and 2.1.2 were made to better visualize the behavior of efficiency as the quality factor and coupling coefficient varies and do not come directly from a cited document.

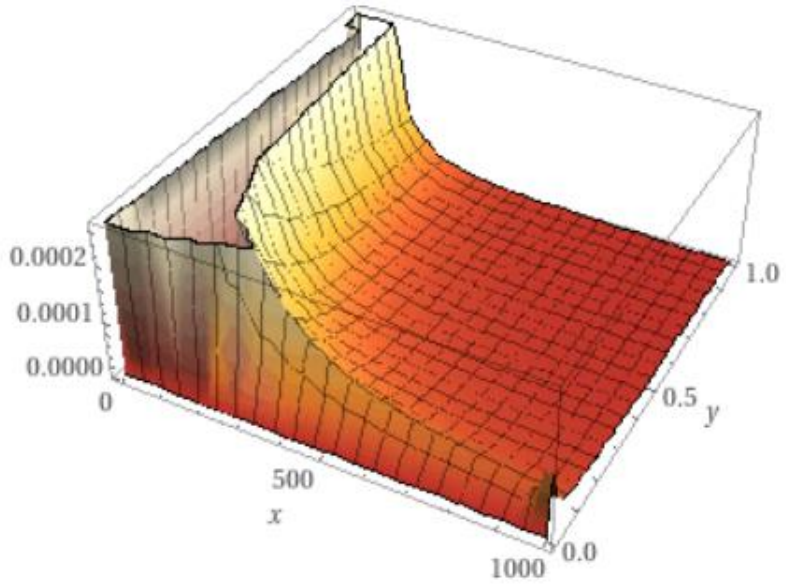

Figure 2.1.1: $\frac{d\eta_{max}}{dQ}$ 3D plot. Where x is Q and y is k

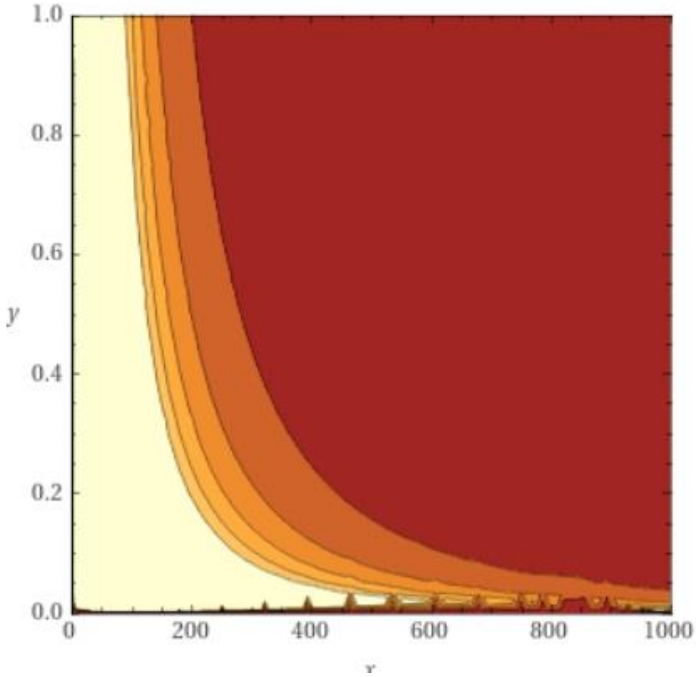

Figure 2.1.2: $\frac{d\eta_{max}}{dQ}$ plot. X-axis is Q and y-axis is k. Darker colors correspond to higher efficiencies.

Considering the function plot, it is possible to achieve large efficiencies, above 90%, for large Q and k values.

With a sufficiently large Q, it is still possible to achieve large efficiencies even with low values for k. For example, with Q = 500 and k = 0.2, efficiency is 98%. Thus, it is possible to construct a system based on resonating coils with high efficiency.

However, k varies with distance, d, and other variables described further below. In practice, if a too low value for k is obtained with a d that is too short, the use of this technology can be compromised. Therefore, it is important to define k in its variables and optimize it to achieve an acceptable efficiency for an acceptable distance.

On the other hand, it can be difficult to obtain a high Q and rising frequency may not be possible, depending on the application and coils used. Thus, achieving high k can be challenging.

This technology can be used underwater, at sea, or in places where weather conditions are adverse because the coils are isolated from water, but the magnetic field still propagates through water. [3]

Furthermore, it is known that the increase in the number of turns of a coil, N, makes the inductance increase, L, and Q as well. However, at too high frequencies, the coil resistance also increases, so the quality factor Q decreases. Thus, there is an optimal value for the frequency-dependent Q.

As already mentioned, it is necessary to take into account frequency and power in order to avoid exposure to too intense electric and magnetic fields. [4] 100 kHz is a common value indicated for the threshold between safe use and the risk of electro stimulation exposure.

Frequencies in the range of GHz and more are possible for sufficiently low power, a fact that means, in the context of this document, the damage caused by high frequencies can be considered negligible due to the fact that low power will be used, inferior to 10W.

There is also the possibility to extend the range of this technology by using more than two coils. Putting consecutive coils, even without an energy supply, the magnetic field of the transmitter reaches the second coil, and another magnetic field emerges, which reaches the third and so on. This way, energy is transmitted from coil to coil in a domino effect, extending the range.

High M guarantees a strong coupling [5]. M can be calculated using the next equations:

$$M = k\sqrt{L_1 L_2} \tag{2.1.5}$$

$$M = \frac{V_2}{\omega I_1} \tag{2.1.6}$$

With V_2 being the induced electromotive force in the secondary and I_1 the primary current.

This way, it is possible to add variables in order to adjust the value of M to obtain a harder coupling.

Given the fact that unplanned coupling is unrelated to the energy transfer between transmitter and receiver, that is, coupling between the transmitter and another device which operates at a similar frequency could cause improper charging, which leads to loss of efficiency due to the fact that part of the energy is being used to charge a device in the vicinity.

There is a need for having a proper frequency plan for a WPT, depending on the technology used [6] for charging only the device or devices that it is designed for. This way, the use of a narrow band can be made viable to allow a large number of frequencies to be used. A way to guarantee selectivity in the work band is with high Q.

It is proposed that a decrease in the resistance value for the coils as coils are capable of storing large amounts of energy and at the same time reducing the energy lost per cycle. [7]

Furthermore, Q is independent of M. This independence is explained by the fact that it is possible to increase L through the increase of the number of turns, which also increases R and Q. However, increasing frequency will increase the value of R without increasing L, thus decreasing Q without M necessarily changing.

In order to increase the range, it is possible to add more coils in resonance with transmitter and receiver without need to supply these coils. Losses from coil to coil will cause efficiency to decrease with distance, almost linearly, but not as much as without any coil in between. After a certain point, losses become too high, so the range can reach a few meters. [8]

This domino effect can also make energy flow in more than one direction, as explained in [4]. This can be useful if bidirectional charge is a requirement because there is only need for one device.

There is also the possibility to use four topologies:

1. Series-Series or SS
2. Series-Parallel or SP
3. PS stands for Parallel-Series.
4. Parallel to Parallel, or PP

Of these, only 1 and 2 are of practical interest, being that SS is the most efficient when load impedance is small and SP is the most efficient when load the impedance is large. [9]

Misalignment between coils of transmitter and receiver, as well as shifting between turns of the respective circuits, leads to a loss of efficiency. [10] This is due to the fact that magnetic field density is not uniform, being more dense in the direction of the centre of the turns and less dense in the exterior. The geometry of the magnetic field of the transmitter can be altered in such a way that performance increases, depending on application.

Using planar coils and varying the section of the turns, as well as geometry, it is possible to find an optimal value for M. This point corresponds to equal sections, both for primary and secondary circuits. [11]

It is also proposed that the radius of the turns be different, that is, the turns of the secondary be at least slightly smaller than the turns of the primary as a way to guarantee that the turns of the secondary are completely immersed in the magnetic field of the primary.

The M dependency on the radius of the turns of the coils of primary and secondary is more evident, according to:

$$M \approx \frac{\pi \mu_0 N_1 N_2 {r_1}^2 {r_2}^2}{2(d^2+{r_1}^2)^{\frac{3}{2}}} \qquad (2.1.7)$$

Doing $\frac{\partial M}{\partial r_1} = 0$ and $\frac{\partial M}{\partial r_2} = 0$

Comes $r_1=\sqrt{2}d$ and $r_2=0$, which correspond to absolute maximum and minimum respectively.

If $r_2 = 0$ there is no transmission. Increasing r_2 will increase performance, at least, until a certain point, but as it will be explained further there are advantages in keeping r_2 smaller than r_1.

This indicates that it is possible to obtain significant distances, d, between the coils if the radius of the turns of the primary is larger than the distance d.

It is evident that from a certain radius, it becomes impractical to increase the radius, so other methods should be used to increase performance.

$r_2 = 0$ has no physical meaning in practice. If $r_2 = 0$ there is no transmission. Increasing r_2 will increase performance, at least, until a certain point, but as it will be explained further there are advantages in keeping r_2 smaller than r_1.

If $r_2 \approx 0$ and $r_2 > 0$, the secondary turns are completely immersed in the magnetic field of the primary, resulting in a large M. [12]

When non identical resonating coils, NIRCs, are used it is possible to achieve more uniformity in transmission rate when compared to IRCs, identical resonating coils [13].

Increasing r_1 while maintaining the same size for r_2 makes M lower for too short range but higher for longer distances. This does not mean that range increases. When an equivalent IRC to an NIRC is used, which consists in using two equal coils with a radius equal to the average size of r_1 and r_2 of NIRC, performance is the same for both at long range and is actually better for equal coils at very short distance, when compared to non identical resonating coils.

The advantage of using r_1 greater than r_2 is the fact that the phenomenon of frequency splitting, which will be described further, is reduced, even at a point where no frequency splitting occurs. Thus, there is no need for systems to compensate this phenomenon which increase losses and building price due to the need for more electronics and control systems.

If the system will work at relatively long range, this method can be used to overcome frequency splitting while decreasing the complexity of the system, energy loss, electronic components and overall price.

When load impedance, R_L, varies and transmission efficiency and global efficiency are measured, it is verified that global efficiency is larger when load impedance is matched, that is when $R_L = Z_0 = 50\Omega$, even though the relationship between the energy that flows from the primary to the secondary and the energy stored in the LC tank of the primary decreases.

This is due to the fact that when R_L increases, the power received by the secondary also increases, at the cost of an increase in the loss of energy.

The loss of efficiency can compromise the use of this and nullify its utility. Thus, maximizing distance and efficiency for that distance is decisive.

There are some aspects which are not possible to change due to the impossibility of controlling some physical phenomena. For example, the magnetic field intensity decreases with the power of three with distance, and this cannot be controlled. [14]

$$B = \frac{\mu_0}{2\pi} \frac{NIA}{x^3\left[1+\left(\frac{r_i}{x}\right)^2\right]^{\frac{3}{2}}} \tag{2.1.8}$$

With A, the area occupied by the coil

r_i, the radius of the coil i

I, the current in the coil

x, the distance to the coil

When distance $x >> r_i$:

$$B = \frac{\mu_0}{2\pi} \frac{NIA}{x^3} \tag{2.1.9}$$

This phenomenon cannot be changed, which, in practice, means that other methods should be used in order to increase system performance. For example, methods that can make this hyperbole into one with higher values for magnetic field density B for the same distance, or in other words, achieving the same magnetic field density B for a greater distance, even though the curve will always be a hyperbole because this is a physical phenomenon that cannot be changed.

However, according to equations (2.1.8) and (2.1.9), there is still the possibility to increase the curve of the magnetic field density in order to increase the distance by adding more turns to the coils, increasing the current in the wire and increasing coil area, which results in the increase of the transmitter coil radius, as already mentioned, which leads to an increase in size.

Even though these methods consist in possible ways to enhance performance, they are not always desirable due to size specifications in many applications. Therefore, other methods to increase performance should be adopted in order to increase performance maintaining size,

which is advantageous to be minimized in order to use this technology in microelectronics or other applications where size is a constraint.

Some methods consist simply of achieving the best performance from the same coil without necessarily increasing the size or number of turns. For example, if there is a method in which the same coil can produce a stronger magnetic field or a stronger coupling, or a method to decrease other losses without occupying more space, this will be advantageous.

There is a method that consists of an increase in energy transmitted by the same coil, not because of an increase in the number of turns or area per turn, but by obtaining good impedance matching instead. This means that energy will be sent from transmitter to receiver at resonant frequency, and when the magnetic field vibrates near this frequency, losses to reflection will be reduced due to good impedance matching, and consequently, the amount of energy sent will increase due to a decrease in energy reflected back, and that increases efficiency and charging speed without increasing size or price. This way, it is proposed that matched impedances should be used in order to obtain an acceptable overall efficiency. It is possible to describe the efficiency mathematically as a function of the S parameters.

$$\eta = |S_{21}|^2 \qquad (2.1.10)$$

If S_{21}=0.897, efficiency is 80.4%

This implies that good matching is essential to guarantee high efficiency. [15]

2.2 The Frequency Splitting Phenomenon

It happens that the value of impedance of a circuit is not constant. For example, in a WPT linked to a battery the circuit impedance will change as time passes and the battery becomes degraded. In other words:

$$L = L(t),\ C = C(t) \text{ and } R = R(t)$$

This variation of impedance will change the transfer function of the circuit as time passes, which results in a need to adjust variable of Laplace, s, as this impedance variation occurs, and that is, to adjust frequency dynamically in order to guarantee a good match of impedances as time passes. This also means that if a controller is used to adjust frequency dynamically the inductance, capacity and resistance of the inductors should be written as a function of time in order to obtain the map of poles and zeros correctly.

In the context of wireless power transfer, this phenomenon may occur because of many factors, such as variation in distance between primary and secondary coils, which varies the secondary impedance seen by the primary, altering the S parameters and shifting the frequency of operation of both primary and secondary, which results in an increase in the absolute value of the difference between the primary and secondary frequencies, which are now split from each other and different from the resonant frequency, which is in between, leading to loss of energy transmitted, thus decreasing efficiency or eventually stopping it. [16]

This phenomenon can also happen with a variation of M. This becomes clearer when observing a transformer:

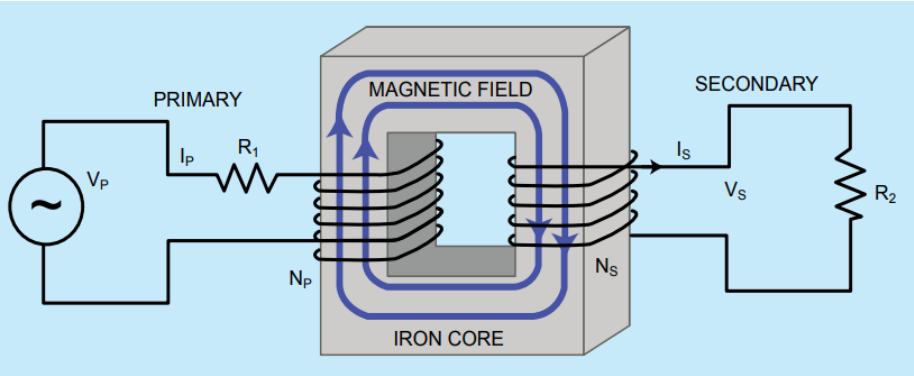

Figure 2.2.1: Transformer

Considering the coils` resistance R_1 and R_2 for primary and secondary, respectively:

$$V_p = I_p R_1 + L_1 \frac{\partial Ip}{\partial t} - M \frac{\partial Is}{\partial t} \quad (2.2.1)$$

$$M \frac{\partial I_p}{\partial t} = I_s R_2 + L_2 \frac{\partial Is}{\partial t} \quad (2.2.2)$$

As it is shown, M in the primary represents the load of the secondary seen by the primary, and the increase of M increases $I_p = I_1$ as a way to compensate for the coupling effect of the secondary with the primary. The same happens for M in the second equation. [17]

However, it is possible to adjust frequencies dynamically as a way to improve performance and avoid degradation due to frequency splitting and S parameter shifting.

Through the use of various algorithms, several methods were developed to improve performance. One algorithm makes the frequency vary in a way that the S parameters lead to an improvement, with:

$$\eta_{21} = |S_{21}|^2 \quad (2.2.3)$$

$$\eta_{11} = |S_{11}|^2 \quad (2.2.4)$$

S_{21} and S_{11} are inversely proportional.

This means that the efficiency measured with S_{21} is the real efficiency, and the other measures how much efficiency is lost to reflection.

At resonance there are two peaks of performance. One peak at a frequency slightly before and the other peak comes after the resonant frequency. As frequency shift occurs the resonant frequencies of primary and secondary circuits will get apart from each other and the peak of performance will change dynamically until it reaches its final state that corresponds to the peak after primary`s resonance and the peak before secondary`s resonance, simultaneously. The final state happens at a single peak that corresponds to the join of both peaks mentioned.

The algorithm used can adjust itself to stay in resonance and obtain an efficiency of 97%. It is maintained constant until it reaches the point where the distance itself is greater than the radius of the primary coil divided by square root of 2, as it is expected to get highly efficient, and after that point, efficiency starts to drop quickly with distance, even though it is still better than without the algorithm, until the point where there is almost no energy being transferred, where it does not compensate anymore to supply the controller. [18]

This system works without the need to transmit signals through the air, unlike telecommunications systems.

Another algorithm adjusts frequency based on the average transmitted power, taking into account that this power is maximized at resonant frequency. Each time power changes, the

algorithm decreases frequency. If power increases, it continues to decrease frequency. If power decreases, the frequency increases. [19]

This algorithm can also reach its maximum power when the frequency splitting phenomenon occurs. This way, it is shown that performance can be improved through the use of algorithms that adjust frequency until the maximum efficiency point is reached, even with frequency splitting.

When using an SS or SP topology, it is possible to install a voltmeter in the transmitter at the capacitor and coil terminals to determine whether or not the circuit has good impedance matching.

When the potential difference is zero Volts, the match is at an optimal value, that is when X_L-X_C=0. When this does not happen, it means that a predominance of magnetic energy stored in the coil over electric energy stored in the capacitor exists, or vice-versa for the SS topology.

With the SP topology, the same happens when an ammeter is put at the output of the LC tank of the secondary and the current reaches its minimum value. [20]

In [21], it is explained that the increase in coupling coefficient k increases the quality factor of the coils Q, thus increasing efficiency.

$$\eta = kQ = kQ(k) \tag{2.2.5}$$

$$\text{With} \quad Q_i = \frac{1}{R_i}\sqrt{\frac{L_i}{C_i}} = \frac{\omega_i L_i}{R_i} = \frac{1}{\omega_i R_i C_i} \tag{2.2.6}$$

i is the number of the coil.

This way is shown that quality factor can be improved by reducing the parasitic capacity, coil resistance or increasing L, for example increasing the number of turns as already shown.

According to theory, it is well known that the number of turns decreases the total parasitic capacity due to an increase of number of capacities between turns entering in parallel:

$$C_{total} = \frac{1}{N-1}C \tag{2.2.7}$$

Where N is the number of turns and C is the parasitic capacity between two adjacent turns.

Thus, increasing the number of turns will increase L and R at the same time C decreases.

On the other hand, it is also known that:

$$Z_0 = \sqrt{\frac{L}{C}} \tag{2.2.8}$$

If it is taken into account the characteristic impedance of 50Ω, as commonly used, it is necessary to increase L and C proportionally in order to maintain matching. This result confirms the need to use an RLC series circuit in the primary, since with high Q a coil with reduced parasitism is obtained, and to balance this, maintaining matching, it is necessary to either decrease frequency, which is not entirely desirable, or alternatively, a capacitor must be used in series with the coil to compensate for the magnetic energy stored in a good quality coil and reach resonance at the same frequency, without degradation of Q, even though frequency decreases.

The critical distance, which is the maximum achievable distance at an acceptable efficiency, is needed in order to maximize k, so there is no need for too high Q. Once critical distance is exceeded, it may not compensate for the continuous adjustment of the S parameters

because efficiency is reduced and/or energy consumption increases over time due to the need for more time to charge. The transmitted energy stops to compensate for the energy necessary to supply the control circuits needed to make the adjustments to the S parameters, thereby the cessation of transmission can turn out to be advantageous. [22]

In [23], a new method is used to reach the maximum efficiency point. It consists of the use of a buck-boost converter in which the duty cycle, D, is altered in order to reach maximum efficiency.

It is suggested that to reach a desired output power, the input voltage should be put at its minimum value at which that output power is reached.

Regulating D, maximum efficiency is obtained for D = 0.53 but the point of minimum input voltage occurs when D = 0.38, even though the value of the input voltage for the maximum efficiency is near its minimum value and just slightly larger.

This improvement on efficiency with the input voltage decreasing is expected according to (2.1.6), and

$$I_1 = \frac{U_1}{Z_1} \tag{2.2.9}$$

$$\text{Thus,} \quad M = \frac{U_2}{U_1}\frac{Z_1}{\omega} \tag{2.2.10}$$

but nothing is mentioned about the variation of input power, and due to the fact that maximum efficiency point and minimum input voltage occur for different values of D it is not clear if this difference in values is due to variation of power, which would vary the primary current I_1, thus varying the magnetic field amplitude and the efficiency obtained or if this difference is due to an error in measurement or even due to variation of buck-boost converter`s efficiency over its operating point.

However, it is clear that there is an increase in efficiency when input voltage decreases, and this method can be used to obtain MEET, which is the point of Maximum Energy Efficiency Transfer.

2.3 Construction Methods and Enhancement Techniques

In [24], the impact on the coupling coefficient k made by the variation of d, L, and the internal and external radius of the coils is analyzed. It is concluded that the parameter with the most significant impact on k is distance, whereby the influence of the other parameters, even if not null, is negligible when compared to distance.

Given the fact that transmission distance is not always constant, for example, in the situation where the transmitter is standing still but the receiver is moving, it can exist a variation of work frequency, of S parameters, and efficiency. Thereby, depending on application, it may be necessary to have a telecommunications system between transmitter and receiver, and depending on system power, it may not introduce significant losses, or it will if the system transfers less or even equal power than the power needed to supply the telecommunications system itself.

In some applications, it can be necessary to have a telecommunications system between transmitter and receiver to determine when the transmitter should send energy or when transmission should be ceased. [25]

An efficiency of about 70% was reached with a similar system, implemented in a device which worked with a power of less than 5W.

Another technique already used in electrical machines, like alternators, has shown that more than one coil can be used to improve performance. According to electrical machine theory, the use of a three-phase sinusoidal voltage system enhances magnetic flux by 50% for the same current as in a single-phase alternator.

The three-phase system in WPT can decrease voltage at the terminals of the LC tank, thereby allowing more power to be put into the same system. There is also the advantage of reducing the number of wires and devices like transistors when compared to a single-phase system for the same power. [26] The efficiency is not necessarily higher, though. The magnetic fields produced by each phase are shifted 120 degrees and can reduce the density of one another and reduce efficiency.

On the other hand, in alternators, the coils are also shifted by 120 degrees in space, which does not happen necessarily in WPT.

In [27], the V-minus method is described, which is compared to a common three-phase system. In the common three-phase system, voltages are shifted 120 degrees from each other as in alternators, but alternators also have coils shifted from each other in space, thus improving performance. Without the shift in space, the three-phase system creates three shifted magnetic fields in the coils that cancel with each other, degrading performance. The V-minus method uses an inverter in one phase to shift it 180 degrees in order to make the magnetic fields add to the others, thus increasing performance compared to the common three-phase system.

In order to model k to obtain longer ranges it is important to know how inductors should be constructed in order that system performance can be predicted for a certain range. Taking into account that the parasitic elements of a coil can change performance, there is the need for considering the coil as a RLC circuit. In [28] is described a method to construct inductors using a math model based on describing each turn of a coil as an LC parallel circuit and the coil as a series of turns which then are LC circuits.

$$L = N \times Lt \tag{2.3.1}$$

$$C_d = \frac{Ct}{N-1} \tag{2.3.2}$$

$$R = \rho \frac{l}{\pi a^2} \tag{2.3.3}$$

Where L_t and C_t are inductance and capacitance per turn of the coil, respectively, a is the wire radius and N the number of turns. R is the total resistance of the coil and l the wire length. Consider the next equation to calculate C_t:

$$Ct = \frac{\pi^2 \varepsilon . 2r}{\ln\left(\frac{p}{2a} + \sqrt{\left(\frac{p}{2a}\right)^2 - 1}\right)} \tag{2.3.4}$$

Where p is pitch, the distance between each turn, r is the turn`s radius and ε the dielectric constant of the material between each turn. But this is the simplified formula, which can be used when p – 2a >> t, where t is thickness of the wire coating. The general formula for C_t is described further below:

$$Ct = \frac{\pi^2 \varepsilon . 2r}{\ln\left(\frac{\frac{p}{2a}}{\left(1+\frac{t}{2a}\right)^{1-\frac{1}{\varepsilon_r}}} + \sqrt{\left(\frac{\frac{p}{2a}}{\left(1+\frac{t}{2a}\right)^{1-\frac{1}{\varepsilon_r}}}\right)^2 - \left(1+\frac{t}{2a}\right)^{1-\frac{1}{\varepsilon_r}}}\right)} \tag{2.3.5}$$

Where ε_r is the wire coating relative dielectric constant.

For L_t there is more than one way to calculate, but it is easier to use the model to calculate the total distributed capacitance, C_d, but calculate L in another form. In [29] the inductance L of a coil is calculated as below:

$$L = \pi\mu_0 \frac{N^2}{h} r^2 K_L \qquad (2.3.6)$$

Where h is coil height and K_L is Nagaoka`s constant which can be calculated or simply taken from the table below:

Table 2.3.1: Nagaoka`s constant

h/D	K_L
0.00	0.0000
0.10	0.2033
0.20	0.3198
0.30	0.4053
0.40	0.4719
0.50	0.5255
0.60	0.5697
0.70	0.6067
0.80	0.6381
0.90	0.6651
1.00	0.6884
1.11	0.7100
1.25	0.7351
1.43	0.7609
1.67	0.7885
2.00	0.8181
2.50	0.8499
3.33	0.8838
5.00	0.9201
10.0	0.9588
11.0	0.9600

Nagaoka`s constant varies with the relation between h and diameter of the coil.

There is more than one way to study the behavior of two resonant coupled coils and achieve an equivalent model that can be used to determined output at a given range and predict the overall performance of the system. In [28] an equivalent model of two resonant coupled coils is proposed and it can be used to simulate the behavior of k, M, output voltage when range is varied. It consists in a T model using 3 different coils. From left to right, the coils have the values of L_1-M, M, and L_2-M, respectively. M(d) denotes M as a function of distance. The input V_1, in the left, produces a V_2, in the right, dependent on M. Variation in distance will cause M to change and for consequence L_1-M and L_2-M, and, as a consequence, V_2 will also change accordingly.

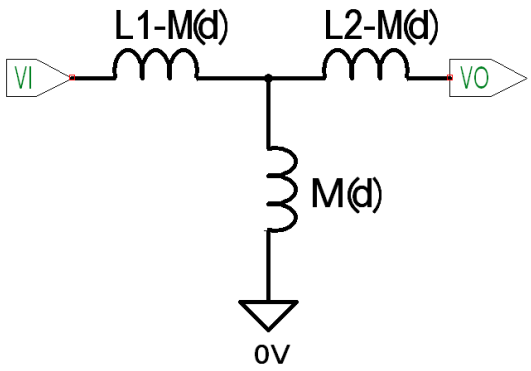

Figure 2.3.1: Equivalent model of a WPT system

2.4 Related Works

As seen early, there are several technologies that can be used to transfer energy wirelessly. All of them can be useful depending on the application. The specifications of the projects will dictate the most suitable of those technologies for that specific use.

The most important factors that need to be considered to choose the most suitable technology are range, power and frequency, even though there are more.

For long range, transmission with lasers or directional antennas is the most suitable option. Usually, both of them use high frequency and can also have high power, but can lead to health issues if the human being is somehow exposed to the laser beams or the radio-waves, but in some applications may be the only options known. If that is the case, there are more related works on these technologies that should be consulted. [29, 30, 31]

For short range, wireless power systems based on induction such as ones using resonating coupling coils for example, have the advantage of having better efficiency than the previous technologies.

In general, if power is low, frequency can be high. But if power needs to be increased, too high frequency can be problematic. Or the equipment is designed to work far from human beings or the frequency needs to decrease but that can degrade performance. Depending on the project specs there is more literature on this theme. [32, 33, 34]

To optimize the inductor construction of the WPT systems there are some important questions that need to be answered.

Is it possible to know what coils should be produced in order to guarantee a certain output power at a determined range? Does combining all these techniques above result in an improvement in WPT? Can these techniques be combined in a way that maximizes k, efficiency, and distance?

Answering these questions, achieving an optimum value for k and other relevant physical quantities and maximize efficiency for a maximized distance are important objectives of this project. What techniques can result in a WPT system with a longer range, better efficiency for that range, and faster charge in a way to compete with fast chargers and the classical wired chargers?

With the optimization and performance prediction, it will be easier to design WPT systems using resonating coupling coils and suitable coils for specific applications. Modeling k, as well as other relevant physical quantities for the distance needed can be a way to create a method that can be used to know what coils should be constructed for a given range and what power will arrive at the secondary.

In the next chapter, some of the information gathered here will be used to develop mathematical models that will be used to predict relevant physical quantities for designing and optimizing the construction of WPT systems using resonating coupling coils.

3

THEORETICAL CONCEPTS AND CONTRIBUTIONS

In this chapter, the objective is to use the information gathered in the previous chapter and funnel the knowledge into mathematical models that can be used to understand the behavior of the energy transfer performance as distance varies due to the importance to maximize this last factor while still guarantying a reasonable amount of energy being transmitted. With the mathematical models developed any system capable of transmitting energy wirelessly, using resonating coupling coils, can be constructed because not only it will be possible to predict the amount of energy that arrives at the receiver at a given distance, but also to combine techniques that enhance performance when projects` specs are considered.

A prototype will be build to study the behavior of the physical quantities considered and, in further chapters, compare its performance with the values calculated with the mathematical models developed.

In a WPT system based on resonant coupling coils it is important to determine which range can be achieved, how much output power can be obtained for that range, what is the efficiency and rate of transferred energy and what coils should be build in order to obtain that performance. Thus, there is the need to model inductance, capacitance and frequency of the coils, then k, M, output voltage, rate of transferred energy and efficiency for the constructed coils for each value of distance, d.

These models will be used to create the system, study its behavior in order to understand if they can be used to predict and enhance overall performance.

Frequency splitting phenomenon will also be taken into to account. There are techniques that consist in changing the geometry of the coils that eliminate this phenomenon but there are also other methods that can be used to adjust frequency, for example, to maintain transmission.

3.1 System behavior Models

What defines the work frequency is the lowest frequency coil. Even when coils are made equal, which means $L_1=L_2$, $N_1=N_2$, $r_1=r_2$ and $h_1=h_2$, they are not exactly equal after construction, that is L_1 will not be exactly equal to L_2 and the parasitic capacitances for both will not be equal either, which in turn result in two similar, but different frequencies. The lowest one

will define the work frequency because after the coils are constructed it is not possible to increase frequency, but additional capacitor can be used in series or parallel in primary or secondary circuit or both in order to decrease the one that has the highest frequency to achieve equal frequencies in both sides. If power is high enough to create health issues due to electro stimulation frequency must be decreased in both transmitter and receiver and that can be made putting capacitors in both sides. Thus frequency can always be decreased but it can only increase if the coils are built in such a way that their natural frequency is high. This way the natural resonating frequency can be used or frequency can be decreased by adding capacitors.

The capacitors could be put in series or parallel, but it is known that SS or SP topologies are the ones of interest, which results always in a series capacitor in the primary but in the secondary it depends on the load impedance. If load impedance is larger than $\sqrt{\frac{L2}{C2}}$ SP topology should be used. If load impedance is lower SS topology should be used.

There are several variables that can change a WPT performance such as transmission power, frequency, transmitter current, coils used and the way they are constructed which are dependent on the number of turns N, radius, r and height of the coil, h. All these variables can be manipulated to enhance performance, reduce complexity of construction and manufacturing costs and minimizing occupied space. Some variables can enhance some indicators but can also degrade others, which means that there will be situations of compromise between one and another.

A theoretical study will be made in order to create mathematical models that will be used to better understand the behavior of the system for a given distance and to predict performance for a given distance even when it varies. There is also the objective of achieving a prototype of a WPT using resonating coupling coils using the methods studied and, in later chapters, the results obtained and simulations done will be compared and discussed.

According to the several variables that can be used, it is already known that when transmitter power increases performance and range will also increase. Frequency depends on the constructed coils, and primary current should be large because the density of magnetic flux, B increases with current, which in practice means that for a given transmitter power changing the electrical characteristic of voltage and current can be used to change performance, in this case, if voltage can be lowered and primary current becomes higher, the density of magnetic flux increases which results in an increase of range.

Inside an inductor the density of magnetic flux is:

$$B_1 = \frac{N_1 \mu_0 I_1}{h_1} \tag{3.1.1}$$

N_1 is the number of turns, I_1 the current and h_1 the height of the primary coil. This formula can be considered when distance to the center of the inductor, d, is zero.

$$V_1 = L_1 \frac{dI_1}{dt} \tag{3.1.2}$$

$$V_2 = M \frac{dI_1}{dt} \tag{3.1.3}$$

When d=0 and losses are not considered, k=1. If L_1=L_2=L, M=L for d=0.
In order to have transmission the current needs to vary over time, thus it will be considered AC:

$$I_1 = Asin(2\pi ft) \quad (3.1.4)$$

$$I_2 = Bsin(2\pi ft) \quad (3.1.5)$$

Where A and B is current I_1 and I_2 intensity, respectively.
Using (3.1.4) in (3.1.1) and (3.1.2):

$$B_1 = \frac{N_1\mu_0 A}{h_1} sin(2\pi ft) \quad (3.1.6)$$

$$V_1 = L_1 \frac{dI_1}{dt} = L_1 2\pi f A cos(2\pi ft) \quad (3.1.7)$$

$$V_2 = M \frac{dI_1}{dt} = M 2\pi f A cos(2\pi ft) \quad (3.1.8)$$

By definition, the electromotive force induced in the secondary coil, V_2, will be the variation of magnetic flux with time. The magnetic flux is the variation with time of the product of the magnetic field intensity and the surface of the secondary coil, s_2, which is constant. Thus:

$$V_1 = -\frac{d\phi_1}{dt} = -\frac{dB_1(t)}{dt} \times s_1 = -s_1 \frac{N_1\mu_0 A}{h_1} 2\pi f cos(2\pi ft) \quad (3.1.9)$$

The magnetic field intensity in the secondary coil is the same of the primary when d<<.

$$V_2 = -\frac{d\phi_2}{dt} = -\frac{dB_1(t)}{dt} \times s_2 = -s_2 \frac{N_1\mu_0 A}{h_1} 2\pi f cos(2\pi ft) \quad (3.1.10)$$

From (2.1.9), and considering d>r_1:

$$B_1(d) = \frac{\mu_0}{2\pi} \frac{N_1 I_1 s_1}{d^3} = \frac{\mu_0}{2\pi} \frac{N_1 s_1}{d^3} Asin(2\pi ft) \quad (3.1.11)$$

As d increases the magnetic field intensity decreases as seen in the previous formula which results in:

$$V_2 = -\frac{d\phi_2}{dt} = -\frac{dB_1(t)}{dt} \times s_2 = -s_1.s_2 \frac{\mu_0}{\pi} \frac{N_1}{d^3} A\pi f cos(2\pi ft) \quad (3.1.12)$$

This means that increasing work frequency will increase V_2 and geometry of the coils can be used to enhance performance. Both the areas of the primary and secondary coils can be increased to enhance energy transfer and if one is decreased the other can be increased to compensate. V_2 is dependent on the current I_1 and the number of turns of the primary coil.

Furthermore, losses come from the resistance of the coils and not from low rate of transferred energy. It is possible to have low losses, which results in high efficiencies, even with low rate of transferred energy, even though the energy output will be low. This means that a WPT system using resonating coupled coils can have, for example, 2% loss from the copper wire, which makes the efficiency of 98%, but as distance increases, efficiency decreases without an increase of loss, but due to a decrease of magnetic flux density instead. In practice, when distance is short both the efficiency and rate of transferred energy are high and when distance d increases, k, M and V_2 decreases, which then decrease the rate of transferred energy, RoTE, while the losses are maintained approximately constant for the same input power. When RoTE is high and the output power needed for a given application is P_2, the input power needed is

$$P_1 = \frac{1}{\eta} P_2 = \frac{1}{\text{RoTE} - \text{losses}} P_2.$$

For the same input power the efficiency stays the same but as d increases less power will arrive at the output, which can leads to an increase of input power to maintain the same output power, and as a consequence, I_1 increases which makes losses increase and an efficiency decrease. Thus, RoTE creates a great impact on input power needed for supply and the output power. Even if losses stayed the same, more energy will be lost overtime due to low RoTE because the device will take more time to charge. RoTE is defined due to the fact that in wireless transfer losses are not the main problem that degrades performance. RoTE does not include Joule losses but it is used to measure the amount of magnetic flux that is being used to produce an electromotive force at the secondary.

$$P_1 = V_1 I_1 \quad \wedge \quad P_2 = V_2 I_2$$

Using (3.1.4) and (3.1.8) for P_1 and (3.1.6) and (3.1.9) for P_2 that makes:

$$P_1 = L_1 \pi f A^2 sin(4\pi f t) \tag{3.1.13}$$

$$P_2 = M \pi f A B sin(4\pi f t) \tag{3.1.14}$$

Note that equation (3.1.14) applies when losses are not considered. That makes:

$$RoTE = \frac{P_2}{P_1} \tag{3.1.15} \quad \wedge \quad \eta = \frac{P_2 - R_{L1} I_1^2 + R_{L2} I_2^2}{P_1} \tag{3.1.16}$$

$$RoTE = \frac{P_2}{P_1} = \frac{M \cancel{\pi f A B sin(4\pi f t)}}{L_1 \cancel{\pi f A^2 sin(4\pi f t)}} \xLeftrightarrow{M = k\sqrt{L_1 L_2}}$$

$$RoTE = k \sqrt{\frac{L_2}{L_1}} . \frac{B}{A} \tag{3.1.17}$$

The relation between L_2 and L_1 can be adjusted in order enhance performance. If $L_2=4L_1$, RoTE doubles for the same distance. RoTE cannot exceed 100% because the output power will never be higher than the input. The consequence is having double RoTE for a system where $L_2=4L_1$ when k is equal or lower than 0.5 and less than double where k is greater than 0.5 for the same system.

A and B are the values of the currents of primary and secondary inductors, respectively, and can be calculated when both inductors are considered as an RLC circuit where R_L is the coil resistance, L the inductance and C_d the distributed capacitance which is the parasitic capacitance. If the coils are equal both will have the same RLC circuit then both currents will be equal when d=0.

When transmission occurs both inductors will be at resonance which nullifies reactive energy. The current in one coil can be divided into two components. The current passing in the coil and the current passing in the parasitic capacitance which is 180 degrees shifted from the coil current. Due to this fact the current can be calculated as RL circuit:

$$\overline{V_1} = (R_{L1} + j\omega L_1)\overline{I_1} \Leftrightarrow \overline{I_1} = \frac{\overline{V_1}}{R_{L1}+j\omega L_1}$$

$$\overline{I_1} = I_1 \angle \varphi$$

φ is the angle between current and voltage. Due to the fact that R_{L1} is small, $\varphi \approx 90°$.

I_1 is the value for current that needs to be calculated. I_2 can be calculated the same way but because V_2 varies with distance the I_2 will be lower as distance increases.

$$\overline{V_2} = (R_{L2} + j\omega M)\overline{I_2} \Leftrightarrow \overline{I_2} = \frac{\overline{V_2}}{R_{L2}+j\omega M} \Leftrightarrow \text{using } (2.1.6)$$

$$\Leftrightarrow \overline{I_2} = \frac{j\omega M}{R_{L2}+j\omega M}\overline{I_1} \Leftrightarrow I_2 = \frac{\omega M}{\sqrt{R_{L2}^2+(\omega M)^2}} I_1 \Leftrightarrow I_2 \approx \frac{\omega M}{R_{L2}+\omega M} I_1 \qquad (3.1.18)$$

For ωM >> R_{L2}, $I_2 \approx I_1$. Even with M being reduced with the increase of distance with relatively high frequency or small coil resistance or both I_2 is near I_1. This makes $A \approx B = A$. Thus, (3.1.14) and (3.1.17) can be rewritten:

$$P_2 = M\pi f A^2 sin(4\pi f t) \qquad (3.1.19)$$

$$RoTE = k\sqrt{\frac{L_2}{L_1}} \qquad (3.1.20)$$

From (3.1.20) it is deduced that L_2 should be larger than L_1 to enhance RoTE. RoTE is directly proportional to k, M, V_2 and output power. According to (2.3.6) L_1 and L_2 can be described as:

$$L_1 = \pi\mu_0 \frac{{N_1}^2}{h_1} {r_1}^2 K_{L1} \qquad L_2 = \pi\mu_0 \frac{{N_2}^2}{h_2} {r_2}^2 K_{L2}$$

$$\frac{L_2}{L_1} = \frac{{N_2}^2}{{N_1}^2} \frac{{r_2}^2}{{r_1}^2} \frac{h_1}{h_2} \frac{K_{L2}}{K_{L1}} \qquad (3.1.21)$$

The Nagaoka`s constant depends on geometry, that is on relation between $\frac{h}{2r}$. The equation (3.1.21) can be rewritten as:

$$L_1 = \left(\frac{N_1}{N_2}\right)^2 \left(\frac{r_1}{r_2}\right)^2 \frac{h_2}{h_1} \frac{K_{L2}}{K_{L1}} L_2 \qquad (3.1.22)$$

or

$$L_2 = \left(\frac{N_2}{N_1}\right)^2 \left(\frac{r_2}{r_1}\right)^2 \frac{h_1}{h_2} \frac{K_{L1}}{K_{L2}} L_1 \qquad (3.1.23)$$

The inductance of one coil is the other multiplied by the relation between the number of turns, of radius and heights. This becomes practical when calculating coils because they can be defined as a relation of the other. From now on, once calculated the inductance for two equal coils, that is $L_1=L_2$, $N_1=N_2$, $r_1=r_2$ and $h_1=h_2$, both coils can then be changed to satisfy requirements by multiplying one of the coils by the relation between the number of turns, radius and heights.

This process is similar to that of a transformer where m = $\frac{N_1}{N_2}$ is used to know the relation of transformation. Here it is used to calculate the relation of inductances.

Consider

m = $\frac{N_1}{N_2}$ (3.1.24), g = $\frac{r_1}{r_2}$ (3.1.25), c = $\frac{h_1}{h_2}$ (3.1.26), q = $\frac{K_{L1}}{K_{L2}}$ (3.1.27)

Equations (3.1.22) and (3.1.23) can be rewritten as:

$$L_1 = \frac{m^2 g^2}{cq} L_2 \qquad (3.1.28)$$

$$L_2 = \frac{cq}{m^2 g^2} L_1 \qquad (3.1.29)$$

These formulas shall later be used to study what happens to RoTE when the parameters change.

By definition, the efficiency is the output power divided by the input power, but it will be useful to distinguish between efficiency and energy transferring, that is to separate losses from rate of transferred energy.

$\eta = \frac{P_2}{P_1}$ and from (3.1.18) $I_2 = I_1$

With losses:

$$P_1 = V_1 I_1 \quad \wedge \quad P_2 = V_2 I_1 - (R_{L1} + R_{L2}){I_1}^2$$

That makes:

$$\eta = \frac{(V_2 - (R_{L1}+R_{L2})I_1)\cancel{I_1}}{V_1\cancel{I_1}} = \frac{V_2 - (R_{L1}+R_{L2})I_1}{V_1} \qquad (3.1.30)$$

Equation (3.1.30) is a general formula. When d increases V_2 decreases but the losses do not increase. When losses are not considered efficiency becomes:

$$\eta = \frac{V_2}{V_1}$$

But with no losses efficiency is 100%. If the secondary becomes too far away and no energy is transferred the output power will be 0, and as a consequence, efficiency will be zero, but the losses will be approximately equal. Rewriting the formula above is needed. According to (3.1.15):

$$RoTE = \frac{V_2}{V_1} \qquad (3.1.31)$$

$$\eta = \frac{P_2}{P_1} = \frac{V_2 - (R_{L1}+R_{L1})I_1}{V_1} = \frac{V_2}{V_1} - \frac{(R_{L1}+R_{L1})I_1}{V_1} = RoTE - losses \qquad (3.1.32)$$

Later in tests V_2 shall be measured, but in reality it is not possible to measure V_2 without losses. V_2 obtained in practice is V_2 of the formula plus losses so (3.1.32) needs rewriting:

$$\eta = \frac{P_2}{P_1} = \frac{V_2^*}{V_1} = \frac{V_2}{V_1} - \frac{(R_{L1}+R_{L1})I_1}{V_1} = \frac{V_2}{V_1} - \frac{V_{losses}}{V_1} = RoTE - losses \qquad (3.1.33)$$

Where V_2^* is the real obtained voltage while V_2 is the voltage without considering losses. If V_{losses}<<, efficiency and RoTE become approximately equal.

According to formulas (3.1.20) and (3.1.23) it is possible to understand the evolution of RoTE with the different possible ways to build the coils in such a way that the rate of transferred energy increases. Consider that initially the coils are made equal, that is $L_1=L_2$, $N_1=N_2$, $r_1=r_2$ and $h_1=h_2$. Then N, r and h are modified to achieve better performance:

If $\begin{cases} N_2^{'} = 2N_2 \\ r_2^{'} = r_2 \\ h_2^{'} = h_2 \end{cases}$ while L_1 = constant implies $L_2^{'}$= 4L_2, M´= 2M and RoTE´=2RoTE

If $\begin{cases} N_2^{'} = N_2 \\ r_2^{'} = 2r_2 \\ h_2^{'} = h_2 \end{cases}$ while L_1 = constant implies $L_2^{'}$= 4L_2, M´= 2M and RoTE´=2RoTE

If $\begin{cases} N_2^{'} = 2N_2 \\ r_2^{'} = r_2 \\ h_2^{'} = 2h_2 \end{cases}$ while L_1 = constant implies $L_2^{'} = \frac{1}{2}L_2$, $M^{'} = \frac{1}{\sqrt{2}}M$ and $RoTE^{'} = \frac{1}{\sqrt{2}}$ RoTE

Where $N_2^{'}$, $r_2^{'}$ and $h_2^{'}$ are the modified values for N_2, r_2, and h_2, that change L_2, M and RoTE into $L_2^{'}$, $M^{'}$, $RoTE^{'}$, respectively. If L_1 needs to be increased L_2 should also be increased.

Furthermore, using more than one coil in transmitter and/or receiver could eventually be used to enhance performance by creating a new mutual inductance M_{AB}. That could amplify the total magnetic field which then could increase range at a cost of more coils.

Consider using two equal coils, A and B with $L_A=L_B$, $N_A=N_B$, $r_A=r_B$ and $h_A=h_B$, where A and B are used in the transmitter or receiver in parallel and side by side. In series it would be the same as doubling the number of turns. More than two coils could be used for both primary or secondary but the final model would use the equivalent inductance thus making just one transmitter and one receiver with one equivalent coil in each side. From theory it is known that:

If both coils are aligned:

$$L_{eq} = \frac{L_A L_B - {M_{AB}}^2}{L_A + L_B - 2M_{AB}} \tag{3.1.34}$$

If the coils are turned on opposite sides:

$$L_{eq} = \frac{L_A L_B - {M_{AB}}^2}{L_A + L_B + 2M_{AB}} \tag{3.1.35}$$

When comparing equations (3.1.34) and (3.1.35) the divisor of the first equations is lower than the second one. This means the first formula can achieve a higher L_{eq} and for that reason (3.1.34) is the only one of interest. Using (2.1.5) to rewrite (3.1.34):

$$L_{eq} = \frac{L_A L_B - k_{AB}^2 L_A L_B}{L_A + L_B - 2k_{AB}\sqrt{L_A L_B}} = \frac{L_A L_B (1 - k_{AB}^2)}{L_A + L_B - 2k_{AB}\sqrt{L_A L_B}} \tag{3.1.36}$$

Where k_{AB} is the coupling coefficient of the coils A and B.

As k_{AB} increases towards unity L_{eq} decreases which is undesirable. If k_{AB} decreases towards zero it is achieved the parallel of two coils which result in a L_{eq} lower than both L_A or L_B alone while occupying more space and increasing the amount of wire needed and cost resulting in no advantage.

One important part of a WPT system design consists in predicting the energy output for a certain distance, or in other words, for a given distance predict what coils should be made and what input power should be used in order to achieve at least a specified amount of power in the secondary without great loss of power. Therefore, modeling k, M, V_2, and RoTE will help to

understand the behavior of these physical quantities as distance changes and that way know what output power can be achieved for a specified range.

To model M as distance varies formula (2.1.7) will be used and then using (2.1.5) to achieve a model for k:

$$\mathrm{M}(d) \approx \frac{\pi\mu_0 N_1 N_2 {r_1}^2 {r_2}^2}{2({d^2}+{r_1}^2)^{\frac{3}{2}}} \overset{(2.1.5)}{\Longleftrightarrow} k(d) \approx \frac{1}{\sqrt{L_1 L_2}} \frac{\pi\mu_0 N_1 N_2 {r_1}^2 {r_2}^2}{2({d^2}+{r_1}^2)^{\frac{3}{2}}}$$

Then equation (2.3.6) is used to rewrite the previous formula:

$$\sqrt{L_1 L_2} = \sqrt{\pi^2 {\mu_0}^2 \frac{{N_1}^2}{h_1}\frac{{N_2}^2}{h_2} {r_1}^2 {r_2}^2 K_{L1} K_{L2}} = \pi\mu_0 N_1 N_2 r_1 r_2 \sqrt{\frac{K_{L1}K_{L2}}{h_1 h_2}}$$

$$k(d) \approx \frac{1}{\cancel{\pi\mu_0 N_1 N_2 r_1 r_2}} \sqrt{\frac{h_1 h_2}{K_{L1}K_{L2}}} \frac{\cancel{\pi\mu_0 N_1 N_2 {r_1}^2 {r_2}^2}}{2({d^2}+{r_1}^2)^{\frac{3}{2}}} \Leftrightarrow$$

$$\Leftrightarrow k(d) \approx \frac{\sqrt{h_1 h_2}}{2\sqrt{K_{L1}K_{L2}}} r_1 r_2 \frac{1}{({d^2}+{r_1}^2)^{\frac{3}{2}}} \qquad (3.1.37)$$

To obtain V_2 it is used (2.1.6) and (2.1.7):

$$\mathrm{M} = \frac{V_2}{\omega I_1} \overset{(2.1.7)}{\Longleftrightarrow} \frac{\pi\mu_0 N_1 N_2 {r_1}^2 {r_2}^2}{2({d^2}+{r_1}^2)^{\frac{3}{2}}} = \frac{V_2}{\omega I_1} \Leftrightarrow V_2(d) \approx \frac{\pi^2 f I_1 \mu_0 N_1 N_2 {r_1}^2 {r_2}^2}{({d^2}+{r_1}^2)^{\frac{3}{2}}} \qquad (3.1.38)$$

For RoTE there is more than one way to obtain, by using (2.3.6) and (3.1.20) it is:

$$RoTE = k\sqrt{\frac{L_2}{L_1}} \overset{(2.3.6)}{\Longleftrightarrow} RoTE = k\sqrt{\frac{\cancel{\pi\mu_0} {N_2}^2 {r_2}^2 h_1 K_{L2}}{\cancel{\pi\mu_0} {N_1}^2 {r_1}^2 h_2 K_{L1}}} = k\frac{N_2}{N_1}\frac{r_2}{r_1}\sqrt{\frac{h_1}{h_2}}\sqrt{\frac{K_{L2}}{K_{L1}}} =$$

Using formulas (3.1.24), (3.1.25), (3.1.26) and (3.1.27):

$$= k\frac{\sqrt{cq}}{mg} \overset{(3.1.37)}{\Longleftrightarrow} RoTE = \frac{\sqrt{h_1 \cancel{h_2}}}{2\sqrt{K_{L1}\cancel{K_{L2}}}} \cancel{r_1} r_2 \frac{1}{({d^2}+{r_1}^2)^{\frac{3}{2}}} \frac{N_2}{N_1}\frac{r_2}{\cancel{r_1}}\sqrt{\frac{h_1}{\cancel{h_2}}}\sqrt{\frac{\cancel{K_{L2}}}{K_{L1}}} \Leftrightarrow$$

$$RoTE(d) \approx \frac{1}{2}\frac{N_2}{N_1}\frac{h_1}{K_{L1}} {r_2}^2 \frac{1}{({d^2}+{r_1}^2)^{\frac{3}{2}}} \qquad (3.1.39)$$

By using (3.1.7), (3.1.8) and (3.1.31) this is what achieved:

$$RoTE = \frac{V_2}{V_1} \overset{(3.1.7),(3.1.8)}{\Longleftrightarrow} RoTE = \frac{M\cancel{2\pi f A cos(2\pi f t)}}{L_1\cancel{2\pi f A cos(2\pi f t)}} = \frac{M}{L_1}$$

Then, by using (2.1.7) and (2.3.6) it is obtained:

$$RoTE = \frac{\frac{\pi\mu_0 N_1 N_2 {r_1}^2 {r_2}^2}{2(d^2+{r_1}^2)^{\frac{3}{2}}}}{\pi\mu_0 \frac{{N_1}^2}{h_1} {r_1}^2 K_{L1}} = \frac{\cancel{\pi\mu_0} N_1 N_2 \cancel{r_1^2} {r_2}^2 h_1}{\cancel{\pi\mu_0} {N_1}^2 \cancel{r_1^2} K_{L1} 2(d^2+{r_1}^2)^{\frac{3}{2}}} \Leftrightarrow$$

$$\Leftrightarrow RoTE(d) \approx \frac{1}{2}\frac{N_2}{N_1}\frac{h_1}{K_{L1}} {r_2}^2 \frac{1}{(d^2+{r_1}^2)^{\frac{3}{2}}}$$

Both forms reach the same formula (3.1.39).

Formulas (3.1.37), (2.1.7), (3.1.38), and (3.1.39) consist on the mathematical model to understand the behavior of k, M, V_2, and RoTE with distance, respectively. Notice that η gives the relation between output power and input power independently from what source reduces the output power. It can be either due to high coil resistance or low performance due to long range that provokes low rate of transferred energy. Inductor parameters should be used to enhance performance. All these formulas are an approximation due to the fact the model for M is an approximation and the other formulas are written according to (2.1.7).

3.2 Calculating frequency

Frequency is an important part of a WPT system because the resonance frequency of the coils will define frequency of the oscillator used later. Due to parasitic elements an inductor can be considered as an RLC circuit as in Figure 3.2.1:

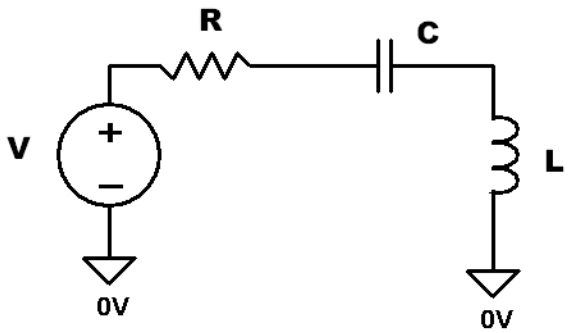

Figure 3.2.1: RLC Circuit

By applying Kirchhoff`s Voltage Law, and considering the initial voltages in the inductor and parasitic capacity null, it is obtained after simplification:

$$\frac{dV(t)}{dt} = \frac{d^2i(t)}{dt^2} + \frac{R}{L}\frac{di(t)}{dt} + \frac{1}{LC} = 0$$

By applying Laplace transform to this equation it is obtained:

$$s^2 + \frac{R}{L}s + \frac{1}{LC} = 0 \Leftrightarrow s = -\frac{R}{2L} \pm \sqrt{\left(\frac{R}{2L}\right)^2 - \frac{1}{LC}} \Leftrightarrow s = -\alpha \pm \sqrt{\alpha^2 - \omega^2}$$

Where α is the attenuation that is provoked by the resistance. When there is no resistance s would equal jω, the angular frequency.

$$\omega = 2\pi f = \frac{1}{\sqrt{LC}} \Leftrightarrow$$

$$f = \frac{1}{2\pi\sqrt{LC}} \qquad (3.2.1)$$

The inductance, L, and the capacity, C, are the variables that define frequency. L can be obtained by using equation (2.3.6).

C can be obtained by putting an external capacity in the circuit. This external capacity will enter in parallel with the parasitic capacity making C being the sum of both. Using an external capacity large enough will make the parasitic one irrelevant, and that way, frequency is defined just by the inductance of the coil and the chosen capacity.

On the other hand, it is an advantage to work at high frequencies because the amount of energy transferred over time will increase with frequency. Adding an external capacity can be used to simplify the model but it always reduces frequency which is undesirable. In some applications, if power is too high frequency will need to decrease in order to avoid electro stimulation that causes health issues. In that case, adding an external capacity is a simple method to decrease frequency. Thus, frequency can always be controlled to be decreased but it cannot increase more than the frequency resulting from the inductance and parasitic capacitance of the coil.

The parasitic capacity will be important to know but it can be difficult to calculate. As it will be explained later, more than one model will be used to calculate the parasitic capacity of the coils.

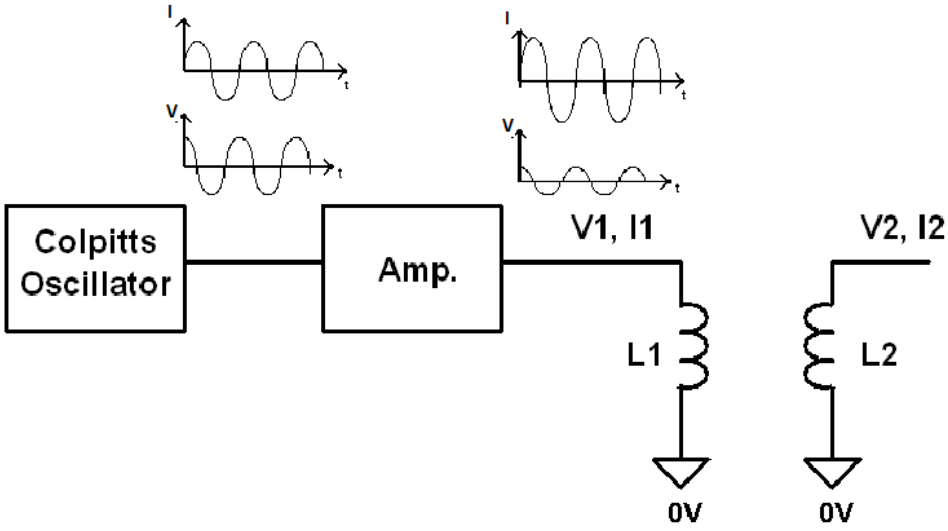

Figure 3.2.2 – High Level Architecture of the work done.

Figure 3.2.2 shows the work done. The math models to predict system performance were made considering V_1, V_2, I_1 and I_2 as seen in Figure 3.2.2. Models for calculating the parasitic capacity of the inductors were also made and are better explained in next subchapter.

Note that the model to predict M was made by another author mentioned in chapter 2. The other models were made based on that model as seen early. The prototype follows this architecture.

3.2.1 Parasitic Capacity

Equations (2.3.2) and (2.3.5) are a model to calculate the parasitic capacitance of an inductor. The model consist in calculating the capacity of just one turn, that is C_t, and because the capacities of each turn of a coil are in series with each other the total capacity is the series of C_t which results in equation (2.3.2).

However, this model has two major problems. One is the fact that all turns are charged and that means that the total capacity of each turn is the sum of all capacities created per turn in every turn. The distance between the first turn and the second, and then the first and the third, and so on… increases per turn which means that every capacity is, one by one, lower than the capacity before it. In practice, for an inductor with just one layer of turns, the total capacity will be slightly larger because the capacity per turn depends on the number of turns.

The second problem is that this only works in a coil with just one layer of turns. By adding more than one layer the total capacity increases because the turns of the second layer are closer than they would if the inductor had the same number of turns but in just one layer and that means that the real capacity is larger than the calculated one.

Due to the fact that the first model failed, other models were studied in order to achieve the best results. In [35] a model proposed by Medhurst was used:

$$C_L = \frac{4\varepsilon_0 h}{\pi}\left[1 + 0.8249\left(\frac{2r}{h}\right) + 2.395\left(\frac{2r}{h}\right)^{\frac{3}{2}}\right]$$

Where h is the height of the inductor, r is the radius; ε_0 is the dielectric constant of air.

This model failed again in calculating the real parasitic capacity. In [36] an alteration to Medhurst model was proposed:

$$k_C = 0.717439\left(\frac{2r}{h}\right) + 0.933048\left(\frac{2r}{h}\right)^{\frac{3}{2}} + 0.106\left(\frac{2r}{h}\right)^{2}$$

$$C_L = \frac{4\varepsilon_0\varepsilon_x h}{\pi}\left[1 + \frac{k_C}{2}\left(1 + \frac{\varepsilon_i}{\varepsilon_x}\right)\right]\frac{1}{cos^2\psi}$$

$$\psi = arctan\left(\frac{p}{2\pi r}\right)$$

Where p is pitch, the distance between one turn and the next, ψ has no particular interest besides being used for calculating, ε_i is the relative dielectric constant of the material inside the coil and ε_x is the relative dielectric constant of the material exterior to the coil.

Even though these equations achieved a value for the parasitic capacity closer to the real value when compared to the previous methods the results were still not satisfying.

After these three methods were used a new model for calculating the parasitic capacity of one inductor was made. There is more than one factor that contributes for the total parasitic capacity and each contribution will be analyzed separately.

The first consists in the capacity of each turn of the inductor to the next in the same layer of turns. Considering a turn as a planar torus or a circle with a smaller circle inside creating a hole for the plate of the capacity, there is a capacity between two adjacent turns. From theory it is known that the capacity between a capacitor of parallel plates is:

$$C = \frac{\varepsilon_0\varepsilon_r A_p}{d} \qquad (3.2.1.1)$$

Where A_p is for plate area and d the distance between them. Considering the circle with a smaller circle inside the area of each plate is:

A_p = The average length of each turn×difference between the radius of the outer circle and the inside circle = $2\pi\left(\frac{R+r}{2}\right) \times (R - r) = \pi(R^2 - r^2)$

R and r are the radius of the large and small circles, respectively. Applying this result to (3.2.1.1):

$$C = \frac{\varepsilon_0\varepsilon_r\pi(R^2 - r^2)}{d} \qquad (3.2.1.2)$$

Other turns also have a contribute to the turn capacity because between the first turn and the third, and the forth turn and so on, there are two charged plates with a distance between them that increases turn by turn, which adds to the total capacity even if just slightly:

$$C_t = \frac{\varepsilon_0 \varepsilon_r \pi (R^2 - r^2)}{d} + \frac{\varepsilon_0 \varepsilon_r \pi (R^2 - r^2)}{2d} + \cdots + \frac{\varepsilon_0 \varepsilon_r \pi (R^2 - r^2)}{(NperLayer - 1) \times d} \Leftrightarrow$$

$$\Leftrightarrow C_t = \frac{\varepsilon_0 \varepsilon_r \pi (R^2 - r^2)}{d} \times \sum_{i=1}^{NperLayer-1} \frac{1}{i} \qquad (3.2.1.3)$$

NperLayer is the number of turns of each layer and Ct is the total turn Capacity.

But the middle turns have a greater capacity because the distance between the middle plates and the extremities is lower. This means that not all turns have the same capacity and equation (3.2.1.3) only applies for extremities. To correct this, the middle turn's capacity will be calculated and then the average between the extremities and middle can be used.

$$C_{tmiddle} = \frac{2\varepsilon_0 \varepsilon_r \pi (R^2 - r^2)}{d} \times \sum_{i=1}^{\frac{Nperlayer}{2}} \left(\frac{1}{i}\right) \qquad (3.2.1.4)$$

$$C_t = \left(\frac{1}{2}\right)\left(\frac{\varepsilon_0 \varepsilon_r \pi (R^2 - r^2)}{d} \times \sum_{i=1}^{Nperlayer-1} \left(\frac{1}{i}\right) + \right.$$

$$\left. + \frac{2\varepsilon_0 \varepsilon_r \pi (R^2 - r^2)}{d} \times \sum_{i=1}^{\frac{Nperlayer}{2}} \left(\frac{1}{i}\right)\right) \qquad (3.2.1.5)$$

C_t is average turn capacity of one given layer.

If the inductor has more than one layer it should be considered that layer by layer the radius increases and C_t only applies for the first layer, but by adding to R and r the diameter of the wire C_t for the other layers can still be calculated with equation (3.2.1.5).

For the total layer capacity equation (2.3.2) can be used:

$$C_{layer} = \frac{Ct}{N_{perLayer}-1} \qquad (3.2.1.6)$$

C_{layer} is the total capacity of one given layer.

The second contribution consists in the fact that there is one capacity between two adjacent turns of two adjacent layers. For this, it can be considered the model for a cylindrical capacity where the first turn is the inside plate and the second turn is the outer plate:

$$C_{cylinder} = \frac{2\pi\varepsilon_0\varepsilon_r D}{\ln\left(\frac{r_C^{'}}{r_C}\right)} \qquad (3.2.1.7)$$

D is the diameter of the wire.

r_C is the distance from the centre of the inductor until the wire.

$r_C^{'}$ is the distance from the centre of the inductor until the outer wire that will be considered for calculation.

The outer layers also contribute for the total capacity even if just slightly because the distance increases. Like in the previous contribution where the middle turns had a greater capacity than the ones of extremities because the distances are shorter the same happens with the middle layers.

The extremities and the middle capacities can be calculated with equation (3.2.1.7). Then the average between them can be considered, that is the interlayer capacity for one turn. The total interlayer capacity is the interlayer capacity for one turn multiplied by the number of turns per layer.

The third contribution consists in the capacities provoked by other conductors that are not adjacent to each other, in other words, all turns create capacities in all the others and because of that a given turn accumulates a capacity from all other turns. The next matrix will be used to better illustrate the problem:

$$\begin{bmatrix} 1 & 0 & 0 & 0 & 0 \\ 1 & 0 & 0 & 0 & 0 \\ 1 & 1 & 1 & 1 & 1 \end{bmatrix}$$

Consider that each position of the matrix represents one conductor or one turn of the coil. In this case, the coil has 15 turns divided in 3 layers with 5 turns per layer.

The bottom line with 1`s represents the contribution given by the all capacities of the layer which were calculated with C_{layer} to the far left turn of the bottom line.

The column with 1`s represents the contribution of the interlayer capacities that were calculated using equation (3.2.1.7) rearranging the radius in the formula accordingly to the far left turn of the bottom line.

The previous calculations were made for the two contributions for all turns. But the contribution that in the matrix is represented with 0`s were not given yet. As distance increases each turn will give different values for each capacity which will be taken into account next, that is the crossed capacity. The crossed capacity can be calculated by using equation (3.2.1.7) by modifying the radius accordingly:

$$C_{crossed} = 2\pi\varepsilon_0\varepsilon_r(2a+2t)\sum_{j=1}^{nLayer}\sum_{i=1}^{Nperlayer-1}\left(\frac{1}{\ln\left(\frac{r+\sqrt{i+j}(2a+2t)}{r+a+t}\right)}\right) \quad (3.2.1.8)$$

nLayer is the number of layers, a is the radius of the wire without the coating, t is the thickness of the coating and r the turn radius.

This is the crossed capacity of the turn of one of the extremities. For the middle turn the equation is:

$$C_{middlecrossed} =$$
$$2\times 2\pi\varepsilon_0\varepsilon_r(2a+2t)\sum_{j=1}^{nLayer}\sum_{i=1}^{Nperlayer-1}\left(\frac{1}{\ln\left(\frac{r+\sqrt{i+j}(2a+2t)}{r+a+t}\right)}\right) \quad (3.2.1.9)$$

The average between (3.2.1.8) and (3.2.1.9) could be used for the calculations, but the maximum that is (3.2.1.8) can also be used for a safety margin that will be explained later. Then the result needs to be multiplied by the number of turns to achieve the total crossed capacity.

The fourth and final contribution is the capacity created in the turn itself due to the fact that the conductor creates an electric field that is radially irradiated and the electric potential in each turn is not equal in every point of the turn. This creates an internal capacity for each turn that is calculated next.

Consider equation (3.2.1.1) and that the area in the equation for an infinitesimal arch of the turn is:

$$A_p = (2a+2t)dx$$

$$dC = \frac{\varepsilon_0\varepsilon_r dA_p}{d} = \frac{\varepsilon_0\varepsilon_r(2a+2t)dx}{D}$$

The total length of the turn is 2πr and, for that reason, to obtain the total internal capacity for one turn the previous equation needs to be integrated:

$$C = \int_0^{2\pi r}\frac{\varepsilon_0\varepsilon_r(2a+2t)}{D}dx = \frac{\cancel{2}\pi\cancel{r}\varepsilon_0\varepsilon_r(2a+2t)}{\cancel{2r}} = \pi\varepsilon_0\varepsilon_r(2a+2t)$$

This is the internal capacity created by the turn itself. In reality the internal capacity is larger because the electric field is not uniform and that means that the other infinitesimal areas

also add to the particular infinitesimal area. Adding to this, when a turn is in presence of other turns in the neighborhood they also create other internal capacities which are in parallel with the internal capacity created by the turn itself and add to the total capacity. The previous result needs to be multiplied by the number of turns. The distance between the other turns varies but also the electric potential of the turns which makes the electrical charge not uniform in all points of the wire. To simplify the problem, this phenomenon will not be considered.

$$C_{int} = \pi\varepsilon_0\varepsilon_r(2a + 2t)N$$

C_{int} is the total internal capacity created by itself and all other turns in the neighborhood. The total internal capacity of the coil has the contribution of all turns:

$$C_{internal} = \pi\varepsilon_0\varepsilon_r(2a + 2t)N^2 \qquad (3.2.1.10)$$

The simplification made means that (3.2.1.10) is an approximation and is actually inferior to the real internal capacity, even if just slightly.

The total parasitic capacity or distributed capacity is the sum of these four contributions because these capacities are in parallel:

$$C_d = \sum_{i=1}^{nLayer} C_{layerTotal_i} + C_{interLayerTotal} + C_{crossedTotal} + C_{internal} \qquad (3.2.1.11)$$

This model is an approximation to the real parasitic capacity. Even though the model has many aspects in consideration there are some not considered. Each turn creates its own capacity inside it, which is the internal capacity, but the other turns also contribute for creating capacities with different values due to distance and electric potential of each turn, and the way a coil is winded up makes the electric potential of each turn different for different positions which then results in some capacities being larger than others. This phenomenon provoked by the way the coil is winded up can be better explained with the next matrix:

$$\begin{bmatrix} 11 & 12 & 13 & 14 & 15 \\ 10 & 9 & 8 & 7 & 6 \\ 1 & 2 & 3 & 4 & 5 \end{bmatrix}$$

When the coil is winded up the first turns became adjacent to each other in the first layer, which means that the electric potential difference for each turn is the same. In the second layer, the same happens for the layer but between one given turn of one layer and another turn in a different layer the electric potential difference is larger than two adjacent turns of the same layer and the amount of electrical charge is not uniform as the number of turns increases. The turns number 1 and 10 have a bigger electric potential difference than 2 and 9 and so on. This also happens for crossed capacities and because the capacity depends on both electric

potential difference and charge which are both not uniform between turns the model is an approximation.

$$\Delta V = Ed = \frac{Qd}{\varepsilon_0 \varepsilon_r A}$$

$$Q = C\Delta V \Leftrightarrow C = \left|\frac{Q}{\Delta V}\right| \Leftrightarrow C = \frac{\varepsilon_0 \varepsilon_r A}{d}$$

These formulas are known from theory and are shown to better explain the problem.

Even though equation (3.2.1.10) is an approximation it can be used to know what parasitic capacity can be achieved and safety margins can be given in order to guarantee that the frequency is at least a value near the real frequency.

On the other hand, if the proposed model shows in later sections that the capacity is relatively near the real value it can be considered for calculating the frequency.

Finally, even if the value is wrong but at least is at the same order of magnitude it can be used to give a perspective of what frequency can be achieved and possible variation can be solved with an external capacitor larger 10 times or more than the calculated value for parasitic capacity and that way compromise between high frequency and frequency predictability.

3.3 The prototype

For the prototype using equal resonating coupling coils it was used a Colpitts oscillator where the inductor is a MCR that is a magnetic controlled reactor. The MCR is used to vary the inductance in order to control work frequency. In the case in study frequency was adjusted manually but a controller could be made and there already algorithms described early that could have been used to adjust frequency automatically.

Due to the fact that for a given transmission power it is useful to have high current in the primary, the characteristic of voltage and current was adjusted using an amplifier, that is, by controlling the gain, voltage decreases and, as consequence, current increases.

The transmitter and receiver consist in equal inductors, that is L_1=L_2, N_1=N_2, r_1=r_2 and h_1=h_2. Different inductors could have been used but the main purpose was to study the model proposed that was described early with equations (2.1.7), (3.1.37), (3.1.38) and (3.1.39) which is a general model.

Other described mathematical models will be used to predict how the coil construction affects inductance, capacitance, resistance and frequency of the coils.

There are techniques that can be used to enhance performance that use different coils but the model is the same.

The main objective was to understand if the mathematical model could be used to predict transmission characteristic for different ranges and that way the model could be used to establish the working range while guaranteeing at least a chosen amount of output power for a specific range which in turn can be used to know the resulting speed of charge.

All secondary voltages measured were no-load tests because the objective was to understand what happens during transmission. After the secondary more power electronics could be added to alter the wave form or convert AC to DC depending on the application, but that was not the objective of this work.

3.3.1 The Constructed Inductors

The first pair of inductors had $N_1=N_2=40$ divided in two layers of 20 each, $r_1=r_2=1.8$cm and $h_1=h_2=4.8$cm. The copper wire had a=0.57mm of radius and a PVC coating with a thickness of t=0.63mm and a total diameter of 2.4mm. There was no pitch because the turns were leaning against each other.

By using equation (2.3.6) the theoretical value for $L_1=L_2=$ $\pi\mu_0 \times \frac{40^2}{0.048} 0.018^2 \times 0.74$ ≈31,7μH.

$$\mu_0 = 4\pi \times 10^{-7} \text{ H/m}$$

The resistance can be calculated with (2.3.3) considering ρ_{Cu} = 1.72× 10^{-8} Ωm

$$R_{L1}=R_{L2}=1.72 \times 10^{-8} \times \frac{2\pi \times 0.018 \times 40}{\pi \times 0.00057^2} \approx 76.2\text{m}\Omega$$

For the capacity the different models achieved different values:
With equation (2.3.5):

This formula considers pitch from the center of the first wire until the center of the other wire.

$$\frac{\frac{p}{2a}}{\left(1+\frac{t}{2a}\right)^{1-\frac{1}{\varepsilon_r}}} = \frac{\frac{2a+2t}{2a}}{\left(1+\frac{t}{2a}\right)^{1-\frac{1}{\varepsilon_r}}} \approx 1.557712 \qquad \left(1+\frac{t}{2a}\right)^{1-\frac{1}{\varepsilon_r}} \approx 1.352023$$

$$Ct = \frac{\pi^2 \varepsilon_0 \varepsilon_r . 2 \times 0.018}{\ln\left(1.557712 + \sqrt{(1.557712)^2 - 1.352023}\right)} \approx 10.5pF$$

Applying equation (2.3.2) per layer:

$$Cd = \left(\frac{Ct}{20-1}\right) * 2 \approx 1.1pF$$

For Medhurst:

$$\frac{2r}{h} = 0.75 \qquad \varepsilon_0 = 8.85 \times 10^{-12} C^2/Nm^2$$

$$C_{d1} = C_{d2} = \frac{4\varepsilon_0 0.018}{\pi}\left[1 + 0.8249(0.75) + 2.395(0.75)^{\frac{3}{2}}\right] \approx 124.06pF$$

For modified Medhurst:

$$\psi = arctan(0) = 0 \qquad \varepsilon_r = 3.18$$

$$k_C = 0.717439\left(\frac{2r}{h}\right) + 0.933048\left(\frac{2r}{h}\right)^{\frac{3}{2}} + 0.106\left(\frac{2r}{h}\right)^{2} \approx 149.68$$

$$C_L = \frac{4\varepsilon_0\varepsilon_r h}{\pi}\left[1 + \frac{k_C}{2}\left(1 + \frac{\varepsilon_0}{\varepsilon_0}\right)\right]\frac{1}{cos^2\psi} \approx 259.16\ pF$$

For the proposed model instead of the average value the maximum value will be used for a better approximation:

$$C_{tmiddle1st} = \frac{2\varepsilon_0\varepsilon_r\pi((0.018 + 3a + 3t)^2 - (0.018 + a + t)^2)}{2t} \times \sum_{i=1}^{\frac{20}{2}}\left(\frac{1}{i}\right) \approx 30.4\ pF$$

The second and outer turn is:

$$C_{tmiddle2nd} = \frac{2\varepsilon_0\varepsilon_r\pi((0.018 + 5a + 5t)^2 - (0.018 + 3a + 3t)^2)}{2t} \times \sum_{i=1}^{\frac{20}{2}}\left(\frac{1}{i}\right) \approx 34.2\ pF$$

For the total capacity of turns in the same layer for the two layers is:

$$C_{layerTotal} = \frac{C_{tmiddle1st}}{N_{perLayer} - 1} + \frac{C_{tmiddle2nd}}{N_{perLayer} - 1} \approx 3.4\ pF$$

For the capacity between the first and second layer is:

$$C_{interLayerTotal} = \frac{2\pi\varepsilon_0\varepsilon_r 2 \times 0.018}{\ln\left(\frac{0.018 + 3a + 3t}{0.018 + a + t}\right)} \times 20 \approx 72.1\ pF$$

Again, the maximum value will be used when calculating the total crossed capacity:

$$C_{middlecrossed} = 2 \times 2\pi\varepsilon_0\varepsilon_r(2a + 2t)\sum_{j=1}^{2}\sum_{i=1}^{20-1}\left(\frac{1}{\ln\left(\frac{0.018 + \sqrt{i+j}(2a+2t)}{0.018 + a + t}\right)}\right)$$

$$\approx 49.573\ pF$$

$$C_{crossedTotal} = C_{middlecrossed} \times N \approx 1.983\ nF$$

For total internal capacity is:

$$C_{internal} = \pi\varepsilon_0\varepsilon_r(2 \times 0.00057 + 2 \times 0.00063)40^2 \approx 0.34\ nF$$

The total distributed capacity is:

$$C_d = 3.4 + 72.1 + 1983 + 340 \approx 2.31\ nF$$

The frequency is:

$$f = \frac{1}{2\pi\sqrt{(31.7\times10^{-6})(2.31\times10^{-9})}} \approx 588\ 145\ Hz$$

The characteristic impedance is:

$$Z_0 = \sqrt{\frac{(31.7 \times 10^{-6})}{(2.31 \times 10^{-9})}} \approx 117.1\Omega$$

The second pair of inductors had N_1=N_2=80 divided in two layers of 40 each, r_1=r_2=1.8cm and h_1=h_2=4.8cm. The copper wire had a=0.57mm of radius and a PVC coating with a thickness of t=0.03mm and a total diameter of 1.2mm. There was no pitch because the turns were leaning against each other.

By using equation (2.3.6) the theoretical value for L_1=L_2= $\pi\mu_0 \times \frac{80^2}{0.048} 0.018^2 \times 0.74$ ≈127μH.

$$\mu_0 = 4\pi \times 10^{-7}\ \text{H/m}$$

The resistance can be calculated with (2.3.3) considering ρ_{Cu} = 1.72× 10^{-8} Ωm.

R_{L1}=R_{L2}=$1.72 \times 10^{-8} \times \frac{2\pi\times0.018\times80}{\pi\times0.00057^2}$ ≈0.15Ω

For the capacity the different models achieved different values:

With equation (2.3.5):

This formula considers pitch from the center of the first wire until the center of the other wire.

$$\frac{\frac{p}{2a}}{\left(1+\frac{t}{2a}\right)^{1-\frac{1}{\varepsilon_r}}} = \frac{\frac{2a+2t}{2a}}{\left(1+\frac{t}{2a}\right)^{1-\frac{1}{\varepsilon_r}}} \approx 1.034053 \qquad \left(1+\frac{t}{2a}\right)^{1-\frac{1}{\varepsilon_r}} \approx 1.017967$$

$$Ct = \frac{\pi^2 \varepsilon_0 \varepsilon_r . 2 \times 0.018}{\ln\left(1.034053 + \sqrt{(1.034053)^2 - 1.017967}\right)} \approx 43.2\, pF$$

Applying equation (2.3.2) per layer:

$$Cd = \left(\frac{Ct}{20-1}\right) * 2 \approx 2.3\, pF$$

For Medhurst:

$$\frac{2r}{h} = 0.75 \qquad \varepsilon_0 = 8.85 \times 10^{-12} C^2/Nm^2$$

$$C_{d1} = C_{d2} = \frac{4\varepsilon_0 0.018}{\pi}\left[1 + 0.8249(0.75) + 2.395(0.75)^{\frac{3}{2}}\right] \approx 124.06\, pF$$

For modified Medhurst:

$$\psi = arctan(0) = 0 \qquad \varepsilon_r = 3.18$$

$$k_C = 0.717439\left(\frac{2r}{h}\right) + 0.933048\left(\frac{2r}{h}\right)^{\frac{3}{2}} + 0.106\left(\frac{2r}{h}\right)^2 \approx 149.68$$

$$C_L = \frac{4\varepsilon_0 \varepsilon_r h}{\pi}\left[1 + \frac{k_C}{2}\left(1 + \frac{\varepsilon_0}{\varepsilon_0}\right)\right]\frac{1}{cos^2\psi} \approx 259.16\, pF$$

For the proposed model:

Instead of the average value the maximum value will be used for a better approximation:

$$C_{tmiddle1st} = \frac{2\varepsilon_0\varepsilon_r\pi((0.018+3a+3t)^2-(0.018+a+t)^2)}{2t} \times \sum_{i=1}^{\frac{40}{2}}\left(\frac{1}{i}\right) \approx 488.5\ pF$$

The second and outer turn is:

$$C_{tmiddle2nd} = \frac{2\varepsilon_0\varepsilon_r\pi((0.018+5a+5t)^2-(0.018+3a+3t)^2)}{2t} \times \sum_{i=1}^{\frac{40}{2}}\left(\frac{1}{i}\right) \approx 977.2\ pF$$

For the total capacity of turns in the same layer for the two layers is:

$$C_{layerTotal} = \frac{C_{tmiddle1st}}{N_{perLayer}-1} + \frac{C_{tmiddle2nd}}{N_{perLayer}-1} \approx 37.6\ pF$$

For the capacity between the first and second layer is:

$$C_{interLayerTotal} = \frac{2\pi\varepsilon_0\varepsilon_r 2\times 0.018}{\ln\left(\frac{0.018+3a+3t}{0.018+a+t}\right)} \times 40 \approx 4.07\ nF$$

Again, the maximum value will be used when calculating the total crossed capacity:

$$C_{middlecrossed} = 2\times 2\pi\varepsilon_0\varepsilon_r(2a+2t)\sum_{j=1}^{2}\sum_{i=1}^{40-1}\left(\frac{1}{\ln\left(\frac{0.018+\sqrt{i+j}(2a+2t)}{0.018+a+t}\right)}\right) \approx 172.19\ pF$$

$$C_{crossedTotal} = C_{middlecrossed} \times N \approx 13.77\ nF$$

For total internal capacity is:

$$C_{internal} = \pi\varepsilon_0\varepsilon_r(2\times 0.00057 + 2\times 0.00003)80^2 \approx 679.02\ pF$$

The total distributed capacity is:

$$C_d = 37.6 + 4070 + 13770 + 679.02 \approx 18.56\ nF$$

The frequency is:

$$f = \frac{1}{2\pi\sqrt{(127\times10^{-6})(18.56\times10^{-9})}} \approx 103\,664\,Hz$$

The characteristic impedance is:

$$Z_0 = \sqrt{\frac{(127 \times 10^{-6})}{(18.56 \times 10^{-9})}} \approx 82.3\Omega$$

3.3.2 The Colpitts Oscillator

To transmit energy wirelessly using resonant coupling coils it is needed to use a current the varies with time in order to create a variation in the magnetic field intensity that induces an electromotive force which then appears on the secondary circuit, transmitting the energy.

Therefore, creating AC current or other method to create a variable current is necessary and, to achieve that, a Colpitts oscillator was built. A different oscillator could be used and signal produced do not need to be necessarily sinusoidal, but initially it was not certain if the coil would or not act as a filter just permitting the passage of the energy of the wave at working frequency and not the harmonics and for that reason an oscillator which produced a sinusoidal wave was chosen due to the fact that triangular or square waves can be decomposed as the sum of sinusoidal waves.

Other LC oscillators could have been used for the prototype, but in this case, the Colpitts oscillator was chosen because it can generate high frequency sinusoidal signals with high frequency stability. Adding to this, the Colpitts oscillator frequency can be varied by varying the capacitors, or in this case, the inductance is changed by using a MCR to adjust the working frequency as the frequency splitting phenomenon occurs while keeping the amplitude of the output of the oscillator approximately constant.

The oscillator consists in using two capacitors and a MCR in a voltage amplifier to generate a sinusoidal wave. The MCR can be varied by voltage using a controller or, in the case, manually because the controller was not the objective of this work. By varying inductance of the MCR frequency can vary and that way frequency splitting can be overcome.

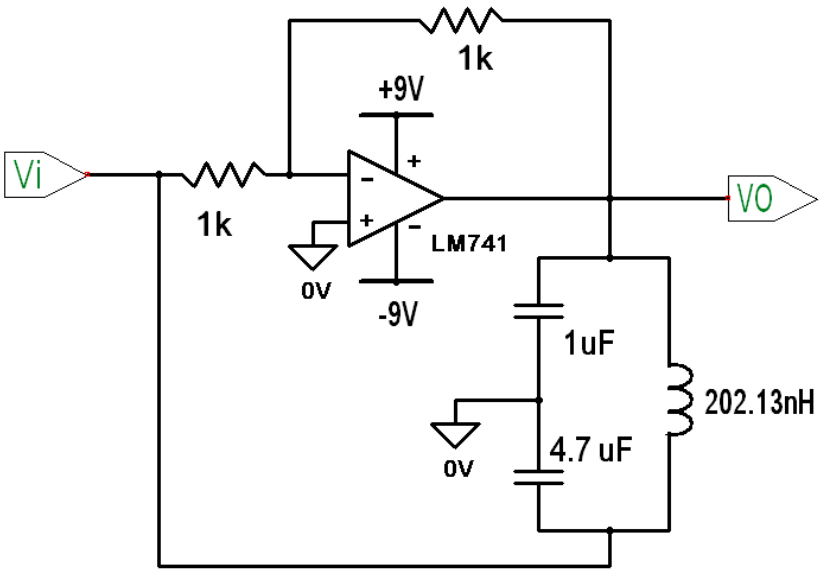

Figure 3.3.2.1: Colpitts Oscillator

LM741 was the amplifier used. Vi is an input signal used to regulate the input power at the transmitter coil that appears at the end of the blocks used.

$$f = \frac{1}{2\pi\sqrt{LC_{eq}}} \qquad C_{eq} = \frac{C_1 C_2}{C_1 + C_2}$$

C_1 = 1µF

C_2 = 4.7µF

C_{eq} = 0.825µF

L is variable between approximately 60nH and 136µH.

The working frequency range will be between 15-700kHz.

Due to the fact that is difficult to predict the parasitic capacity of the inductor, and as consequence, the resonating frequency, it is a good practice to measure this frequency before the construction of the oscillator in a case where frequency range is short because the real inductor frequency can be out of that range. A signal generator can be used by regulating frequency of the signal wave in the first coil until the second coil achieves the maximum voltage with no-load. The frequency obtained is the real resonator frequency and the oscillator should be constructed for that central frequency.

3.3.3 The Amplifier

As explained early, having high values for the current in the primary circuit is useful to transmit energy at farthest distance possible. Therefore, a voltage amplifier was used to increase current that came from the oscillator. By varying resistors the voltage gain can be controlled. For high gain values the voltage increases and current decreases, if low gain values are used the voltage does not increase significantly or can even be decreased resulting in larger primary current. The amplifier does not have a buffer stage which results in a voltage gain decrease, and as a consequence, primary current increases. The topology is presented next:

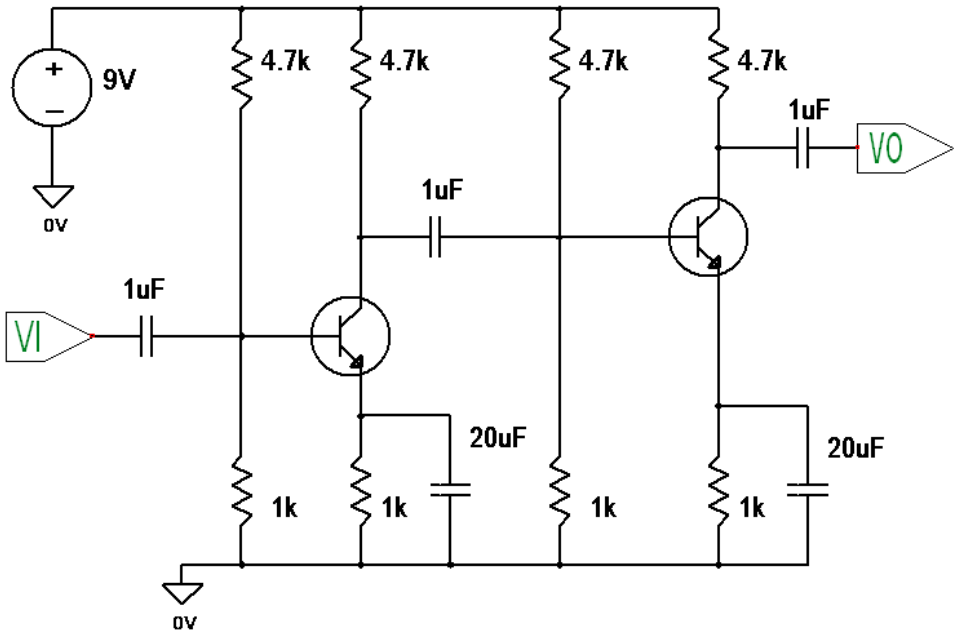

Figure 3.3.3.1: Amplifier

In this case, a two-stage common emitter with emitter degeneration amplifier was used. Capacitors of 20µF were used to increase the voltage gain at high frequencies. Other amplifier topologies could be used. This topology was chosen for its simplicity, insensibility to static gain of current and high gain.

There is no need for a buffer stage because the resistance of the primary coil, which is a very low value, will enter in parallel with the output impedance of the amplifier. Therefore, the voltage gain will decrease drastically and current will increase as a result.

3.4 Controller

The objective of this work was not to do the controller, even though its presence would have been advantageous. The control that here is done by manually adjusting the magnetic permeability of the MCR, consists in adjusting frequency to achieve MEET point as distance varies. This makes possible for the secondary to move while the primary stands still and still maintain transmission optimized, for that distance.

By observing the map of poles and zeros of the transfer function MEET can be achieved by automatically regulating frequency using a controller. Even though, the controller was not the main objective of this project, here is presented the transfer function and the map of poles and zeros in complex plain.

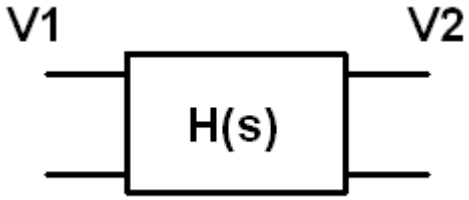

Figure 3.4.1: Two-port transfer function.

Considering a RLC circuit for primary and secondary, Z_1 and Z_2 can be expressed as function of s:

$$Z_1(s) = R_{L1} + \frac{1}{sC_1} + sL_1 = L_1 \frac{s^2 + \frac{R_{L1}}{L_1}s + \frac{1}{L_1C_1}}{s} \wedge Z_2(s) = L_2 \frac{s^2 + \frac{R_{L2}}{L_2}s + \frac{1}{L_2C_2}}{s}$$

$V_2(t)$ is the convolution of h(t) and $V_1(t)$:

$$V_2(t) = h(t) * V_1(t) \Leftrightarrow Z_2I_2(t) = h(t) * Z_1I_1(t) \overset{I_1(t)=I_2(t)}{\Longleftrightarrow} Z_2 = h(t) * Z_1 \Leftrightarrow$$

$$\Leftrightarrow H(s) = \frac{Z_2(s)}{Z_1(s)} = \frac{L_2}{L_1} \frac{s^2 + \frac{R_{L2}}{L_2}s + \frac{1}{L_2C_2}}{s^2 + \frac{R_{L1}}{L_1}s + \frac{1}{L_1C_1}} =$$

$$= \frac{L_2}{L_1} \frac{\left(s + \alpha_2 - \sqrt{{\alpha_2}^2 - {\omega_{02}}^2}\right)(s + \alpha_2 + \sqrt{{\alpha_2}^2 - {\omega_{02}}^2})}{\left(s + \alpha_1 - \sqrt{{\alpha_1}^2 - {\omega_{01}}^2}\right)(s + \alpha_1 + \sqrt{{\alpha_1}^2 - {\omega_{01}}^2})}$$

$$with\ \alpha_1 = \frac{R_{L1}}{2L_1}, {\omega_{01}}^2 = \frac{1}{L_1C_1},\ \alpha_2 = \frac{R_{L2}}{2L_2},\ \ {\omega_{02}}^2 = \frac{1}{L_2C_2}$$

Where h(t) is the impulse response of the channel between primary and secondary and H(s) its Laplace transform.

H(s) has the same number of poles and zeros and all of them have a negative real part, being located in the left side of the imaginary plain. Thus, H(s) is stable by Routh-Hurwitz criteria. When $\omega >> \alpha$ H(s) is marginally stable.

The whole plant consists in the product of the transfer functions of Colpitts oscillator, amplifier and H(s).

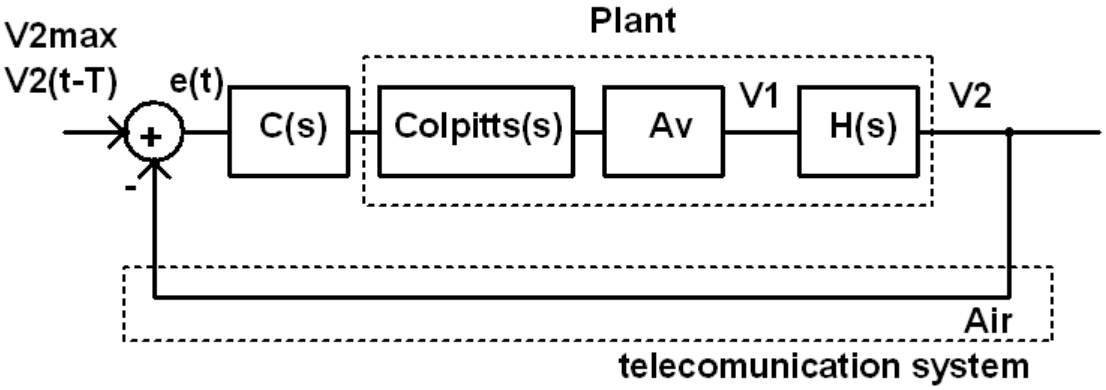

Figure 3.4.2: Block diagram of the full system with automatic controller.

The transfer function of the plant is the product of the transfer functions of the Colpitts oscillator, amplifier and H(s).

When manually controlling the system V_2 is observed in an oscilloscope and frequency is regulated until the maximum of V_2, V_{2max} is obtained. Due to the fact that V_2 is obtained in the secondary electric circuit which is physically apart from the primary with air in between, an automatic controller would need a telecommunication system to send the obtained V_2 to compare with the previous V_2 obtained, $V_2(t-T)$, until V_{2max} is reached.

If the frequency shift between the primary and secondary resonant frequencies was predictable, V_{2max} could be achieved without a telecommunication system.

In the next chapter, simulations and experimental results obtained with the prototype as well as the performance indicators calculated with the described models will be shown for comparison. There, a detailed discussion about the simulations, experimental results and theoretical concepts is also found.

4

SIMULATIONS AND EXPERIMENTAL RESULTS

In this chapter, simulations done using LTSPICE program are shown for further comparison with the calculations done and the obtained results from the prototype.

Later, the mathematical models made in the theoretical analysis will be applied and due to the fact that they depend on distance, the values will be put in tables which then will be used to produce graphs that present the functions described by the application of the models to the distances tested with the prototype.

Finally, in the Discussion subsection, the mathematical models will be compared to the obtained results from the prototype and simulations to describe how the models can be used to plan and design WPT systems using resonating coupling coils. Different construction methods that can be used depending on project specs will also be explained in order to build systems most suitable for specific applications.

4.1 Simulations

Each simulated block will be presented one by one as well as the whole system simulation. Simulated behavior considered relevant will also be present. The advantages of simulating consist not only in better block design and the ability to make small changes to components for better system design with less effort but also for better understanding of how the system will work before being built due to the fact that if simulations are relatively close to the actual performance obtained from the prototype that makes the simulations well suited for system design. The WPT system created was designed in LTSPICE program according to prototype subsection, beginning in page 34.

In this case, it was used a variable voltage supply. The simulations are used to study the behavior of V_2 as distance varies. When distance changes M is manually changed accordingly which then also changes the value of L_1-M and L_2-M. The resistance of 1 Ω is used to simulate losses and can be changed if needed, even though, it is known from theory that losses are low in general and performance is mostly affected by distance. To avoid

misinterpretations L_1-M and L_2-M and M of the simulations will be called the first, second and third inductances, respectively.

The objective of this work is not to explain how to simulate electrical circuits on LTSPICE, but the blocks used will be shown and it will be explained how to simulate the WPT behavior.

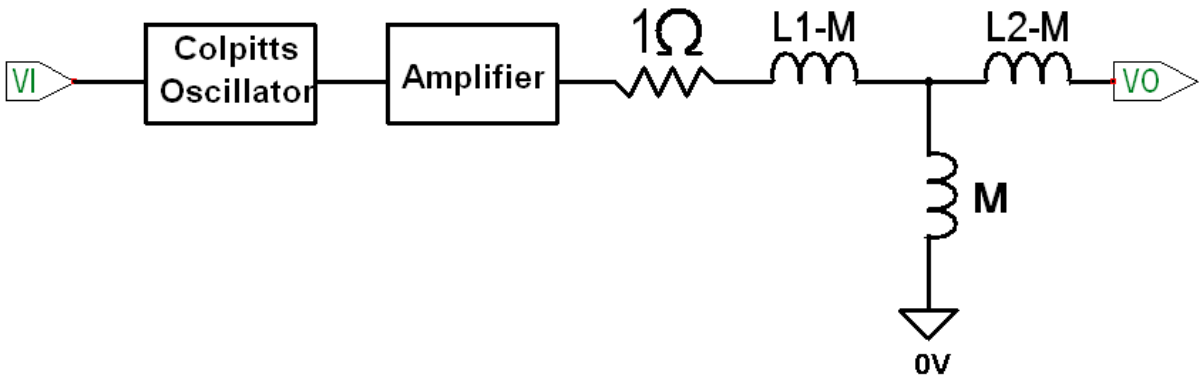

Figure 4.1.1: The Complete schematic of the constructed WPT

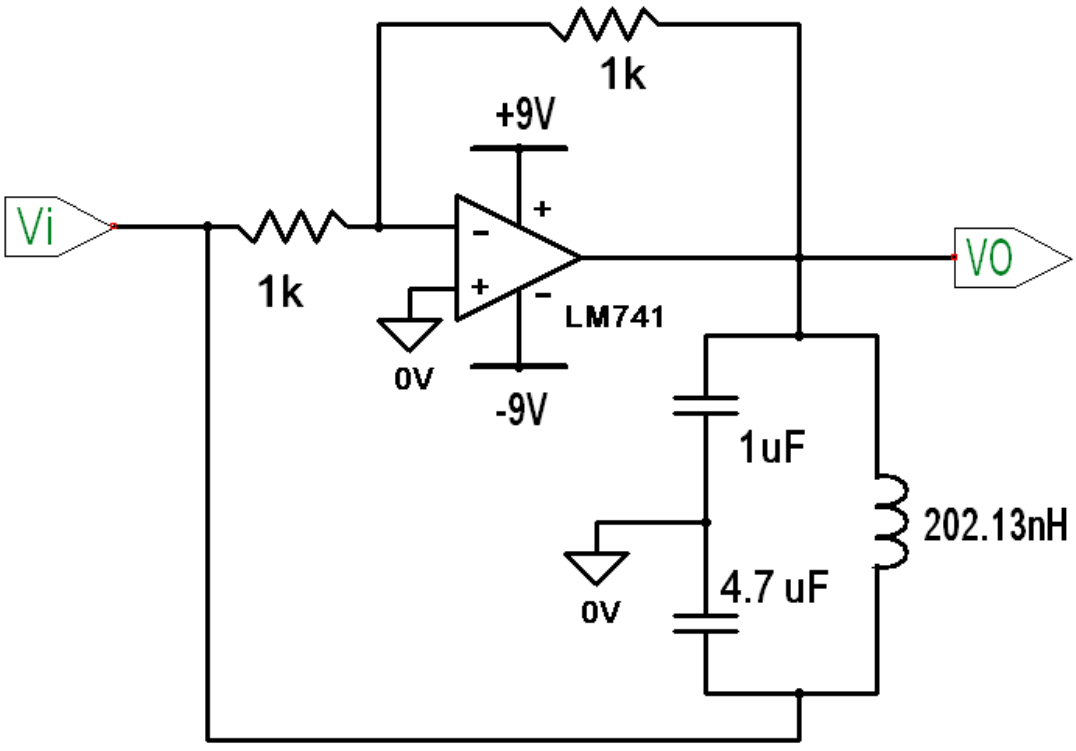

Figure 4.1.2: Schematic of the Colpitts Oscillator

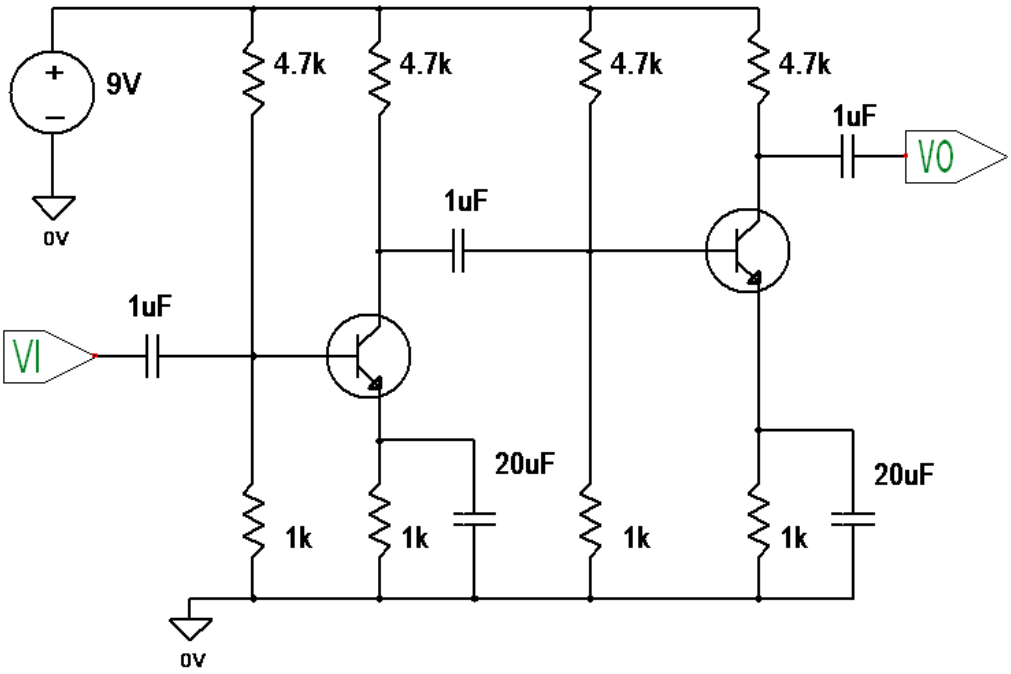

Figure 4.1.3: Schematic of the Amplifier

After creating and testing the schematics in figures 4.1.2 and 4.1.3 individually they can be turned into symbols using the LTSPICE. In figure 4.1.1 both symbols of Colpitts oscillator and voltage amplifier are used to create the schematic of the full WPT system. The T model with three inductors is used to simulate the behavior of the energy transferring.

There is more than one type of analysis, AC, DC, noise, etc…but when there is energy transferring, which is the part of interest, AC analysis of the simulator should be used. There is no energy being transferred in DC and noise is not of particular interest in the context of energy transferring using this technology.

After the schematic is done, clicking in the run button will show in the screen the type of analysis and its own specifications. AC analysis and the next specifications were chosen:

Type of sweep: decade

Number of points per decade: 1000

Start frequency: 300000

Stop frequency: 500000

After running the simulation the points before the first and after the second inductances are clicked, which correspond to V_1 and V_2, respectively. Then a graph appears in the screen with the values for V_1 and V_2 in dB by default, but units can be converted to Volt by clicking in y-axis with the right button of the mouse and choosing the proper setting. Both ways can be used to simulate the behavior of the WPT. The behavior is not tested directly in the simulator for all distances, but for each value of distance V_2 can be obtained. There is no need for V_1 being shown in the graph, but only to check if it is the proper value needed for primary voltage in the real WPT.

In this case, V_I was manually adjusted to obtain 6.01 V in the point before the first inductance which corresponds to V_1. After checking V_1, there is only need to click in the point after the second inductance, or V_O, to simulate V_2.

When d = 2cm for the coils with an inductance of 31.7 µH calculated in section 3 it will be shown how to simulate, as an example.

If the scale in dB is used, the graph should be zoomed in the peak which happens in the resonance frequency. This way the values for V_1 and V_2 can be easier to see. For this case, V_1 = 21.5 dB and V_2 = 16.0 dB.

$$dB = 20\log_{10}\left(\frac{V_2}{V_1}\right)$$

16.0-21.5 = -5.5 dB

$$-5.5 = 20\log_{10}\left(\frac{V_2}{V_1}\right) \Leftrightarrow \frac{V_2}{V_1} \approx 0.531 \Leftrightarrow V_2 = 0.531 \times 6.01 \approx 3.19\,V$$

If the scale is in V, the graph should be zoomed in and the values are obtained directly.

By using the calculated M for the third inductance and 31.7 µH minus M for the first and second inductances all values can be simulated for each distance. Each value is put in a table, as it is shown in tables 4.1.1 and 4.1.2 and then RoTE can be calculated by dividing the simulated value for V_2 and the chosen V_1, that is for this case is 6.01V and multiplied by 100 to obtain the value for RoTE in %. Then, the simulated values can be compared with the calculations. The calculations for k, M, V_2 and RoTE will be better explained in subsection 4.2. There it will be seen that the values for calculated k is 1.2, which is higher than the maximum theoretical value of 1, and as a consequence, M, V_2 and RoTE will also be greater than their maximum theoretical values. For that reason, consider using the maximum theoretical values for each physical quantity in the simulations when the calculations exceed those values.

Table 4.1.1: Calculated and simulated values for V_2 and RoTE when L_1=L_2=31.7µH.

d(cm)	Mcalc(µH)	V2calc(V)	V2sim(V)	Rotecalc(%)	RoTEsim(%)
1	38.0	7.00	6.00	116	99.8
2	17.0	3.07	3.19	51.1	53.1
3	7.73	1.34	1.45	22.4	24.1
4	3.93	0.635	0.740	10.6	12.3
5	2.21	0.313	0.415	5.2	6.91
7	0.878	0.0648	0.165	1.08	2.75
9	0.428	-0.0192	0.0805	-0.319	1.34
11	0.239	-0.0544	0.0450	-0.906	0.749
13	0.146	-0.0717	0.0275	-1.19	0.458
15	0.0961	-0.0811	0.0182	-1.35	0.303

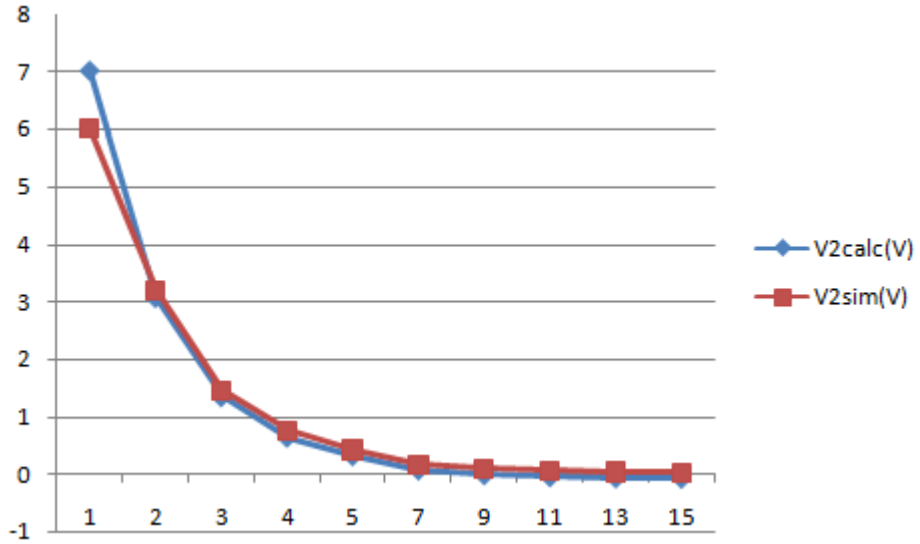

Figure 4.1.4: Comparison between calculated and simulated V_2 for L_1=L_2=31.7µH.

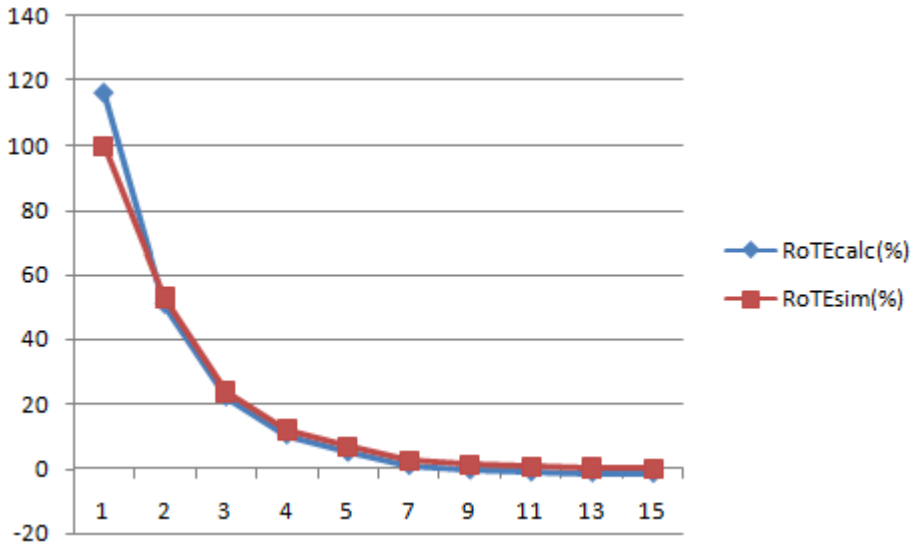

Figure 4.1.5: Comparison between calculated and simulated RoTE for L_1=L_2=31.7µH.

For inductors with calculated value for inductance of 127 µH, the simulation process is similar. Only the first, second and third inductances should changed properly, and V_I can be used to obtain the value of 9V for primary voltage. Note that the resistance before the T model can be adjusted for having the calculated value of the sum of primary and secondary coil resistances and this way simulated V_2 and RoTE already include losses, which will be better explained lately.

Table 4.1.2: Calculated and simulated values for V_2 and RoTE when L_1=L_2=127μH.

d(cm)	Mcalc(μH)	V2calc(V)	V2sim(V)	Rotecalc(%)	RoTEsim(%)
1	152	10.5	8.99	117	99.9
2	68.1	4.61	4.79	51.2	53.2
3	31	2.01	2.18	22.3	24.2
4	15.7	0.938	1.10	10.4	12.2
5	8.84	0.453	0.623	5.03	6.92
6	5.4	0.211	0.380	2.35	4.22
8	2.4	0.000911	0.169	0.0101	1.88
10	1.27	-0.0784	0.0894	-0.872	0.993
12	0.743	-0.115	0.0523	-1.28	0.581
14	0.471	-0.135	0.0332	-1.49	0.369
16	0.318	-0.145	0.0224	-1.61	0.249

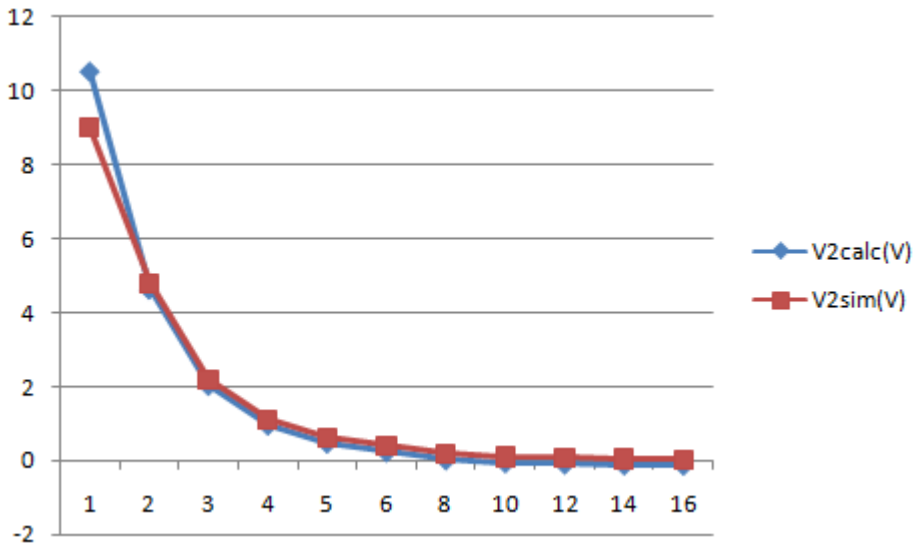

Figure 4.1.6: Comparison between calculated and simulated V_2 for L_1=L_2=127μH.

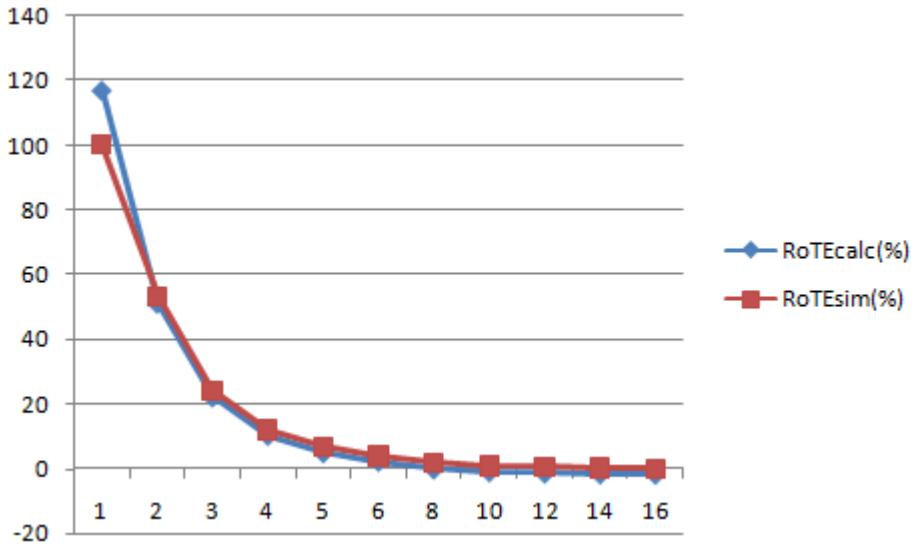

Figure 4.1.7: Comparison between calculated and simulated RoTE for L_1=L_2=127µH.

4.2 Experimental Results

Both the obtained values of the tests done with the prototype and the calculated values from the models will be shown for further comparison. The calculations shall be detailed for better understanding of how to apply the models to predict the behavior of energy transferring. The results obtained with the prototype will be used for comparison with the models in order to understand if the models can be used or not for performance prediction. The detailed calculations will show how to use the models with the developed method in this work to predict system performance and that way simulate the behavior of WPT systems before building it to avoid low quality construction and too expensive inductors.

The prototype of a WPT was constructed according to section 3. The next images correspond to the obtained values of k, M, V_2, and RoTE for the constructed inductors. The quality of the mathematical models for predicting k, M, V_2 and RoTE that are used to calculate efficiency and understand the behavior of the WPT system as distance varies will be analyzed in the next section as well as the overall performance.

To overcome frequency splitting phenomenon the system was designed to adjust frequency using a MCR that acts as a variable inductor in the Colpitts oscillator. When coils are already constructed it is difficult to get values for inductance and capacitance exactly equal to calculated values and even though the work frequency of the oscillator can be controlled varying the work point, this can lead to distortion increasing which can lead to loss of energy if the inductors act as a filter and just pass the energy at resonance frequency.

It is common in industrial production, after manufacturing large quantities of standardized devices that they are not entirely equal. If inductors and oscillators manufactured vary too much transmission could be compromised. To analyze the behavior of a WPT when inductors vary it was constructed two pairs of different inductors with different frequencies of resonance. The overall performance will be analyzed for the two models.

Table 4.2.1: Nagaoka`s constant

h/D	K_L
0.00	0.0000
0.10	0.2033
0.20	0.3198
0.30	0.4053
0.40	0.4719
0.50	0.5255
0.60	0.5697
0.70	0.6067
0.80	0.6381
0.90	0.6651
1.00	0.6884
1.11	0.7100
1.25	0.7351
1.43	0.7609
1.67	0.7885
2.00	0.8181
2.50	0.8499
3.33	0.8838
5.00	0.9201
10.0	0.9588
11.0	0.9600

To obtain a continuous function for Nagaoka`s constant, K_L, Microsoft Excel was used to find a function to simulate its behavior. To obtain a better approximation, the table was divided in two and two functions were obtained. One function is for h/D less than 1 and the other is for h/D greater than 1.

Two pairs of identical inductors were used to make the experience, the first pair having a good impedance matching, that is Z_0 is near 50Ω, and the second pair differencing significantly from that value. Each pair in turn was put in alignment along a graduated axis. For each pair, the first inductor was held stationary while the second was moved along a distance d and the voltage at the second inductor's terminals was measured. Then, k, M, and RoTE were calculated using the measured values for V_2.

The measured and calculated values were done for all values of d and were put in tables which later were used to produce graphs that show the behavior of each physical quantity as distance varies.

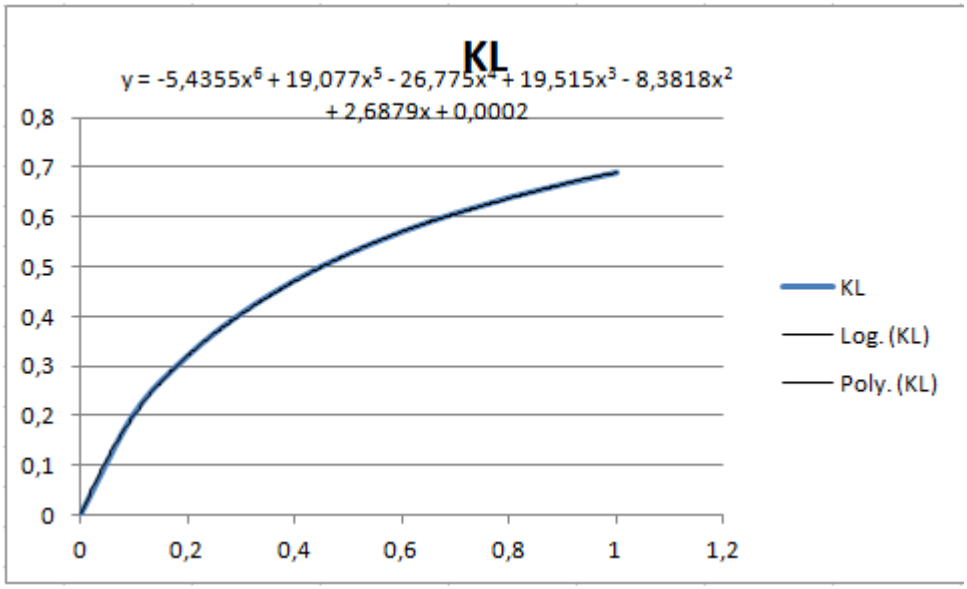

Figure 4.2.1: Function than simulates $\frac{h}{D}$ less than 1

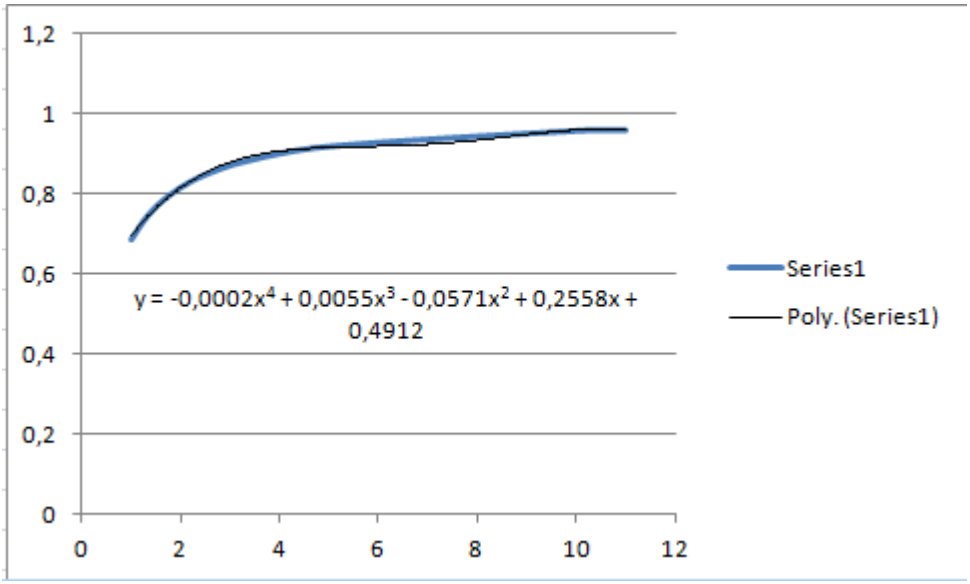

Figure 4.2.2: Function than simulates $\frac{h}{D}$ greater than 1

A LCR multimeter was used to measure resistance, inductance and capacitance of the constructed inductors.

The first pair of inductors have L_1=28µH, L_2=30µH, C_{d1}=7.31nF, C_{d2}=6.93nF, R_{L1}=85mΩ and R_{L2}=86mΩ. From equation (2.2.8) comes Z_{01}=61.9Ω and Z_{02}=65.8Ω. Using equation (3.2.1) comes f_1=351789 Hz and f_2=349054 Hz, which are approximately equal.

The second pair of inductors have L_1=124µH, L_2=126µH, C_{d1}=511nF, C_{d2}=502nF, R_{L1}=0.169Ω and R_{L2}=0.171Ω. Z_{01}=15.6Ω and Z_{02}=15.8Ω. f_1=19994 Hz and f_2=20012 Hz. Notice that these coils are mismatched from the characteristic impedance of 50Ω. f_1=19994 Hz and f_2=20012 Hz.

Results for inductors with L_1=28µH and L_2=30µH can be consulted in Appendix A figures A1 to A22. Results for inductors with L_1=124µH and L_2=126µH can be consulted in Appendix A figures B1 to B11.

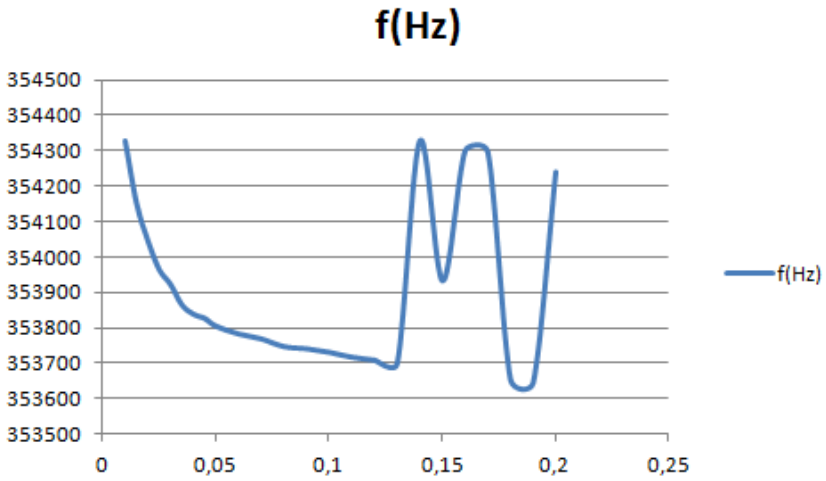

Figure 4.2.3: Frequency adjustment for L_1=28µH and L_2=30µH

Table 4.2.2: Obtained values for k, M, V_2 and RoTE when L_1=28µH and L_2=30µH

d(cm)	V_2obt(V)	V_1(V)	f(Hz)	Mobt(µH)	Kobt	RoTEobt(%)
1	4.24	6.01	354328	20.1	0.694	71.8
1.5	3.71	6.01	354152	17.6	0.607	62.8
2	2.82	6.01	354046	13.4	0.461	47.8
2.5	2.65	6.01	353964	12.6	0.434	44.9
3	2.29	6.01	353922	10.9	0.375	38.8
3.5	1.76	6.01	353864	8.35	0.288	29.8
4	1.49	6.01	353838	7.07	0.244	25.2
4.5	1.20	6.01	353826	5.69	0.196	20.3
5	0.990	6.01	353804	4.70	0.162	16.8
6	0.707	6.01	353782	3.36	0.116	12.0
7	0.530	6.01	353768	2.51	0.0868	8.98
8	0.424	6.01	353746	2.01	0.0694	7.19
9	0.354	6.01	353740	1.68	0.0580	6.00
10	0.283	6.01	353730	1.34	0.0463	4.80
11	0.230	6.01	353716	1.09	0.0377	3.90
12	0.194	6.01	353708	0.921	0.0318	3.29
13	0.156	6.01	353698	0.740	0.0255	2.64
14	0.141	6.01	354328	0.668	0.0231	2.39
15	0.127	6.01	353932	0.602	0.0208	2.15
16	0.113	6.01	354300	0.535	0.0185	1.91
17	0.0990	6.01	354296	0.469	0.0161	1.68
18	0.0850	6.01	353652	0.404	0.0139	1.44
19	0.0710	6.01	353644	0.337	0.0116	1.20
20	0.0640	6.01	354240	0.303	0.0105	1.08

The values obtained in table 4.2.2 will be explained next. All calculations will be done for d=1cm. The other values are calculated the same way but distance, d, changes. All distances used in calculations were converted to meters.

V_1 and V_2 are obtained in appendix A figureA1 in yellow and blue, respectively, by dividing the peak-to-peak voltages by 2 to obtain the amplitude, and then dividing by square root of 2 to get the rms value.

$$V_1 = \frac{peak-to-peak_{yellow}}{2\sqrt{2}} = 6.01\ V \qquad V_2 = \frac{peak-to-peak_{blue}}{2\sqrt{2}} = 4.24\ V$$

For primary current measurement was used a voltmeter linked to a resistance, R_1=1.028Ω. By applying Ohm`s law current can be known. Voltage on coil terminals cannot be measured directly because resonance occurs when energy is being transmitted which makes voltage 0V. This phenomenon happens because the inductive and capacitive reactances of the inductor reach the same value which results in the same voltage for both but with opposite signals. The sum of the two results is 0V.

The current could also be calculated, but in this first case, it was measured using a relatively small resistance before the primary inductor. This was used in the first pair of inductors to confirm the calculations below. In the second pair of inductors current was not measured but simply calculated due to the fact that the first pair of coils already had confirmed that current can simply be calculated and that the measured value is almost the same as the calculated one and the small differences that may exist are due to the fact that laboratory equipment cannot keep frequency steady for long periods. In practice, there is no need to add a resistance, but when it is added it must be considered in calculations.

$$I_1 = \frac{V_1}{R_1+R_{L1}+\omega L_1} = \frac{6.01}{1.028+0.085+2\times\pi\times354328\times28\times10^{-6}} = 94.7\ mA$$

$$M = \frac{V_2}{\omega I_1} = \frac{4.24}{2\times\pi\times354328\times0.0947} = 20.1\ \mu H$$

$$k = \frac{M}{\sqrt{L_1 L_2}} = \frac{20.1\times10^{-6}}{\sqrt{28\times10^{-6}\times30\times10^{-6}}} = 0.694$$

$$RoTE(\%) = k\sqrt{\frac{L_2}{L_1}} \times 100\ \% = 0.694 \times \sqrt{\frac{30\times10^{-6}}{28\times10^{-6}}} \times 100 = 71.8\%$$

The other values are calculated by repeating the process described only changing the value of the peak-to-peak voltages for each distance according to appendix A, figuresA2 to A22.

Table 4.2.3: Calculated values for k, M, V_2 and RoTE when L_1=28μH and L_2=30μH

d(cm)	Kcalc	Mcalc(μH)	V_2calc(V)	RoTEcalc(%)
1	1.20	38.0	6.99	116
1.5	0.812	25.7	4.70	78.3
2	0.536	17.0	3.07	51.1
2.5	0.357	11.3	2.01	33.5
3	0.244	7.73	1.34	22.4
3.5	0.171	5.42	0.913	15.2
4	0.124	3.93	0.635	10.6
4.5	0.0918	2.91	0.444	7.39
5	0.0696	2.21	0.313	5.20
6	0.0425	1.35	0.152	2.54
7	0.0277	0.878	0.0648	1.08
8	0.0189	0.599	0.0128	0.212
9	0.0135	0.428	-0.0192	-0.319
10	0.0100	0.317	-0.0399	-0.663
11	0.00754	0.239	-0.0544	-0.906
12	0.00585	0.185	-0.0644	-1.07
13	0.00462	0.146	-0.0717	-1.19
14	0.00371	0.118	-0.0771	-1.28
15	0.00303	0.0961	-0.0811	-1.35
16	0.00250	0.0793	-0.0842	-1.40
17	0.00209	0.0663	-0.0867	-1.44
18	0.00177	0.0561	-0.0886	-1.47
19	0.00150	0.0476	-0.0902	-1.50
20	0.00129	0.0409	-0.0914	-1.52

The calculations will be explained again for the first value of distance, which is d = 1cm, for better understanding.

$$\frac{h}{D} = \frac{4.8}{1.8 \times 2} = 1.333$$

Due to the fact the value for the relation between height and diameter of the coils cannot be directly extracted from table 4.2.1 it shall be used the equation in figure 4.2.2 that gives K_L for $\frac{h}{D}$ greater than 1.

$$K_L = -0.0002 \times 1.333^4 + 0.0055 \times 1.333^3 - 0.0571 \times 1.333^2 + 0.2558 \times 1.333 + 0.4912$$
$$\approx 0.7432$$

$$k(0.01) \approx \frac{\sqrt{h_1 h_2}}{2\sqrt{K_{L1}K_{L2}}} r_1 r_2 \frac{1}{(d^2 + {r_1}^2)^{\frac{3}{2}}} =$$

$$= \frac{\sqrt{0.048 \times 0.048}}{2\sqrt{0.7432 \times 0.7432}} 0.018 \times 0.018 \frac{1}{(0.01^2 + 0.018^2)^{\frac{3}{2}}} =$$

$$= 1.0463 \times 10^{-5} \times \frac{1}{(0.01^2 + 0.018^2)^{\frac{3}{2}}} \approx 1.20$$

$$L_1 = \pi \mu_0 \frac{{N_1}^2}{h_1} {r_1}^2 K_{L1} = \pi \times 4\pi \times 10^{-7} \times \frac{40^2}{0.048} \times 0.018^2 \times 0.7432 \approx 31.7\ \mu H$$

$$M(0.01) \approx \frac{\pi \mu_0 N_1 N_2 {r_1}^2 {r_2}^2}{2(d^2 + {r_1}^2)^{\frac{3}{2}}} = \frac{\pi \times 4\pi \times 10^{-7} \times 40 \times 40 \times 0.018^2 \times 0.018^2}{2} \frac{1}{(0.01^2 + 0.018^2)^{\frac{3}{2}}} =$$

$$= 3.31543 \times 10^{-10} = \frac{1}{(0.01^2 + 0.018^2)^{\frac{3}{2}}} = k(0.01) \times \sqrt{L_1 L_2} =$$

$$= 1.20 \times \sqrt{31.7 \times 10^{-6} \times 31.7 \times 10^{-6}} \approx 38.0\ \mu\text{H}$$

It is a good practice to measure the frequency before doing the calculations due to the fact that the model to estimate the parasitic capacity is not precise enough. For frequency measurement a signal generator was linked to the primary inductor terminals and a sinusoidal wave was generated. The frequency is controlled until a signal appears in the secondary inductor that can be seen using an oscilloscope. When the signal appears in the secondary and frequency is adjusted to reach the maximum output voltage the resonance is reached and the frequency where it occurs is the resonant frequency. After measuring the resonance frequency of the pair of inductors this value should be used for calculations. If the parasitic capacity of the coil is not used, but another capacity is added to impose frequency, there will be no need for building a pair of inductors and measuring because the frequency calculated will be precise enough. In this case, it was used the parasitic capacity because the most difficult case in study corresponds to the highest resonant frequency that a pair of inductors can achieve which is the natural resonant frequency. In this case, the frequency achieved with the real inductors was around 354 kHz.

Even though the inductances can be measured, it is used for the calculations the value from equation (2.3.6) because this value is usually more precise. In a mass production process most of the inductors will have an inductance relatively near the calculated value and some of them will have higher or lower than the calculated value. When the value is equal or higher it is expected that performance is at least equal or even higher than the model prediction. The worst

case happens when obtained values for inductances are lower than calculated which corresponds to the case in study.

$$I_1 = \frac{V_1}{R_1 + R_{L1} + \omega L_1} = \frac{6.01}{1.028 + 0.0762 + 2 \times \pi \times 354000 \times 31.7 \times 10^{-6}} \approx 83.9\, mA$$

$$V_2(0.01) \approx \frac{\pi^2 f I_1 \mu_0 N_1 N_2 {r_1}^2 {r_2}^2}{(d^2 + {r_1}^2)^{\frac{3}{2}}} = M(0.01) \times 2\pi \times f \times I_1 = 38 \times 10^{-6} \times 2\pi \times$$

$$\times 354000 \times 0.0839 \approx 7.09\, V$$

Note that both formulas for calculating V_2 are equivalent and the differences in the calculated values that may occur are due to approximations in intermediate calculations. The same happens for calculating k, M and RoTE, where it is possible to use one equation or the other. This fact does not make the formulas achieved in section 3 useless because they can still be used to understand the behavior of k, M, V_2 and RoTE as inductor construction changes.

The measured value for output voltage is V_2* but the calculated value does not have losses included. To compare the model with reality it is necessary to add the losses to the measured value or subtract them to the calculated one. Thus, V_2 shall be calculated again:

$$V_2(0.01) = M(0.01) \times 2\pi \times f \times I_1 - (R_1 + R_{L1} + R_{L2}) I_1 =$$

$$= 38 \times 10^{-6} \times 2\pi \times 354000 \times 0.0839 - (1.028 + 0.0762 + 0.0762) \times 0.0839$$
$$\approx 6.99\, V$$

For a constant transmitter power the losses on both coils are constant, at least, until a distance far enough that equation (3.1.18) requirements are not fulfilled anymore, which also happens for a distance out of range that is not of particular interest. For example, for the worst obtained case, which happens when d = 20 cm:

$$I_2 = \frac{\omega M}{R_{L1} + \omega M} I_1 = \frac{2\pi \times 354000 \times 0.303 \times 10^{-6}}{0.0762 + 2\pi \times 354000 \times 0.303 \times 10^{-6}} I_1 = 0.903 I_1 \approx I_1$$

All other cases I_2 is even near I_1.

$$RoTE(0.01) \approx \frac{1}{2} \frac{N_2}{N_1} \frac{h_1}{K_{L1}} {r_2}^2 \frac{1}{(d^2 + {r_1}^2)^{\frac{3}{2}}} = k \sqrt{\frac{L_2}{L_1}} \times 100\% = \frac{V_2}{V_1} \times 100\% =$$

$$= \frac{6.99}{6.01} \times 100 \approx 116\%$$

The differences between kcalc and RoTEcalc(%) are explained by the losses that are added to V_2calc and approximations in intermediate calculations. Note that V_2 used for the calculation of RoTE already has losses included. Thus, RoTE calculated is the same as efficiency and both terms can be used interchangeably. If the value for V_2 used is the value without losses, RoTE will be slightly higher than efficiency. Remember that the distinction between efficiency and RoTE consists in the first being the relation between the output power and input power, but the last being the relation between output power and input power without considering joule effect. This definition was used in order to better understand that efficiency is most affected by distance and inductor construction than it is by joule effect. This way, RoTE and efficiency are two different physical quantities, but when RoTE is calculated considering joule effect makes RoTE and efficiency one and the same. If joule effect did not exist there were no losses and efficiency would be 100%, but the output power that arrived would still decrease with distance which would result in RoTE loss. Efficiency will be calculated for d = 1cm for better understanding of how RoTE and efficiency can be used almost interchangeably.

$$P_1 = V_1 I_1 = 6.01 \times 0.0839 \approx 0.504\ W$$

$$P_2 = V_2 I_2 = V_2 \frac{\omega M}{R_{L1} + \omega M} I_1 = 6.99 \times \frac{2\pi \times 354000 \times 38 \times 10^{-6}}{0.0762 + 2\pi \times 354000 \times 38 \times 10^{-6}} I_1 =$$

$$= 6.99 \times 0.999 I_1 \approx 6.99 \times 0.0839 \approx 0.586\ W$$

$$\eta = \frac{P_2}{P_1} \times 100\% = \frac{0.586}{0.504} \times 100 \approx 116\%$$

When losses are not considered in the calculation of V_2 and RoTE:

$$RoTE(0.01) = \frac{V_2}{V_1} \times 100\% = \frac{7.09}{6.01} \times 100 \approx 118\%$$

Thus, if losses are considered in the calculation of RoTE this becomes equal to efficiency.

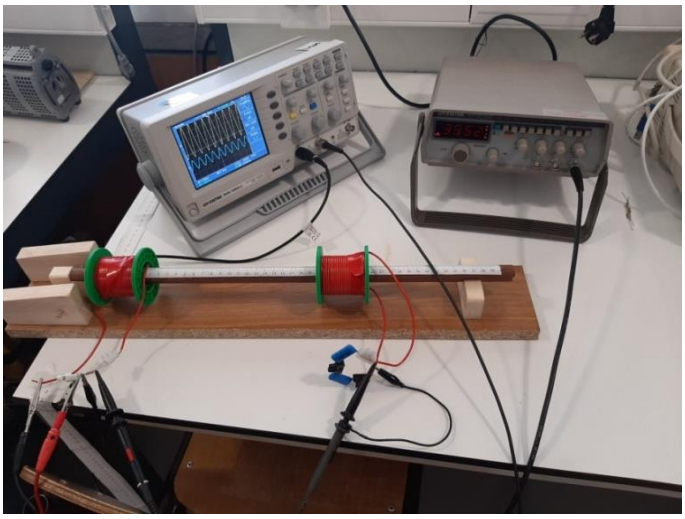

Figure 4.2.4: Equipment for inductor frequency measurement.

Table 4.2.4: Absolute Error for k, M, V_2 and RoTE when L_1=28μH and L_2=30μH

d(cm)	Ek	EM(μH)	EV_2(V)	ERoTE(%)
1	0.506	17.9	2.75	44.2
1.5	0.205	8.15	0.994	15.5
2	0.0746	3.62	0.252	3.35
2.5	0.0767	1.25	0.637	11.4
3	0.131	3.13	0.946	16.4
3.5	0.117	2.93	0.847	14.6
4	0.119	3.14	0.855	14.7
4.5	0.105	2.78	0.756	12.9
5	0.0925	2.49	0.677	11.6
6	0.0733	2.01	0.554	9.45
7	0.0591	1.64	0.465	7.90
8	0.0505	1.41	0.411	6.97
9	0.0445	1.25	0.373	6.32
10	0.0363	1.03	0.323	5.46
11	0.0301	0.853	0.284	4.80
12	0.0259	0.735	0.258	4.36
13	0.0209	0.594	0.228	3.84
14	0.0193	0.550	0.218	3.67
15	0.0178	0.506	0.208	3.50
16	0.0160	0.456	0.197	3.31
17	0.0141	0.403	0.156	3.12
18	0.0122	0.347	0.174	2.91
19	0.0101	0.290	0.161	2.70
20	0.00918	0.262	0.155	2.60

$$Ek(0.01) = |kcalc(0.01) - kobt(0.01)| = 1.20 - 0.694 = 0.506$$

$$EM(0.01) = |Mcalc(0.01) - Mobt(0.01)| = 38.0 - 20.1 = 17.9\ \mu H$$

$$EV_2(0.01) = |V_2calc(0.01) - V_2obt(0.01)| = 6.99 - 4.24 = 2.75\ V$$

$$ERoTE(0.01) = |RoTEcalc(0.01) - RoTEobt(0.01)| = 116 - 71.8 = 44.2\ \%$$

Table 4.2.5: Relative Error for k, M, V_2 and RoTE when L_1=28µH and L_2=30µH

d(cm)	ERROk(%)	ERROM(%)	ERROV$_2$(%)	ERRoTE(%)
1	72.9	89.1	64.9	61.6
1.5	33.8	46.4	26.8	24.6
2	16.2	27.1	8.93	7.02
2.5	17.7	9.96	24.0	25.4
3	34.9	28.8	41.3	42.3
3.5	40.6	35.1	48.2	49.1
4	49.2	44.4	57.4	58.2
4.5	53.2	48.9	63.0	63.7
5	57.1	53.0	68.4	69.0
6	63.3	59.8	78.4	78.8
7	68.1	65.1	87.8	88.0
8	72.8	70.2	97.0	97.0
9	76.7	74.5	105	105
10	78.4	76.4	114	114
11	80.0	78.1	123	123
12	81.6	79.9	133	133
13	81.9	80.2	146	145
14	83.9	82.4	155	154
15	85.4	84.1	164	163
16	86.5	85.2	175	173
17	87.1	85.9	188	186
18	87.3	86.1	204	202
19	87.1	85.9	227	225
20	87.7	86.5	243	240

$$ERROk(0.01) = \frac{Ek(0.01)}{kobt(0.01)} \times 100\% = \frac{0.506}{0.694} \times 100 \approx 72.9\ \%$$

$$ERROM(0.01) = \frac{EM(0.01)}{Mobt(0.01)} \times 100\% = \frac{17.9}{20.1} \times 100 \approx 89.1\ \%$$

$$ERROV_2(0.01) = \frac{EV_2(0.01)}{V_2obt(0.01)} \times 100\% = \frac{2.75}{4.24} \times 100 \approx 64.9\ \%$$

$$ERRoTE(0.01) = \frac{ERoTE(0.01)}{RoTEobt(0.01)} \times 100\% = \frac{44.2}{71.8} \times 100 \approx 61.6\ \%$$

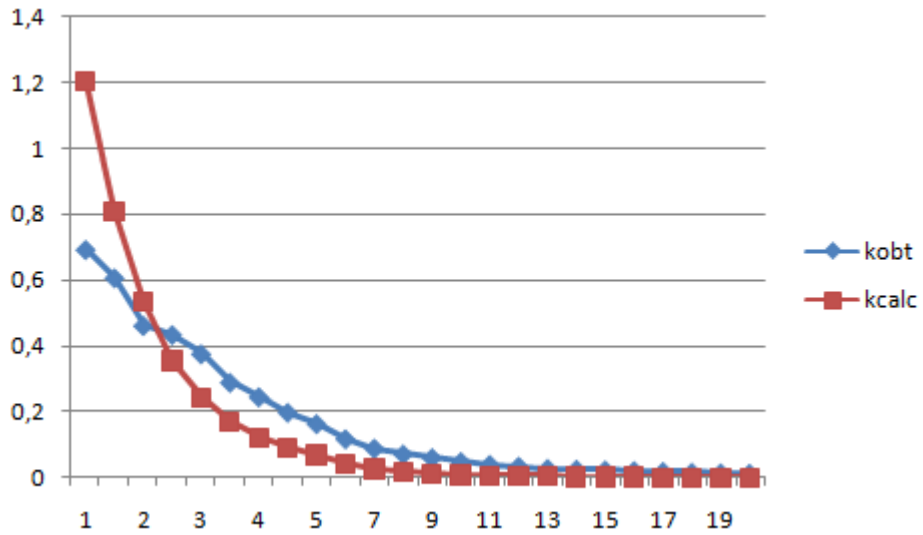

Figure 4.2.5: Comparison between calculated and obtained k when L_1=28μH and L_2=30μH. y-axis is dimensionless and x-axis in cm.

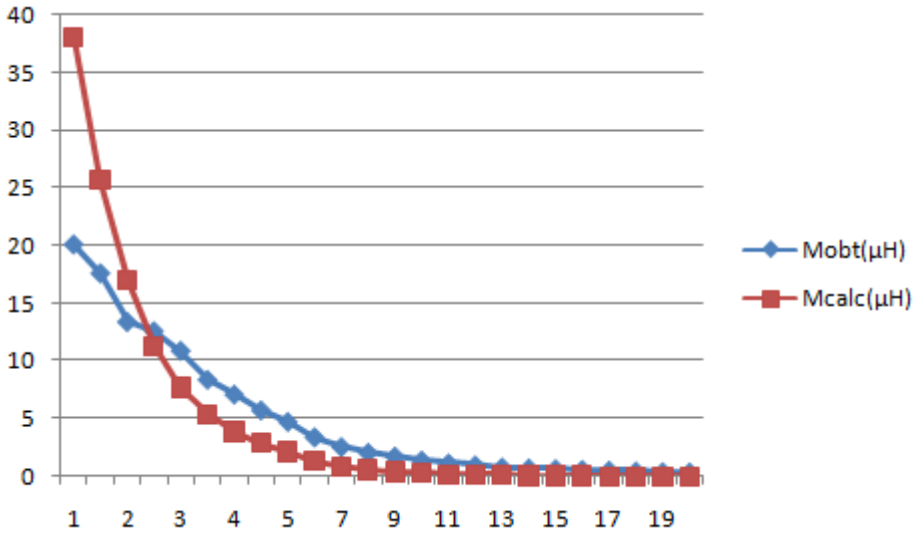

Figure 4.2.6: Comparison between calculated and obtained M when L_1=28μH and L_2=30μH. y-axis in μH and x-axis in cm.

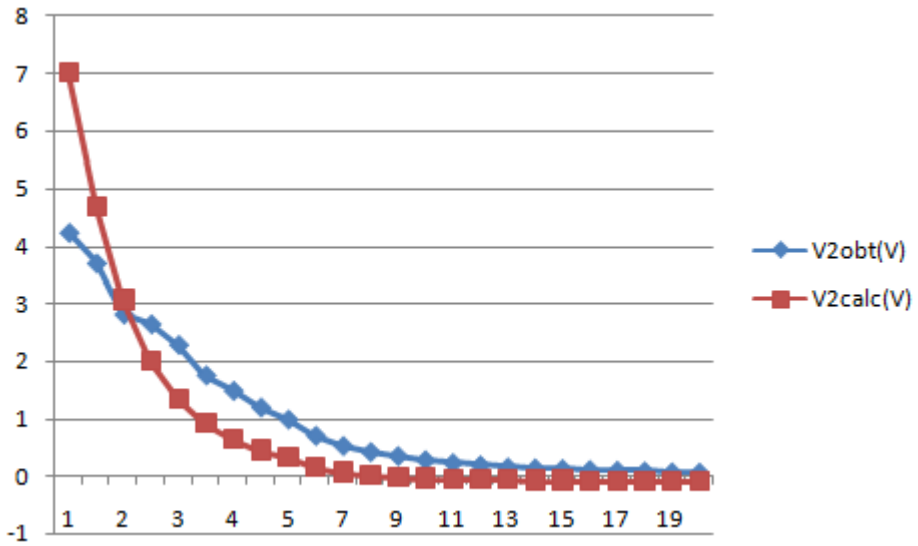

Figure 4.2.7: Comparison between calculated and obtained V_2 when L_1=28µH and L_2=30µH. y-axis in V and x-axis in cm.

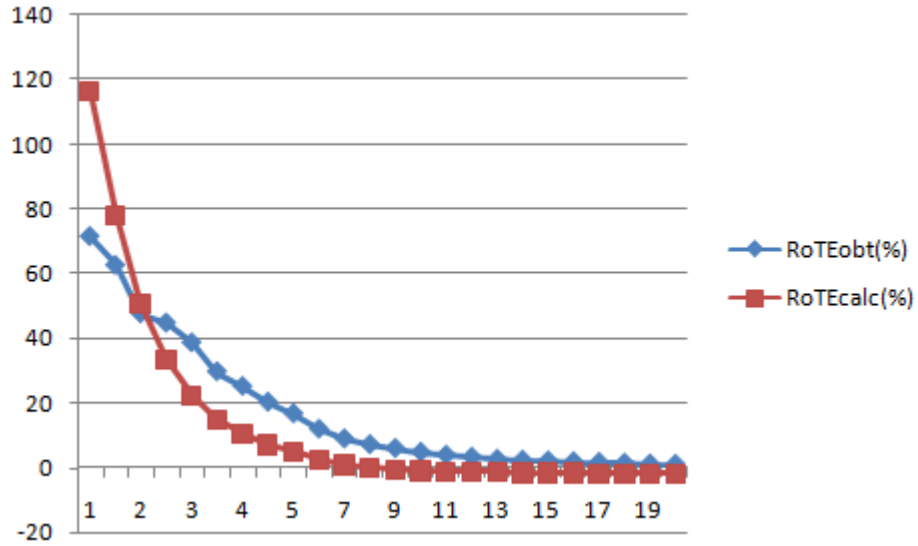

Figure 4.2.8: Comparison between calculated and obtained RoTE when L_1=28µH and L_2=30µH. y-axis in % and x-axis in cm.

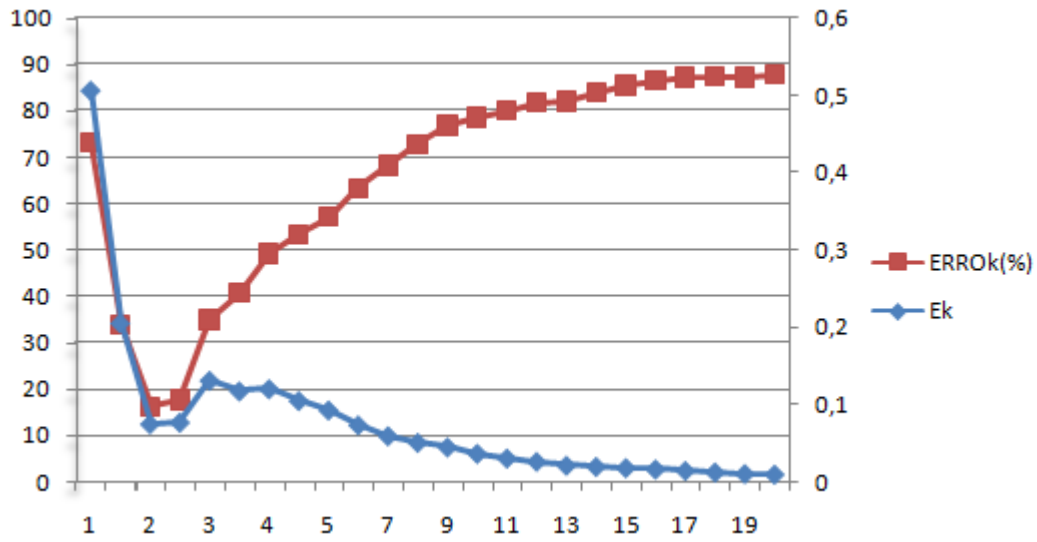

Figure 4.2.9: Comparison between relative and absolute error for k when L_1=28μH and L_2=30μH. y-axis in left in %, y-axis in right is dimensionless and x-axis in cm.

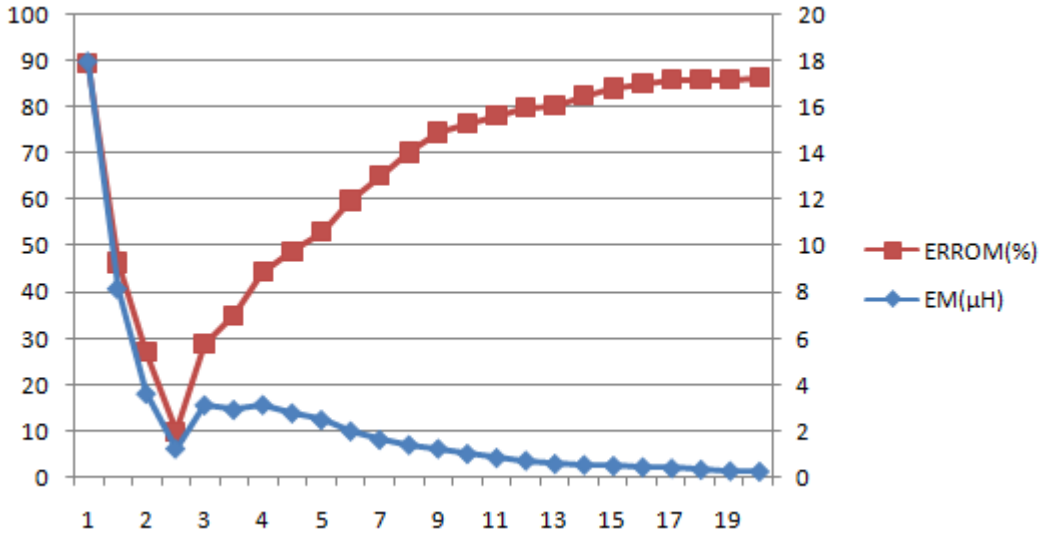

Figure 4.2.10: Comparison between relative and absolute error for M when L_1=28μH and L_2=30μH. y-axis in left in %, y-axis in right in μH and x-axis in cm.

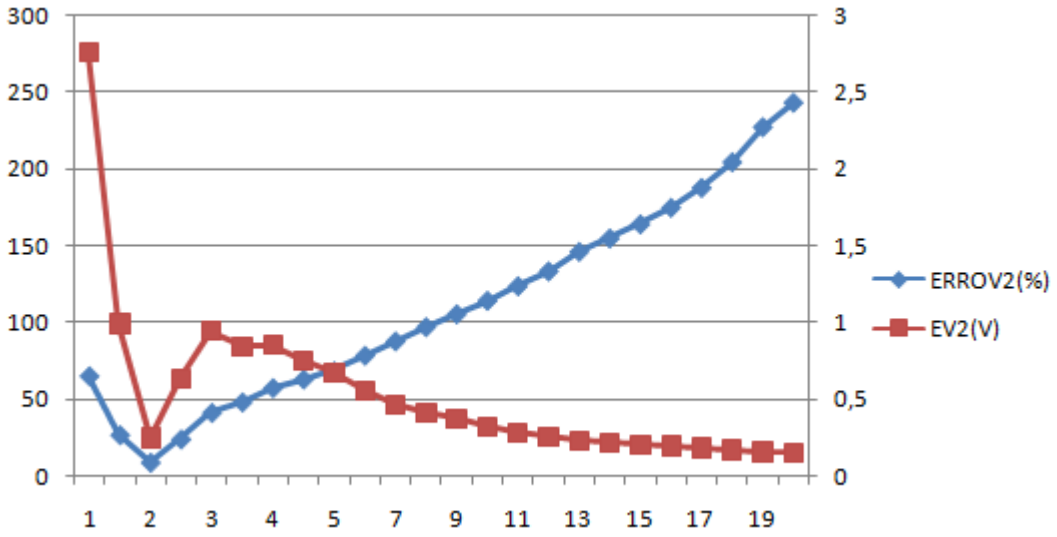

Figure 4.2.11: Comparison between relative and absolute error for V_2 when L_1=28µH and L_2=30µH. y-axis in left in %, y-axis in right in V and x-axis in cm.

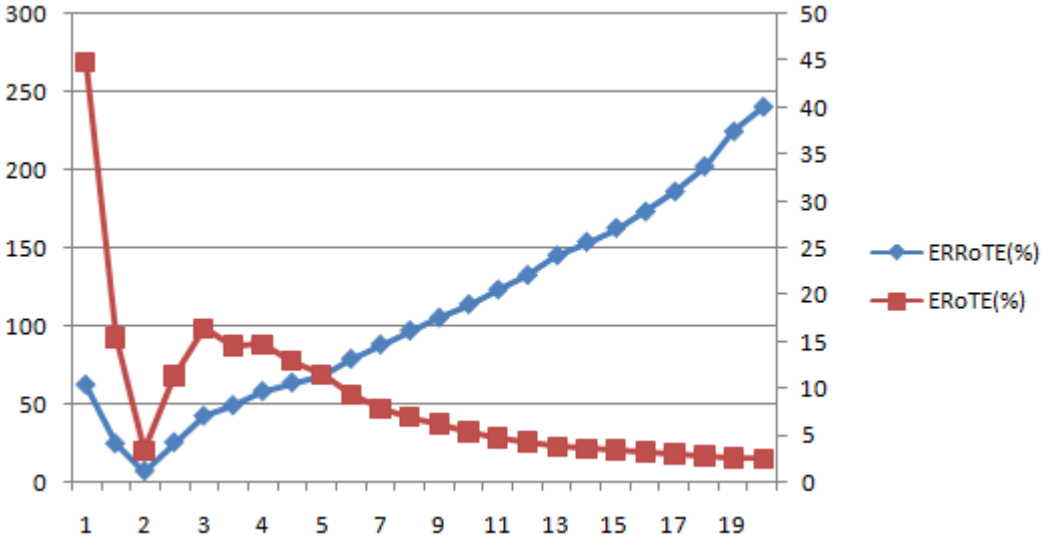

Figure 4.2.12: Comparison between absolute and relative error for RoTE when L_1=28µH and L_2=30µH. y-axis in left in %, y-axis in right in % and x-axis in cm.

Results obtained for coils with L_1=124μH and L_2=126μH shall be analyzed next:

Table 4.2.6: Obtained values for k, M, V_2 and RoTE when L_1=124μH and L_2=126μH

d(cm)	V_2(V)	V_1(V)	f(Hz)	I_1(A)	kobt	Mobt(μH)	RoTEobt(%)
1	8.80	9	23393	0.490	0.976	122	98.6
2	8.32	9	27893	0.411	0.923	115	93.1
3	8.00	9	30935	0.371	0.887	111	89.4
4	7.84	9	33178	0.346	0.869	109	87.6
5	7.28	9	39054	0.294	0.806	101	81.3
6	6.80	9	42777	0.269	0.753	94.1	75.9
8	4.88	9	50060	0.230	0.540	67.5	54.4
10	3.44	9	55199	0.209	0.380	47.6	38.4
12	2.74	9	17189	0.665	0.305	38.2	30.8
14	2.74	9	17191	0.665	0.305	38.2	30.8
16	2.72	9	17201	0.664	0.303	37.9	30.6

d(cm)	f.I_1	exactI_2(A)	P_1(W)	η(%)	η*(%)
1	11457	0.486	4.41	97.8	97.0
2	11472	0.408	3.70	92.4	91.8
3	11480	0.369	3.34	88.9	88.3
4	11485	0.344	3.12	87.1	86.5
5	11495	0.293	2.65	80.9	80.4
6	11500	0.267	2.42	75.6	75.1
8	11507	0.228	2.07	54.2	53.8
10	11511	0.207	1.88	38.2	37.9
12	11424	0.641	5.98	30.4	29.4
14	11424	0.641	5.98	30.4	29.4
16	11424	0.641	5.98	30.2	29.2

The values in table 4.2.6 are obtained similarly as in table 4.2.2. There are physical quantities in this table for better understanding of the physical phenomena involved. Again, all calculations will be done for d=1cm. The other values are calculated the same way but distance, d, changes. All distances used in calculations were converted to meters.

V_2 is obtained in appendix A figureB1 in by dividing the peak-to-peak voltage by 2 to obtain the amplitude, and then dividing by square root of 2 to get the rms value. V_1 is 9 V.

$$V_2 = \frac{peak - to - peak}{2\sqrt{2}} = 8.80\ V$$

$$I_1 = \frac{V_1}{R_{L1}+\omega L_1} = \frac{9}{0.15+2\times\pi\times23393\times124\times10^{-6}} \approx 0.490\ A$$

$$M = \frac{V_2}{\omega I_1} = \frac{8.80}{2\times\pi\times23393\times0.490} \approx 122\ \mu\text{H}$$

$$k = \frac{M}{\sqrt{L_1 L_2}} = \frac{122\times10^{-6}}{\sqrt{124\times10^{-6}\times126\times10^{-6}}} \approx 0.976$$

$$RoTE(\%) = k\sqrt{\frac{L_2}{L_1}} \times 100\ \% = 0.976 \times \sqrt{\frac{126\times10^{-6}}{124\times10^{-6}}} \times 100 \approx 98.4\ \%$$

The other values are calculated by repeating the process described only changing the value of the peak-to-peak voltages for each distance according to appendix A, figuresB2 to B11.

In this case the frequency adjustment produced a larger frequency range that is roughly from 17 KHz to 55 KHz. This changed the current in the primary. The input voltage was kept the same but the distances with higher frequencies had lower current and the ones with lower frequencies had higher current. As it can be seen in equation $V_1 = (R_{L1}+j\omega L_1).I_1$, as frequency increases or decreases the primary current decreases or increases, respectively, and primary voltage is kept constant. This can also be verified by multiplying frequency by primary current. If it produces an approximately equal constant for all distances the input voltage is maintained constant, even though the input power does not. This fact made the input power vary but this does not compromise the experience. Equation (3.1.18) as already shown that I_2 is approximately equal to I_1 when $\omega M >> R_{L1}$. Thus, simply dividing V_2* by V_1 can be used to calculate efficiency and V_2/V_1 can be used to calculate RoTE.

For calculating V_2calc losses need to be subtracted in order to compare with V_2obt due to the fact that obtained V_2 already has losses included, as seen earlier.

Due to frequency being lower than in the previous experience the exact value of I_2 was used, even though for most values the approximate value is near the real one.

$$I_2(0.01) = \frac{\omega M}{R_{L1}+\omega M} I_1(0.01) = \frac{2\pi\times23393\times122\times10^{-6}}{0.15+2\pi\times23393\times122\times10^{-6}} I_1 \approx 0.992 I_1 \approx 0.486\ A$$

ŋ and ŋ* correspond to efficiency. The first happens when equation (3.1.18) is considered and consequently $I_2=I_1$. When equation (3.1.18) requirements are not fulfilled the exact value of I_2 can be used.

$$\text{ŋ}(\%) = \frac{P_2}{P_1}\times100\% = \frac{V_2 I_2}{V_1 I_1}\times100 \approx \frac{V_2 \cancel{I_1}}{V_1 \cancel{I_1}}\times100 = \frac{V_2}{V_1}\times100$$

$$\eta^*(\%) = \frac{P_2}{P_1} \times 100\% = \frac{V_2 I_2}{V_1 I_1} \times 100 \approx \frac{V_2 \frac{\omega M}{R_{L1} + \omega M} \cancel{I_1}}{V_1 \cancel{I_1}} \times 100 = \frac{V_2}{V_1} \frac{\omega M}{R_{L1} + \omega M} \times 100$$

$$\eta(\%)_{(0.01)} = \frac{8.80}{9} \times 100 \approx 97.8\ \%$$

$$\eta^*(\%)_{(0.01)} = \frac{8.80}{9} \frac{2\pi \times 23393 \times 122 \times 10^{-6}}{0.15 + 2\pi \times 23393 \times 122 \times 10^{-6}} \times 100 \approx 97.0\ \%$$

As it is shown, it is not a great difference. But if a relatively long range want to be measured η* will be slightly more precise.

Table 4.2.7: Calculated values for k, M, V_2 and RoTE when L_1=124μH and L_2=126μH

d(cm)	kcalc	Mcalc(μH)	V_2calc(V)	RoTEcalc(%)
1	1.20	152	10.5	117
2	0.536	68.1	4.61	51.2
3	0.244	31.0	2.01	22.3
4	0.124	15.7	0.938	10.4
5	0.0696	8.84	0.453	5.03
6	0.0425	5.40	0.211	2.35
8	0.0189	2.40	0.000911	0.0101
10	0.0100	1.27	-0.0784	-0.872
12	0.00585	0.743	-0.115	-1.28
14	0.00371	0.471	-0.135	-1.49
16	0.00250	0.318	-0.145	-1.61

$$\frac{h}{D} = \frac{4.8}{1.8 \times 2} = 1.333$$

$$K_L = -0.0002 \times 1.333^4 + 0.0055 \times 1.333^3 - 0.0571 \times 1.333^2 + 0.2558 \times 1.333 + 0.4912 \approx 0.7432$$

$$k(0.01) \approx \frac{\sqrt{h_1 h_2}}{2\sqrt{K_{L1} K_{L2}}} r_1 r_2 \frac{1}{(d^2 + {r_1}^2)^{\frac{3}{2}}} =$$

$$= \frac{\sqrt{0.048 \times 0.048}}{2\sqrt{0.7432 \times 0.7432}} 0.018 \times 0.018 \frac{1}{(0.01^2 + 0.018^2)^{\frac{3}{2}}} =$$

$$= 1.0463 \times 10^{-5} \times \frac{1}{(0.01^2 + 0.018^2)^{\frac{3}{2}}} \approx 1.20$$

$$L_1 = \pi\mu_0 \frac{{N_1}^2}{h_1} {r_1}^2 K_{L1} = \pi \times 4\pi \times 10^{-7} \times \frac{80^2}{0.048} \times 0.018^2 \times 0.7432 \approx 127\ \mu H$$

$$M(0.01) \approx \frac{\pi\mu_0 N_1 N_2 {r_1}^2 {r_2}^2}{2(d^2+{r_1}^2)^{\frac{3}{2}}} = \frac{\pi\times 4\pi\times 10^{-7}\times 80\times 80\times 0.018^2\times 0.018^2}{2} \frac{1}{(0.01^2+0.018^2)^{\frac{3}{2}}} =$$

$$= 1.32 \times 10^{-9} = \frac{1}{(0.01^2+0.018^2)^{\frac{3}{2}}} = k(0.01) \times \sqrt{L_1 L_2} =$$

$$= 1.20 \times \sqrt{127 \times 10^{-6} \times 127 \times 10^{-6}} \approx 152\ \mu H$$

Again, if an imposed frequency can be used for calculating, but in the case where the parasitic capacity is used it is a good practice to measure the frequency first. Due to the fact that the lowest values for frequency are around 20 kHz consider this value for frequency.

$$I_1 = \frac{V_1}{R_{L1} + \omega L_1} = \frac{9}{0.15 + 2 \times \pi \times 20000 \times 127 \times 10^{-6}} \approx 0.559\ A$$

$$V_2(0.01) \approx \frac{\pi^2 f I_1 \mu_0 N_1 N_2 {r_1}^2 {r_2}^2}{(d^2 + {r_1}^2)^{\frac{3}{2}}} = M(0.01) \times 2\pi \times f \times I_1 = 152 \times 10^{-6} \times 2\pi \times$$

$$\times 20000 \times 0.559 \approx 10.7\ V$$

This value does not consider losses. When losses are considered:

$$V_2(0.01) = M(0.01) \times 2\pi \times f \times I_1 - (R_{L1} + R_{L2}) I_1 =$$

$$= 152 \times 10^{-6} \times 2\pi \times 20000 \times 0.559 - (0.15 + 0.15) \times 0.559 \approx 10.5\ V$$

$$RoTE(0.01) \approx \frac{1}{2} \frac{N_2}{N_1} \frac{h_1}{K_{L1}} {r_2}^2 \frac{1}{(d^2 + {r_1}^2)^{\frac{3}{2}}} = k \sqrt{\frac{L_2}{L_1}} \times 100\% = \frac{V_2}{V_1} \times 100\% =$$

$$= \frac{10.5}{9} \times 100 \approx 117\%$$

Again, note that V_2 used for the calculation of RoTE already has losses included. Thus, RoTE calculated is the same as efficiency and both terms can be used interchangeably. If the value for V_2 used is the value without losses, RoTE will be slightly higher than efficiency. If input power was increased several times as a way to increase range losses would also increase and even though both RoTE and efficiency would be higher for the same distance when compared with the input power used, the difference between RoTE calculated without losses and efficiency would be higher. This means that even though input power can be used to increase range until a certain point it is not a proper method to increase range endlessly, and for that reason, bigger coils, with higher radius and increased number of turns should also be used. In practice, a compromise between inductor size, price and input power needs to be achieved.

$$\eta(\%)_{(0.01)} = \frac{10.5}{9} \times 100 \approx 117\ \%$$

$$\eta^*(\%)_{(0.01)} = \frac{10.5}{9} \frac{2\pi \times 20000 \times 152 \times 10^{-6}}{0.15 + 2\pi \times 20000 \times 152 \times 10^{-6}} \times 100 \approx 116\ \%$$

Again, η and η* do not create a great difference but for relatively long range η* is slightly more precise. When losses are considered in the calculation of the rate of energy transferring RoTE and η can be used interchangeably.

The tables for the absolute and relative errors for inductors with L_1=124μH and L_2=126μH are not present due to the fact that they are done with the same formulas used in table 4.2.4 and table 4.2.5. The tables 4.2.4 and 4.2.5 were used to produce the figures 4.2.11 to 4.2.18 in order to better understand the behavior of k, M, V_2 and RoTE with distance and if the mathematical models can be used or not to predict the behavior of those characteristics.

Furthermore, the relative errors observed in tables 4.2.4 and 4.2.5 are considerable, even with matched coils and for that reason more will be explained in subsection 4.3.

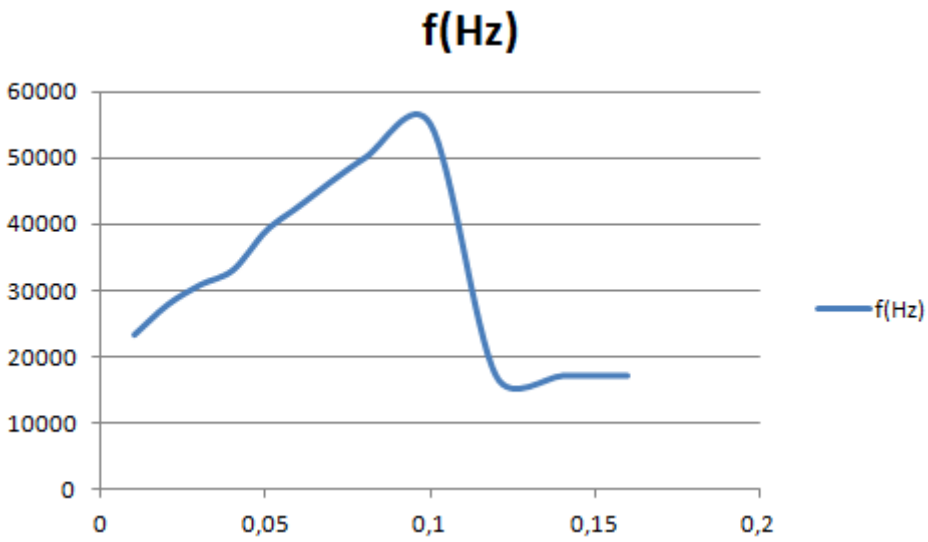

Figure 4.2.13: Frequency adjustment for L_1=124μH and L_2=126μH

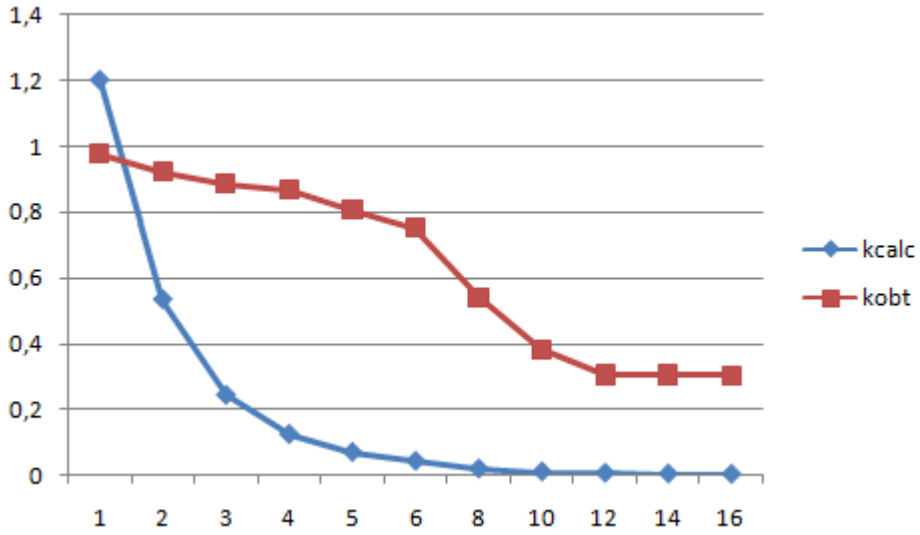

Figure 4.2.14: Comparison between obtained and calculated k when L_1=124µH and L_2=126µH. y-axis is dimensionless and x-axis in cm.

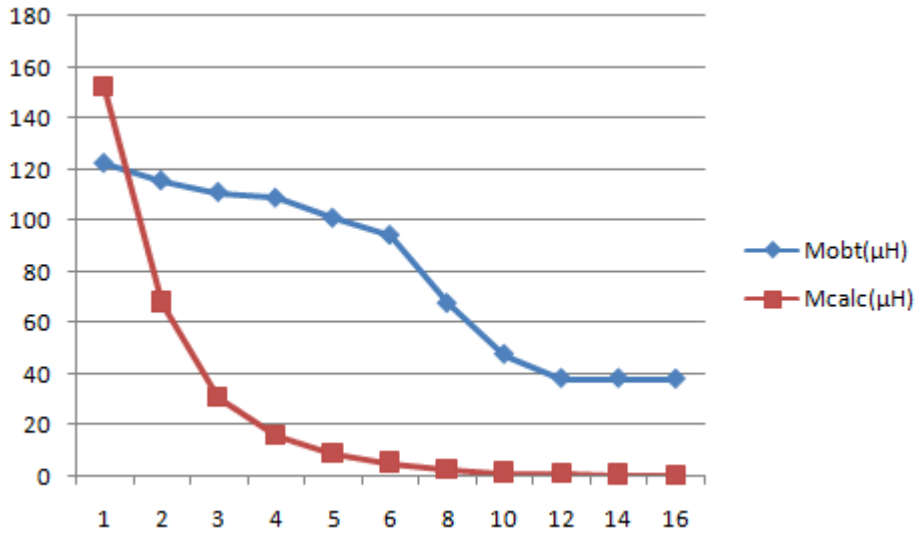

Figure 4.2.15: Comparison between calculated and obtained M when L_1=124µH and L_2=126µH. y-axis in µH and x-axis in cm.

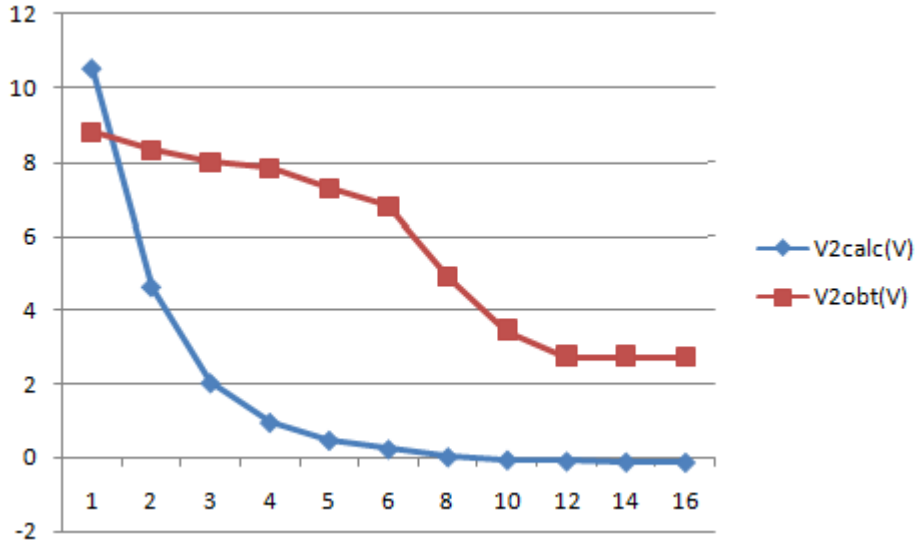

Figure 4.2.16: Comparison between obtained and calculated V_2 when L_1=124µH and L_2=126µH. y-axis in V and x-axis in cm.

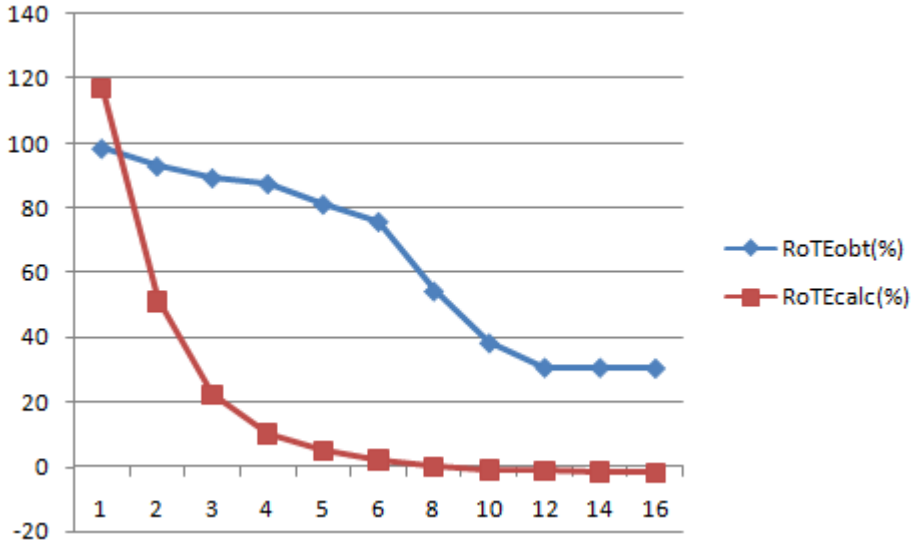

Figure 4.2.17: Comparison between calculated and obtained M when L_1=124µH and L_2=126µH. y-axis in % and x-axis in cm.

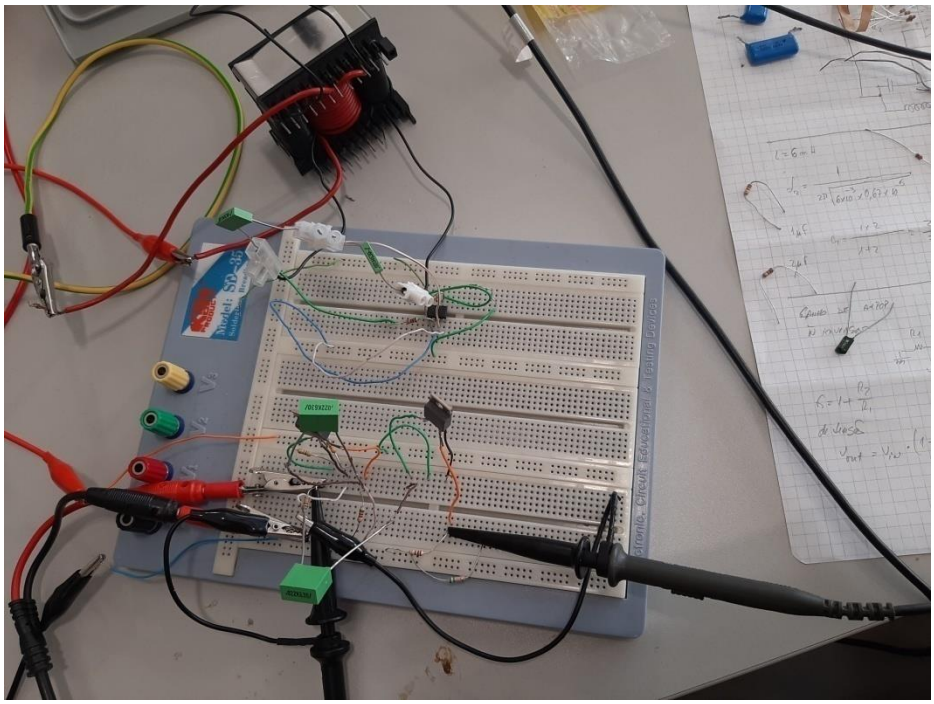

Figure 4.2.18: Prototype blocks before primary inductor.

The prototype was built using the Colpitts oscillator and amplifier linked to the primary inductor which is held on the support with the graduated axis in Figure 4.2.4. While the primary inductor was held stationary the secondary was moved along a distance d and the voltage at the second inductor's terminals was measured using an oscilloscope. Figure 4.2.18 shows the blocks linked to the primary coil including MCR used for frequency adjustment.

Simulations can be useful for more detailed information about the functioning of a full system and test the blocks designed, firstly, one by one, and then all blocks added together. Small changes in block`s components made to achieve the best possible performance can result in time consuming calculations in a theoretical approach, but easily achieved with try and error method in simulations.

4.3 Discussion

In general, the results show that the mathematical model for predicting the behavior of k, M, V_2, RoTE and efficiency with distance can be used to plan and design a WPT system for having a given output power for a determined distance, even though the relative errors achieved are relatively high and some aspects have to be taken in consideration.

The main purpose of the model is to find the output for a given distance. The system can be built to work where RoTE and global efficiency are high or compensate low rate of transferred energy with input power or even constructing inductors with larger inductances and smaller capacities that have higher frequency which result in inductors that occupy more space but have better performance. As explained earlier, input power can be used to increase range until a certain point where losses become too high and after that point inductors with larger inductances and smaller parasitic capacity should be used to increase range and overall performance.

Both the matched pair of inductors that have L_1=28µH, L_2=30µH, C_{d1}=7.31nF, C_{d2}=6.93nF, R_{L1}=85mΩ, R_{L2}=86mΩ, Z_{01}=61.9Ω and Z_{02}=65.8Ω and the mismatched pair of inductors that have L_1=124µH, L_2=126µH, C_{d1}=511nF, C_{d2}=502nF, R_{L1}=0.169Ω, R_{L2}=0.171Ω, Z_{01}=15.6Ω and Z_{02}=15.8Ω achieved similar values for inductance and resistance when compared with the theoretical values of 31.7 µH and 76.2mΩ for the matched pair and 127 µH and 0.15Ω for the mismatched one.

On the other hand, for both cases the parasitic capacities are higher than calculated, and as a consequence the characteristic impedances and frequencies differ from theory, due to the proposed model for calculating parasitic capacities being an approximation and not having in consideration that each turn creates capacities with different values due to distance, electric potential difference of each turn in the neighborhood of others and the non uniformity of electrical charge in the coil. The way coils are winded up can also make difference in the parasitic capacity. The already complex model for calculating parasitic capacities would become even more complex if it was reconsidered.

Comparing the four models analyzed in section 3 for calculating the parasitic capacities with the obtained values all models fail to reach the exact value of the parasitic capacity even though the proposed model achieved the best results. The parasitic capacities calculated with equation (2.3.2) and (2.3.5), Medhurst model, modified Medhurst and proposed model are 1.1pF, 124.06pF, 259.16pF and 2.31nF for the matched inductors and 2.3pF, 124.06pF, 259.16pF and 18.56nF for the mismatched inductors, respectively, while the obtained values were 7.31nF and 6.93nF for the matched pair and 511nF and 502nF for the mismatched pair, respectively.

As observed, for the matched pair the error of parasitic capacity calculation is of one order of magnitude while for the mismatched it is of two orders of magnitude when comparing the obtained values for parasitic capacities and the values calculated with the proposed model. This is consistent with theory because the model tries to calculate the capacity of one turn firstly and then the value is multiplied by the number of turns. Therefore, the error of calculation of the capacity of one turn, which is unknown, is multiplied by the number of turns which results in a greater error. This resulted in a difference between the calculated and obtained values for

frequency. For the matched pair 588 145 Hz were calculated while the obtained value was approximately 354 kHz and for the mismatched pair 103 664 Hz were calculated while the obtained value was approximately 20 kHz.

Due to the error of the calculated capacities, initially the matching changed between the two pairs of inductors because the calculated value for the characteristic impedance of the matched pair was 117.1Ω but the obtained value was around 65Ω while for the mismatched pair was 82.3Ω for the calculated value and between 15Ω and 16Ω for the obtained value. It is noteworthy that a perfect matching is hard to obtain even if the model achieved the exact result because when dimensioning the inductors the number of turns, height and radius, as well as wire thickness and dielectric properties and thickness of the wire coating influences inductance and capacity, and as a consequence, frequency and characteristic impedance.

Even though the proposed model is far from perfect and modifications can be considered the problem of prediction of parasitic capacity can be solved by choosing a capacity ten or a hundred times superior to the value calculated with the proposed model and that gives predictability but frequency is decreased. Thus, coils can be constructed with a safety margin for parasitic capacity or can be made to work on a higher frequency on purpose because that frequency will decrease after adding an external capacity.

The mathematical model for k, M, V_2 and RoTE achieved curves that were inferior to the obtained values in almost all points except for the values where the secondary inductor is almost leaning to the primary inductor. The points where k, M, V_2 and RoTE have less relative error is the range of points with best performance which happens approximately when these functions start to drop, which correspond to the best working range. That does not mean that the working range must be necessarily at MEET point, though. Working range can be further from MEET depending on factors such as needed output power, RoTE or efficiency and input power can even be used to compensate low RoTE and efficiency until a certain point. If the inductors are suitable for the specific application the input power does not necessarily must be kept constant, it can be increased or decreased depending on the secondary inductor position.

By analyzing the relative errors in figures 4.2.9, 4.2.10, 4.2.11 and 4.2.12 it becomes clear that as distance increases the relative error increases which means that at MEET point the relative error is minimum and as the secondary gets far away from the primary the relative error increases.

However, the relative errors are relatively low for the peak of the performance and are high for the zone where the secondary becomes out of range, and thereby, of less interest. This is consistent with absolute errors given by the same figures, where the absolute error decreases with the distance, which means that for long range the model is relatively far from the obtained values but the difference is not much and happens in the zone where transmission should cease.

The minimum and maximum relative errors for k, M, V_2 and RoTE are between 16.2% and 87.7%, 9.96% and 86.5%, 8.93% and 243%, 7.02% and 240%, respectively, and happen in the points where d is 2cm, 2.5cm, 2cm and 2cm, respectively, which is relatively near $d=\frac{r_1}{\sqrt{2}}$, where is the maximum of M. The maximum relative error was for d=20cm which was the farthest point tested.

Before d=$\frac{r_1}{\sqrt{2}}$ the model achieves k>1, and as a consequence, M, V_2 and RoTE can achieve values greater than the maximum for M, than V_1 and greater than 100% for rate of transferred energy which in practice is impossible. For that reason, values before the maximum of M should be considered as $k \approx 1$, $M \approx \sqrt{L_1 L_2}$, $V_2 \approx V_1$ and RoTE≈100%. The difference between the models and the obtained values is due to the fact that all models were calculated from equation (2.1.7) which is the math model for M and is an approximation made for working in the maximum M, and in this point, the relative errors are low. Thus, the models can be used to understand the behavior of the k, M, V_2 and RoTE with distance because even in the zones where errors are high the curves obtained had better performance than expected from the mathematical models.

By analyzing figures 4.2.3 and 4.2.13 it is seen that the frequency varies between 353650 Hz and 354350 Hz for the matched pair of inductors and between 17 kHz and 55 kHz in the mismatched pair. The first has a variation of less than 1 kHz with frequency adjustment and the second a variation of about 38 kHz. This happened because, as seen in section 2, there are two points in the band, one before and the other after the central frequency which is the resonance frequency, where the transmission has better performance and the adjustment is always made to achieve one of this points for a given distance. As distance varies frequency shifting occurs and for each distance the central frequencies of primary and secondary shift from each other apart until a point there is no transmission or the power that arrives at secondary is too low. If frequency was not adjusted performance would decrease drastically and to achieve always the best performance for a given point the frequency was adjusted manually by regulating the MCR of the Colpitts oscillator that acted as a variable inductor, to stay always at one of those two points. One point comes before the central frequency of the inductor and the other comes after the central frequency. From now on, these two points shall be called the first and second point in the band or simply the first and second points, respectively.

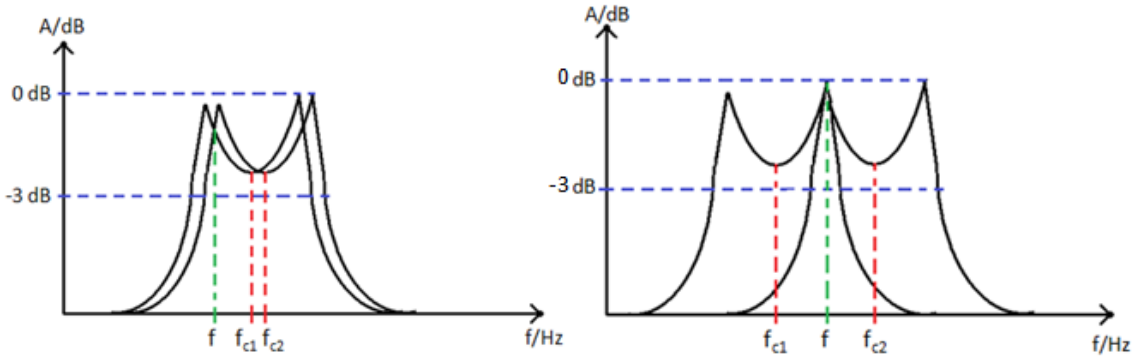

Figure 4.3.1: Work band as frequency shifts.

In the matched pair, the first point was used and as distance varied the frequencies of both coils moved. The transmitter inductor frequency decreased and the receiver increased. Initially both frequencies are almost coincident, but after the receiver becomes farther away the working frequency moves gradually to a point corresponding to both second point of the transmitter and the first point of the receiver. As distance increases the work frequency moves from the first to the second point of the primary while staying always in the first point of the

receiver. Thus, transmission begun in the first point and ended in the second point of the primary while stayed in the first point of the secondary.

If transmission had begun in the second point of the transmitter, as distance varies the central frequencies of both transmitter and receiver would still move, but in this case, the working frequency would correspond to the second point of transmitter and receiver initially, and as frequencies become shifted the working frequency will stay in the second point of the primary coil but will move from the second to the first point of the receiver until a place in the band where transmission should cease.

Due to the fact that the quality factor of the coils varies with k, which in turn varies with distance, the selectivity of the band will also change and it is also difficult to predict what will be the shift of frequencies for both transmitter and receiver. Therefore, frequency shifting can be overcome with the technique used for frequency adjustment but it is unpredictable how much will be the shift.

If the shift is short for a relatively high working frequency the frequency adjustment will be relatively small and k, M, V_2 and RoTE will have curves that will describe the hyperbole similarly to what happened with the matched pair of coils.

In the mismatched pair of inductors, the working frequency shifted more than the matched pair for a lower working frequency which resulted in high variation of performance with distance because in this case, frequency cannot be assumed almost equal in the entire range. Therefore, the curve obtained is not a perfect hyperbole and have a considerable shift in performance in the frequency range where working frequency decreases drastically and slightly better performance where the working frequency increases as distance increases.

The simulated values for V_2 after analyzing tables 4.1.1 and 4.1.2 and figures 4.1.4 to 4.1.7 are near the calculated values, with a difference of 2% or less for between calculated and simulated RoTE. The only exception happens when the calculated value exceeds the maximum theoretical value and in simulations the maximum theoretical value is used instead.

By using the resistance in the simulator V_2 and RoTE can be simulated including losses. Thus, these values can be compared with obtained V_2 and efficiency, respectively.

The calculated values are similar to simulations. The negative value calculated for V_2 simply means that losses at the respective distances do not compensate transmission, even though the error of V_2 increases with distance.

Efficiency is approximately equal to RoTE when $\omega M >> R_{L1}$ and losses are small. By subtracting V_{losses} divided by V_1, which is a small value, to RoTE efficiency is obtained. For that reason the curve of efficiency is approximately equal to RoTE. If input power is overused the losses increase significantly the difference between RoTE and efficiency will also increase, but if proper inductors are built for the desirable range RoTE and efficiency will be near one another and if losses are included in RoTE calculation efficiency and RoTE can be used interchangeably. The factor that most contributes to decrease of efficiency is the distance due to the magnetic field intensity decreasing with the cube of distance.

The mismatched inductors provoked distortion due to the fact that the characteristic impedance was far from 50Ω. The oscillator also contributes with some distortion. Initially, the tests were made to verify if regulating the MCR in the oscillator frequency could be adjusted to resonance, which theoretically happens when reactive energy is nullified and that way distortion would decrease, but that did not happen.

By regulating the magnetic permeability of the MCR, the inductance changes permitting the frequency adjustment of the oscillator and transmission can be maintained but because the inductors were mismatched distortion occurs. With the MCR it is possible to continuously adjust frequency to achieve the best possible results for MEET point due to the fact that there are not discrete jumps between frequencies which could result in point not exactly at MEET.

Firstly, the hypothesis was that the mismatched inductors would act like a filter and just the resonance frequency would be transmitted, and a sinusoidal wave would appear in the receiver, even if the total power was lower. It would be useful to know if power could be transmitted in a case of mismatch because it is hard to find the parasitic capacitance and even though this problem can be solved by adding an external capacity this decreases frequency which degrades the speed of charge and overall performance. The speed of charge is directly proportional to secondary current.

The results show, by analyzing FiguresB1 to B11 of appendix A, that the voltage that appeared in the secondary is not sinusoidal which means that a distorted signal was transmitted. This means that efficiency is not compromised by distortion and there is no loss of power to distortion, even though, after receiving the signal the next blocks would need to accept a distorted signal which in some cases can be compromising or the next blocks should somehow eliminate or at least decrease distortion. Distortion can also be handled by using matched coils that in worst case use an external capacity to impose frequency and matching if the parasitic capacity does not match. The coils can be made with a safety margin for inductance and especially for parasitic capacity in order to obtain a calculated frequency higher than needed and then by adding an external capacity that lowers the work frequency but gives predictability while still guarantying that project specifications are reached.

The amplifier can be used to increase the transmitter inductor`s current without increasing transmitter power and that way the magnetic field intensity increases without need of components that can withstand more power. The amplifier does not necessarily need a buffer stage because its output impedance will enter in parallel with primary inductor impedance which will make, for this amplifier topology, the voltage gain collapse, and as a consequence, the input voltage will achieve its minimum value while the primary current will increase, maintaining input power constant.

The results show that the mathematical models can be used to plan and design a WPT system using resonating coupling coils for a determined range and output power. The inductors should be designed with a margin for inductance and especially for parasitic capacity due to its unpredictability. For more predictability, adding an external capacity to impose the work frequency and matching can be useful to avoid distortion. The coils should be designed for the point where d=$\frac{r_1}{\sqrt{2}}$ and its neighborhood because this is the zone where the mathematical model has less error and is also the peak of performance. In the zone before d=$\frac{r_1}{\sqrt{2}}$ performance should be considered approximately equal to the peak. In the zone after d=$\frac{r_1}{\sqrt{2}}$ performance will be better than the mathematical model prediction but the mathematical model will not give the true performance for this zone, even though transmission can be maintained at least to some point. By voltage control, the magnetic permeability of the inductor of the oscillator can be varied and that way frequency splitting can be overcome. It is hard to predict what will be the

frequency shift but if the range of work frequencies of the oscillator is large enough transmission can be maintained in the maximum efficiency point for each distance.

The theoretical analysis shows that using more than one inductor in primary or secondary do not necessarily enhance performance.

The most limiting factor of a WPT system using resonating coupled coils is the short range. High efficiencies can be obtained with relatively cheap components when compared to other technologies like lasers or others, but range is always short, which can compromise the use of this technology in many applications.

There are applications where this technology can be indispensible. For example, pacemakers need to be charged from time to time and there is need of microsurgeries for recharging which have costs for the patients or for the healthcare systems of countries due increasing man labor of doctors and other specialists to treat these patients. It is not possible or at least not practical, to use a laser and put a solar cell somehow linked to the pacemaker to charge it, but with a small coil inside the pacemaker a transmitter made with this technology can be used to charge it by maintaining the transmitter leaning against the body with a few centimeters of skin away from the pacemaker without need for microsurgeries and saving money used in healthcare systems while giving more quality of life to patients.

4.3.1 The Method to Optimize System Construction

After knowing the project specs, a WPT system can be planned and constructed using the models described in this work. First, it is important to know the range, the output power needed or the speed of charge because the last will dictate how much output power will be needed. Depending on the size needed for the transmitter or receiver, choose NIRC or IRC. For example, if the receiver needs to be small but transmitter does not have hard to achieve restrictions NIRC should be used and depending on the relation between the radiuses of the inductors frequency adjustment may not be needed. If both have size restrictions IRC should be used. Note that the equivalent inductance of IRC is the average of the two different inductances of NIRC. Thus, the models described can even be made for IRC and in the end the relation between the two coils `radiuses can be changed to get NIRC.

By using the models described for k, M, V_2, RoTE and efficiency there are at least two possible ways to know what coils should be constructed. One consists in beginning with two relatively large inductances which may lead to an over dimensioning of the inductors and then using the relations described in section 3 between formulas (3.1.33) and (3.1.34) to change coil parameters, that is radius, height and number of turns in order to have two equal coils suited for intended application. The other consists in beginning with two relatively small inductances even if at start they are under dimensioned and then, by using the same relations, suited inductors for the application can be achieved. Microsoft Excel can be a helpful tool to dimension the coils because all alterations in inductor parameters can automatically change the values obtained for the curves of k, M, V_2 and RoTE without need for manually recalculating them.

After this step, the inductors may still need to change. With the proposed model for calculating parasitic capacity the frequency can be calculated, but not with precision, though. If it is a low power application and frequency wants to be increased, the inductors should have at least a radius equal to range multiplied by square root of two, the height should be increased,

which means that, even with the same number of turns, the coils will have less layers of turns, and increasing the number of turns will also increase the natural resonance frequency. High frequency may compromise the use of NIRC because usually the transmitter coil of NIRCs has large radius, small height, and this way it can be difficult to achieve the same frequency for both, and if that happens, an external capacity needs to be added to the highest frequency coil in order to transmission occur. Dimensioning the inductors can be the most challenging part to do because by changing one inductor parameter, more than one effect can occur, that is, by changing the inductor radius, for example, inductance will increase, but size and parasitic capacity will also increase, and as a consequence, frequency will decrease. Thus, radius, height, number of turns, wire diameter, pitch, dielectric constant of the wire coating, and wire coating thickness should always be taken into account when the coils are being dimensioned.

Table 4.3.1.1 – Inductors Parameters

N_1 – Number of turns of coil 1	p - pitch
N_2 – Number of turns of coil 2	a – wire radius
H_1 – Height of coil 1	ε_r - Relative dielectric constant
H_2 – Height of coil 2	t – wire coating thickness
R_1 – Radius of coil 1	
R_2 – Radius of coil 2	

The inductors should be dimensioned in a way that the working range is equal or lower than transmitter inductor radius divided by square root of two, but this is not mandatory, though. If the range is at a point with low performance, the input power can also be increased to compensate, at least until a certain point. If an increase of input power is overused losses in copper wire will increase too much and that will lead to a great difference between RoTE and efficiency, which can result in low performance, and that is counter-productive. Range should not be increased just by increasing input power but by coil dimensioning as well.

If range is variable between a minimum and maximum, inductors can be dimensioned to the maximum range or to the minimum and then compensated with regulation of input power. For example, increasing input power in the maximum range and decreasing it at minimum. There is also the possibility to find something in between, for example, dimensioning the inductors for the average range and increasing input power slightly, depending on the application and loss increase.

Note that optimizing inductor construction consists in choosing the proper inductor parameters that optimize performance but also size, price, input power needed and other relevant factors for that specific application.

Finally, the other blocks are chosen and dimensioned. Oscillators and amplifiers for the transmitter, and the receiver should have AC/AC converters, AC/DC converters or even both depending on the application. Note that all components need to withstand the current when dimensioning both the blocks and the coils.

The conclusions reached in this work are described in the next and final chapter.

5

CONCLUSIONS AND FUTURE WORK

5.1 Conclusions

To sum up, the obtained curves for k, M, V_2, RoTE and efficiency had better performance than the mathematical models for calculating them. Thus, the models can be used to design and optimize inductor construction for a WPT system using resonating coupled coils for a given distance and to obtain a determined output power.

The mathematical models for calculating inductance and resistance of the inductors work while the four models used to calculate the parasitic capacity failed, even though the proposed model for parasitic capacity calculation achieved the best results.

Using as oscillator that produces a sinusoidal wave with low distortion can maintain its performance for relative long frequency ranges and can be used to overcome frequency splitting phenomenon by varying an inductor or MCR in a continuous way manually or by voltage control.

The matched pair of coils was capable of transmit a sinusoidal wave to the secondary without increasing distortion while the mismatched pair of coils distorted the signal.

The most limiting factors of this technology are the short range and low power applications, even though, there are applications where this technology is indispensable.

Inductor parameters like radius, height, number of turns, wire diameter, pitch, dielectric constant of the wire coating and wire coating thickness have to be considerate when dimensioning the inductors. A change in a coil parameter will produce more than one effect which makes coil dimensioning challenging.

This technology is still not mature enough and there is still further development to be done.

5.2 Future Work

There are several technologies to transfer energy wirelessly that can be used, each with its own advantages and disadvantages, depending on efficiency, design simplicity, costs, power, range and work frequency. Considering just resonating coupling coils some future works can be done.

One consists in WPT systems for car batteries charge. Using this technology implies that enough energy is transferred on time because when considering a receiver in a car and many transmitters in roads the battery needs to charge quick enough when passing by the first transmitter to reach the second one and still have energy under the risk of not reaching the next second transmitter before its energy is depleted. Planning, designing and even testing should be done before creating too long infrastructures with high cost for taxpayers of a country without understanding if the system can or cannot work properly with the fewer transmitters as possible and to withstand high traffic and high speed vehicles that have less time to charge when passing by a transmitter due to high speed.

Works about size decreasing can also be an important contribution when considering pacemakers, for example, due to the fact that they involve human life and well-being. Size decreasing can also be important for saving planet resources, reduce manufacturing costs and make more maneuverable devices as well.

Finally, creating new forms of frequency increase and even frequency control without the need to change the coils once created can be useful not just for increasing efficiency but also to increase range, especially if the systems works with a variable distance. By frequency control it will be possible to extend range further without necessarily increasing input power and losses.

REFERENCES

[1] S. K. Singh, T. S. Hasarmani, "Wireless Transmission of Electrical Power Overview of Recent Research and Development", *International Journal of Computer and Electrical Engeneering*, Vol. 4, No. 2, April 2012.

[2] B. M. Faruk, U. S. Jawarkar, T. G. Pal, A. S. Gugliya, and T. E. Department, "Wireless Power Transfer Electric Vehicle," *Jawaharlal Darda Inst. Eng. Technol.*, vol. 4, 2017, doi: 10.17148/IARJSET.

[3] H. M. Santos, M. R. Pereira, L. M. Pessoa, and H. M. Salgado, "Design and optimization of air core spiral resonators for magnetic coupling wireless power transfer on seawater."

[4] S. Y. R. Hui, W. Zhong, and C. K. Lee, "A critical review of recent progress in mid-range wireless power transfer," *IEEE Transactions on Power Electronics*, vol. 29, no. 9. Institute of Electrical and Electronics Engineers Inc., pp. 4500–4511, 2014, doi: 10.1109/TPEL.2013.2249670.

[5] M. Frivaldsky, P. Spanik, M. Piri, and V. Jaros, "Mutual Inductance of Two Helical Coils-Theory, Calculation, Verification."

[6] D. B. Kshatri, S. Shrestha, and B. Shrestha, "A Brief Overview of Wireless Power Transfer Techniques," *Int. J. Adv. smart Converg.*, vol. 4, no. 2, pp. 1–5, Nov. 2015, doi: 10.7236/ijasc.2015.4.2.1.

[7] J. R. Lucas, "Resonance & Mutual Inductance", Univ. of Moratuwa, Moratuwa, Sri Lanka, 2001.

[8] C. K. Lee, W. X. Zhong, and S. Y. R. Hui, "Effects of magnetic coupling of nonadjacent resonators on wireless power domino-resonator systems," *IEEE Trans. Power Electron.*, vol. 27, no. 4, pp. 1905–1916, 2012, doi: 10.1109/TPEL.2011.2169460.

[9] J. Wang, │mark Leach, │ Eng, G. Lim, Z. Wang, and │yi Huang, "Investigation of Magnetic Resonance Coupling Circuit Topologies for Wireless Power Transmission."

[10] X. L. Huang, H. Qiang, and L. L. Tan, "The Coil Misalignment Model of Inductively Coupled Wireless Power Transfer System: Mutual Inductance Analysis and Transfer Efficiency Optimization."

[11] Y. Han and X. Wang, "Calculation of Mutual Inductance Based on Field-Circuit Coupling Analysis for WPT", in *5th International Conference on Power Electronics Systems and Applications (PESA)*, Harbin, 2013, pp. 1-5.

[12] A. Wasif Reza and N. Kumar, "Efficiency Maximization of Resonant Coupled Wireless Power Transfer System via Impedance Matching Based on Coupling Tuning," 2014. [Online]. Available: https://www.researchgate.net/publication/269405905.

[13] S. Wang et al, "Optimization Analysis of coil configuration and circuit model for asymmetric wireless power transfer system", IET Microwaves, Antennas and Propagation, 2018, Vol. 12, pp. 1132-1139, Jan. 2018.

[14] F. Sodré, "Campo Magnético e Distância", *Revista Brasileira de Física*, Vol.1, no. 2, pp. 325-334, Set 1971.

[15] M. Rehman, Z. Baharudin, P. Nallagownden, and B. Islam, "Modelling and efficiency-analysis of wireless power transfer using magnetic resonance coupling," *Indones. J. Electr. Eng. Comput. Sci.*, vol. 6, no. 3, pp. 563–571, Jun. 2017, doi: 10.11591/ijeecs.v6.i3.pp563-571.

[16] X. Wei, Z. Wang, and H. Dai, "A critical review of wireless power transfer via strongly coupled magnetic resonances," *Energies*, vol. 7, no. 7. pp. 4316–4341, 2014, doi: 10.3390/en7074316.

[17] A. Gopinath.(2013, April). "All About Transferring Power Wirelessly", *Electronics For You* [Online], pp. 52-56, https://www.electronicsforu.com/electronics-projects/electronics-design-guides/transferring-power-wirelessly-2.

[18] University of Michigan--Dearborn., Vehicular Technology Society., IEEE Power Electronics Society., and Institute of Electrical and Electronics Engineers., *5th International IEEE Vehicle Power and Propulsion Conference : September 7-11, 2009, Dearborn, Michigan, USA*.

[19] C. Özdemir and A. N. Mete, “A Frequency-Tracking Algorithm for Inductively Coupled Wireless Power Transfer Systems. M.S. Thesis, Dep. of Elect. and Electron. Eng., Mersin, Turkey, 2017.”

[20] T. L. Floyd, “Chapter 13 RLC Circuits and Resonance”, in *Electronics Fundamentals*, 6e, M. Scardino, Upper Saddle River, New Jersey: Pearson Education, Inc., 2004.

[21] A. E. Vijayan and E. Zurich, “Magnetically Coupled Resonators for Wireless Power Transfer.” [Online]. Available: https://www.researchgate.net/publication/304396671.

[22] A. Agcal, S. Ozcira, and N. Bekiroglu, “Wireless Power Transfer by Using Magnetically Coupled Resonators,” in *Wireless Power Transfer - Fundamentals and Technologies*, InTech, 2016.

[23] W. X. Zhong and S. Y. R. Hui, “Maximum energy efficiency tracking for wireless power transfer systems,” *IEEE Trans. Power Electron.*, vol. 30, no. 7, pp. 4025–4034, Jul. 2015, doi: 10.1109/TPEL.2014.2351496.

[24] M. Al-Saadi, S. Valtchev, and A. Craciunescu, “New Analytical Formulas for Coupling Coefficient of Two Inductively Coupled Ring Coils in Inductive Wireless Power Transfer System Wireless power transfer (WPT) for battery charging View project Development of a Three-Phase Hybrid Unidirectional Rectifier with Boost Converter View project SEE PROFILE.” [Online]. Available: https://www.researchgate.net/publication/338720570.

[25] B. Johns, “An introduction to the Wireless Power Consortium standard and TI’s compliant solutions”, T.I. Inc., Dallas, Texas, Sci. Rep. SLYT401, 2011.

[26] Y. Tanikawa, M. Kato, T. Imura, and Y. Hori, “Experiment of Magnetic Resonant Coupling Three-phase Wireless Power Transfer.”

[27] D. Kimura, S. Member, T. Imura, M. Hiroshi Fujimoto, S. Member, and Y. Hori, “IEEJ International Workshop on Sensing, Actuation, and Motion Control Three-phase Wireless Power Transfer for Dynamic Charging of Electric Vehicle for High Efficiency and Reducing Voltage Unbalancing Considering Magnetic Flux Canceling.”

[28] E. Fernandes, “Transmissão de Potência Sem Fios”, M.S. Thesis, DEEC, FEUP, Porto, Portugal, 2015.

[29] Leopold S., Oisin P., “Concepts for Wireless Energy Transmission Via Laser”, ESA – Advanced Concepts Team, Noordwijk, The Netherlands, ACT-RPR-NRG-2009-SPS-ICSOS, 2009.

[30] Sheng Q. et al, “Adaptative Wireless Power Transfer via Resonant Laser Beam Over Large Dynamic Range”, IEEE INTERNET OF T., vol.10, no10, May, 2023.

[31] Hongzuo L. Et al, “Laser Power Transmission and Its Application in Laser-Powered Electrical Motor Drive: A Review”, Power Electronics and D., vol. 6, no. 41, pp.167-184, Sept., 2021, doi: 10.2478/pead-2021-0010

[32] Rodrigo D. et al, “Limits of WPT through the Human Body using Radio Frequency”, M.S. Thesis, Centro de Investig. em Serv. Dig., Pol. de Viseu, Viseu, Portugal, 2020.

[33] Elena N. Baikova, Stanimir S. Valtchev et al. “Electromagnetic Interference Impact of Wireless Power Transfer System on Data Wireless Channel”, 7th Doctoral Conference on Computing, Electrical and Industrial Systems (DoCEIS), Apr 2016, Costa de Caparica, Portugal. pp.293-301, ff10.1007/978-3-319-31165-4_29ff. ffhal-01438256f

[34] Karina F., Sara L., Peter S., “Interference Risks from Wireless Power Transfer for Electric Vehicles”, FOI, Swedish Defense R. A., Bromma, Sweden, FOI-R--4808--SE ISSN 1650-1942, Dec. 2019.

[35] H. Nagaoka, “The Inductance Coefficient of Solenoids”, Journal of college of Science, Imperial College, Tokyo, Japan, vol. XXVII, article 6, 1909.

[36] D. W. Knight. (2016, May 4) “The self-resonance and self-capacitance of solenoid coils: applicable theory, models and calculation methods”[Online]. Available: http://g3ynh.info/orcid.org/0000-0003-0499-3938

A

APPENDIX

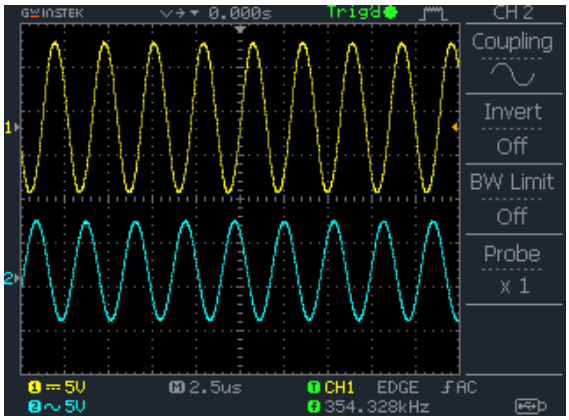

FigureA1:(Blue) V_2(d=1) for L_1=28µH and L_2=30µH

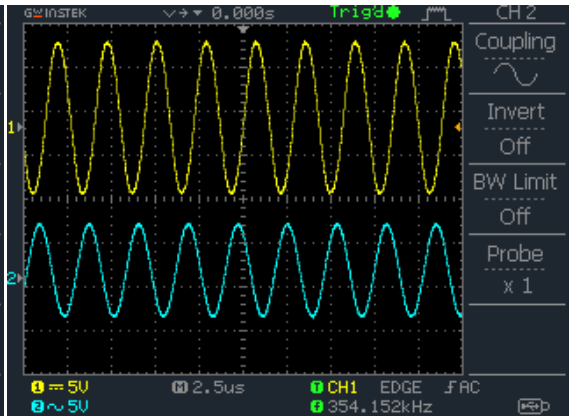

FigureA2:(Blue) V_2(d=1.5) for L_1=28µH and L_2=30µH

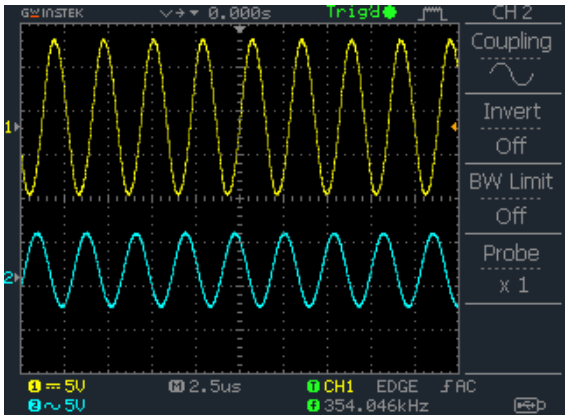

FigureA3:(Blue) V_2(d=2) for L_1=28µH and L_2=30µH

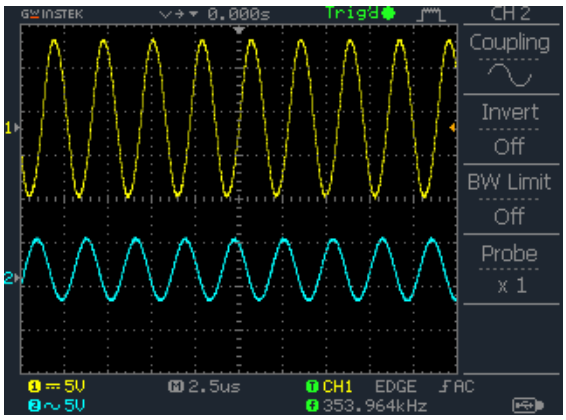

FigureA4:(Blue) V_2(d=2.5) for L_1=28µH and L_2=30µH

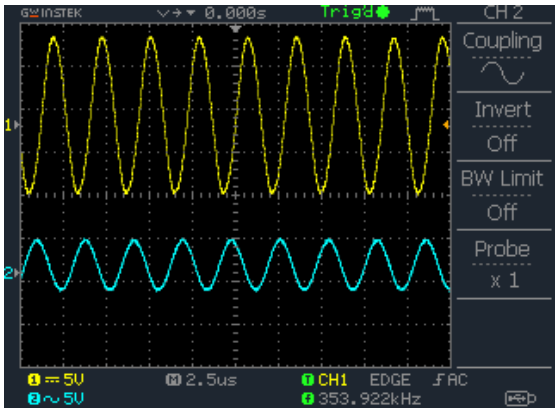

FigureA5:(Blue) V_2(d=3) for L_1=28µH and L_2=30µH

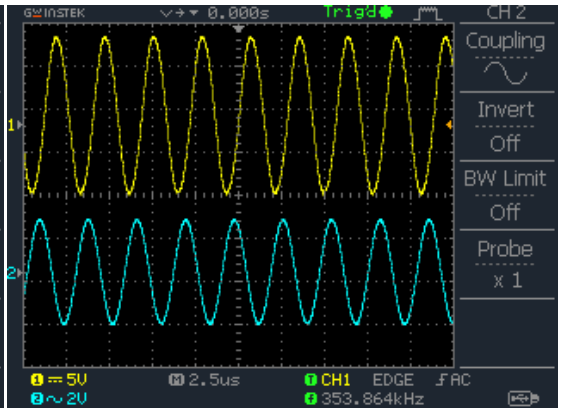

FigureA6:(Blue) V_2(d=3.5) for L_1=28µH and L_2=30µH

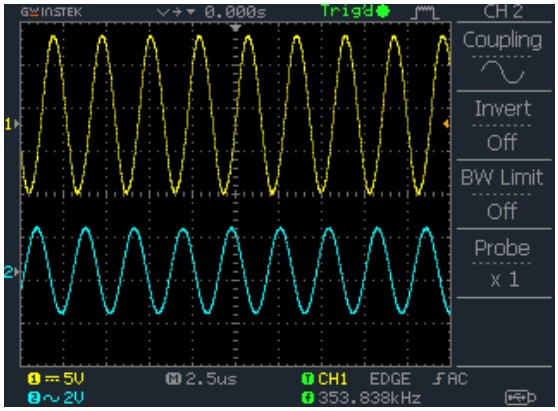

FigureA7:(Blue) V_2(d=4) for L_1=28µH and L_2=30µH

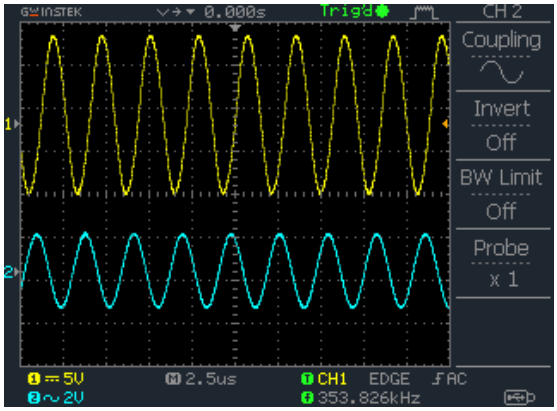

FigureA8:(Blue) V_2(d=4.5) for L_1=28µH and L_2=30µH

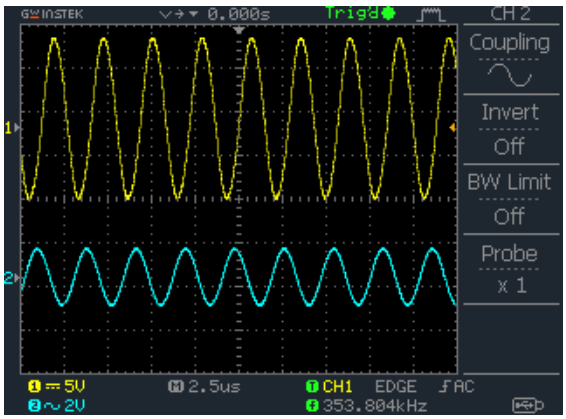

FigureA9: (Blue) V_2(d=5) for L_1=28µH and L_2=30µH

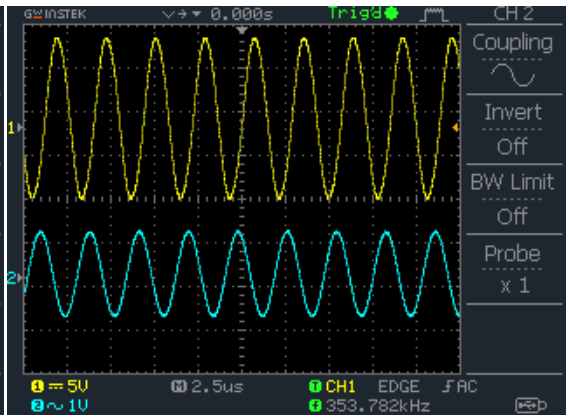

FigureA10: (Blue) V_2(d=6) for L_1=28µH and L_2=30µH

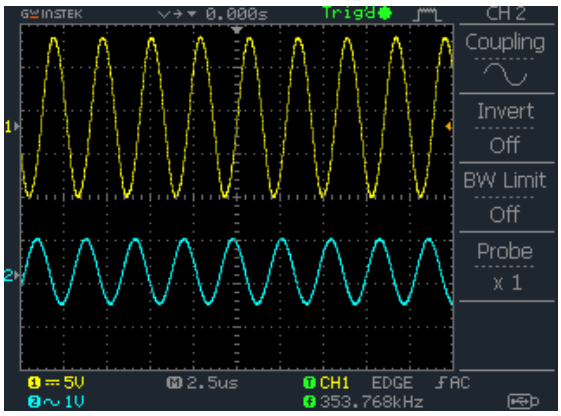

FigureA11: (Blue) V_2(d=7) for L_1=28µH and L_2=30µH

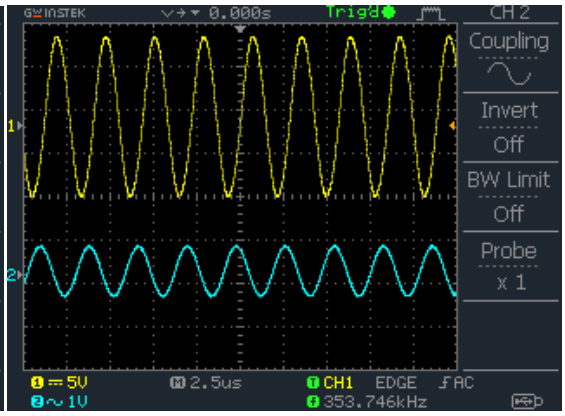

FigureA12: (Blue) V_2(d=8) for L_1=28µH and L_2=30µH

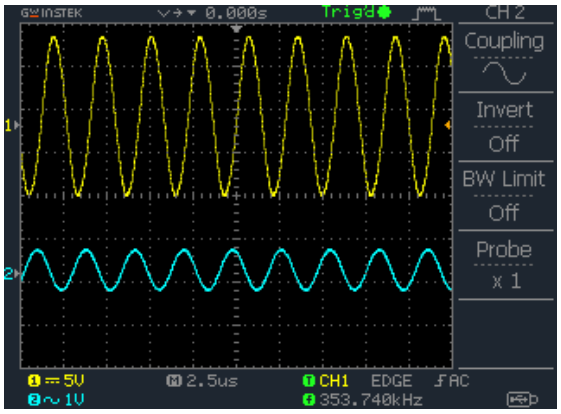

FigureA13: (Blue) V_2(d=9) for L_1=28µH and L_2=30µH

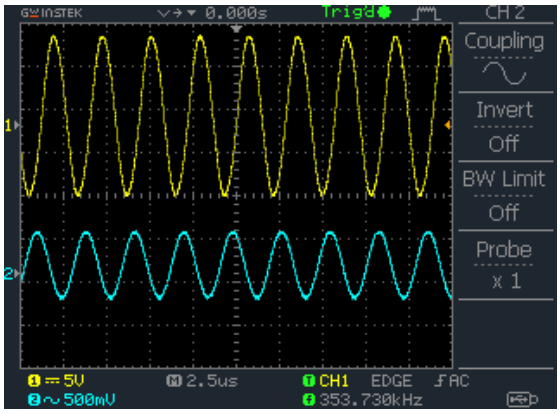

FigureA14: (Blue) V_2(d=10) for L_1=28µH and L_2=30µH

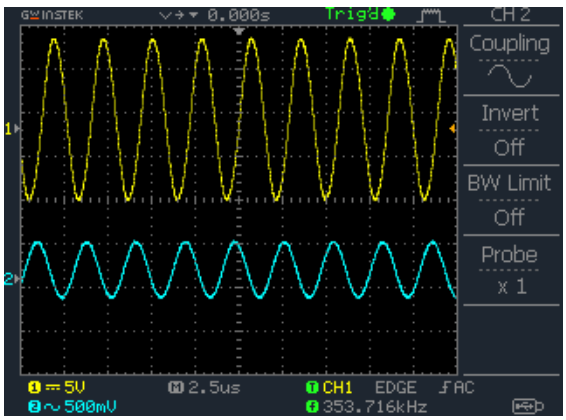

FigureA15: (Blue) V_2(d=11) for L_1=28µH and L_2=30µH

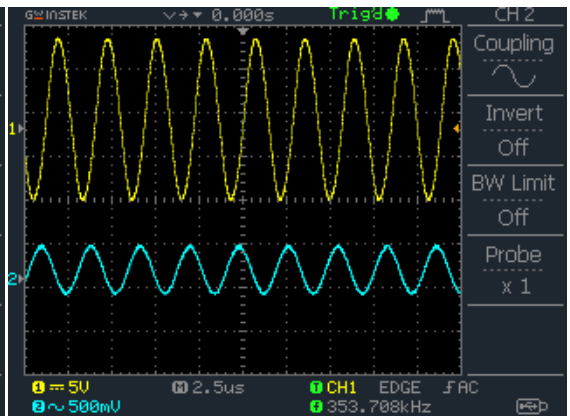

FigureA16: (Blue) V_2(d=12) for L_1=28µH and L_2=30µH

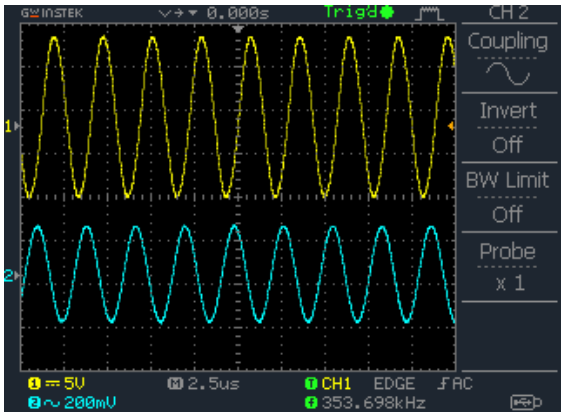

FigureA17: (Blue) V_2(d=13) for L_1=28µH and L_2=30µH

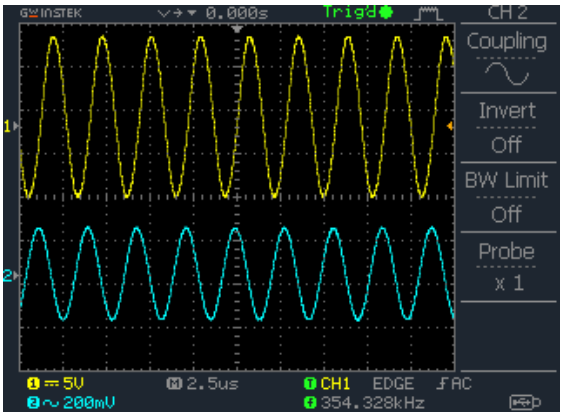

FigureA18: (Blue) V_2(d=14) for L_1=28µH and L_2=30µH

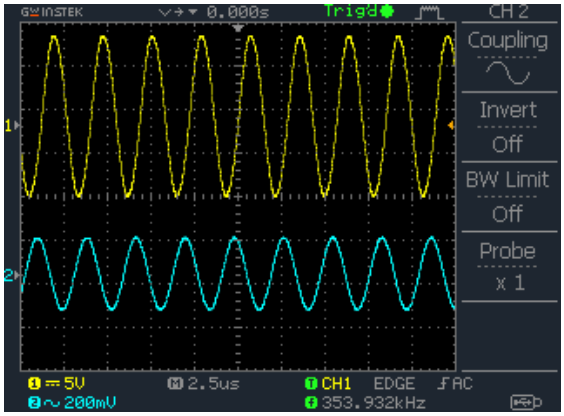

FigureA19: (Blue) V_2(d=15) for L_1=28µH and L_2=30µH

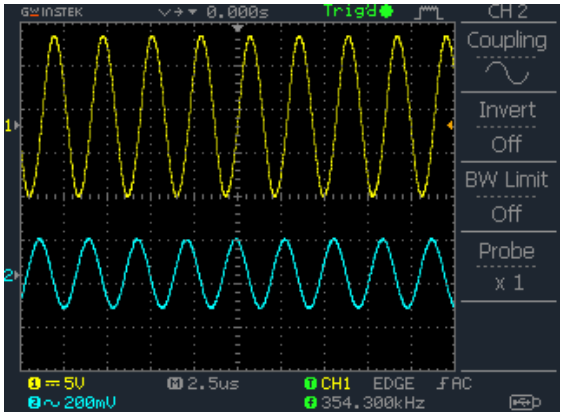

FigureA20: (Blue) V_2(d=16) for L_1=28µH and L_2=30µH

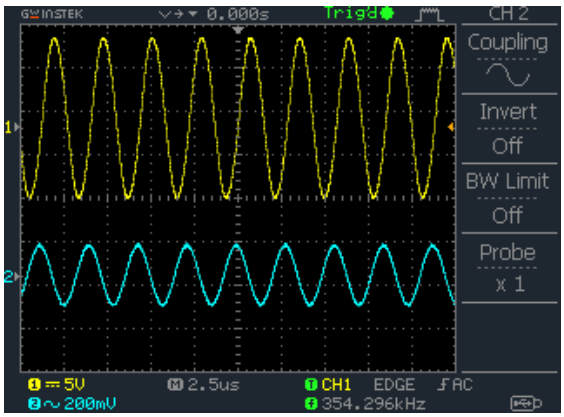

FigureA21: (Blue) V_2(d=17) for L_1=28µH and L_2=30µH

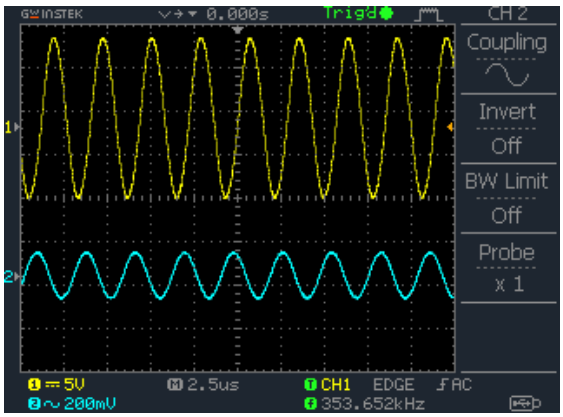

FigureA22: (Blue) V_2(d=18) for L_1=28µH and L_2=30µH

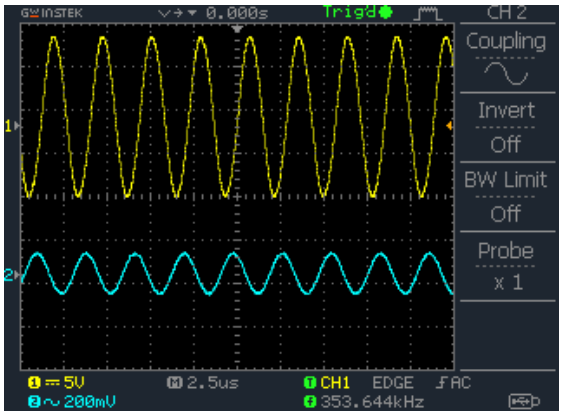

FigureA23: (Blue) V_2(d=19) for L_1=28µH and L_2=30µH

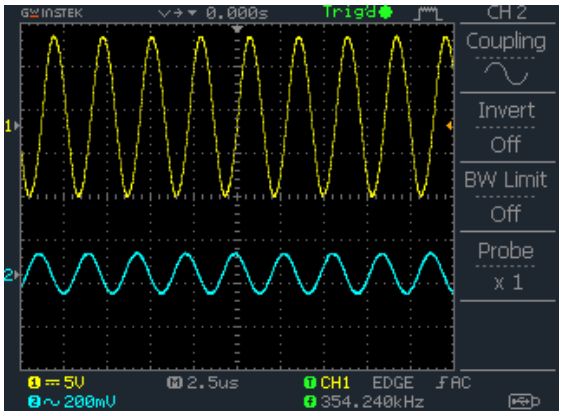

FigureA24: (Blue) V_2(d=20) for L_1=28µH and L_2=30µH

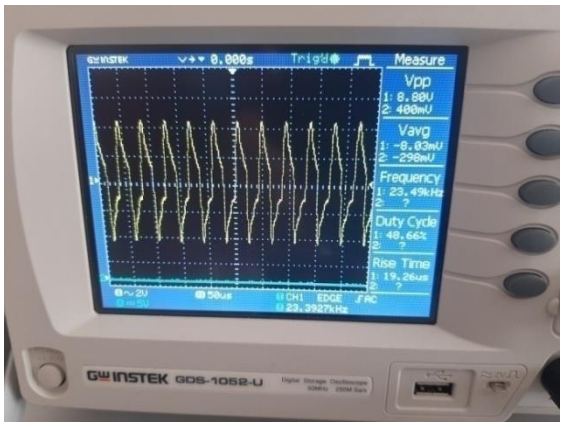

FigureB1: V_2(d=1) for L_1=124µH and L_2=126µH

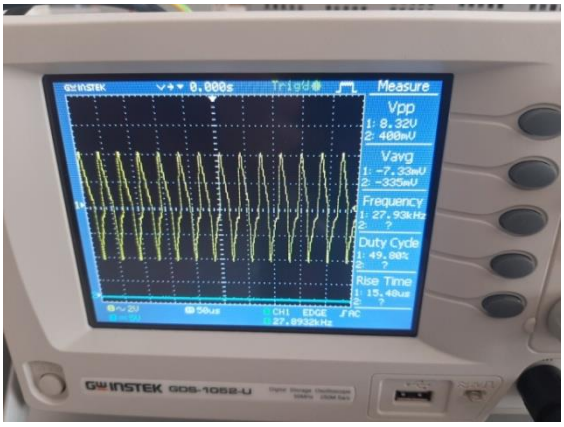

FigureB2: V_2(d=2) for L_1=124µH and L_2=126µH

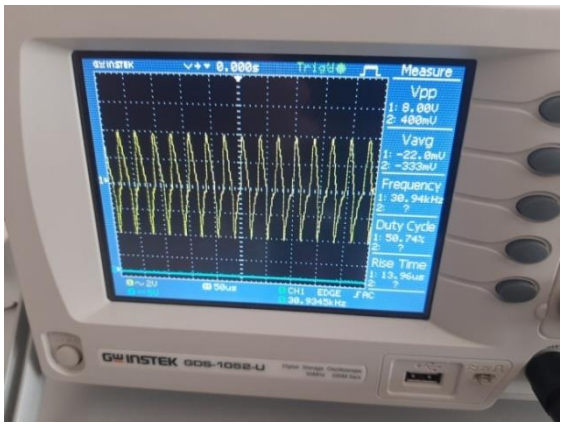

FigureB3: V_2(d=3) for L_1=124µH and L_2=126µH

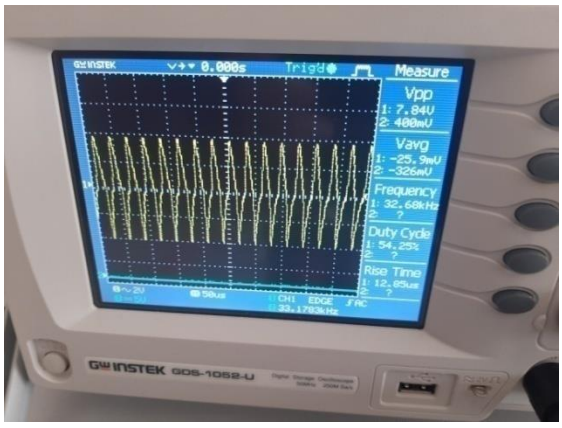

FigureB4: V_2(d=4) for L_1=124µH and L_2=126µH

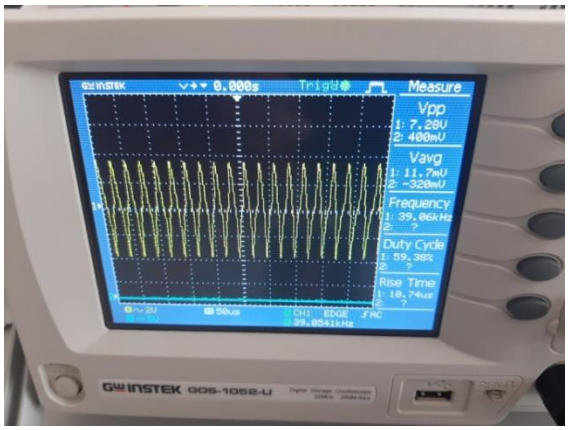

FigureB5: V_2(d=5) for L_1=124µH and L_2=126µH

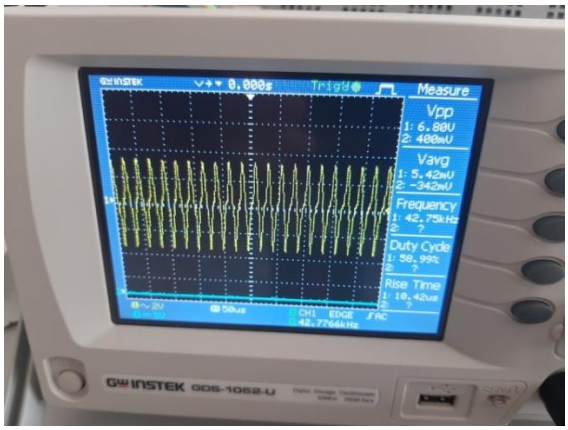

FigureB6: V_2(d=6) for L_1=124µH and L_2=126µH

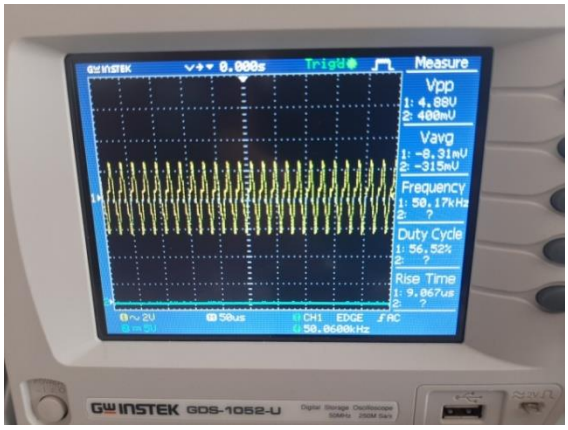

FigureB7: V_2(d=8) for L_1=124µH and L_2=126µH

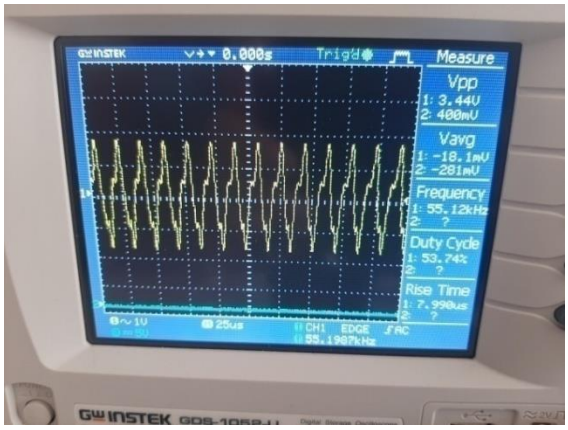

FigureB8: V_2(d=10) for L_1=124µH and L_2=126µH

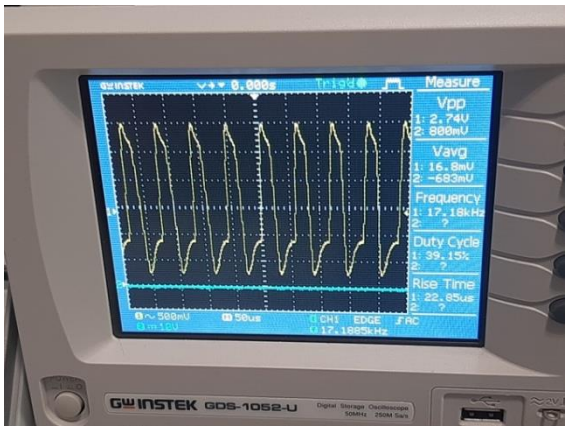

FigureB9: V_2(d=12) for L_1=124µH and L_2=126µH

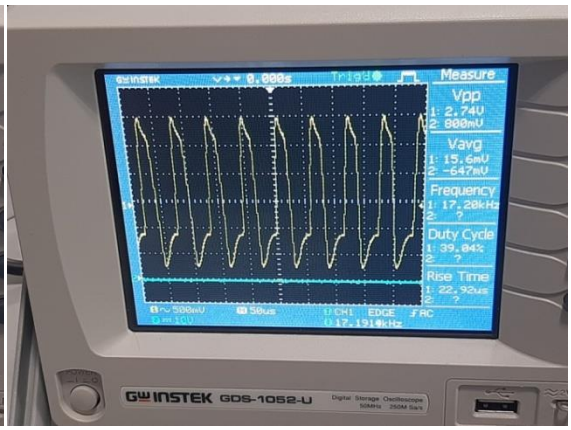

FigureB10: V_2(d=14) for L_1=124µH and L_2=126µH

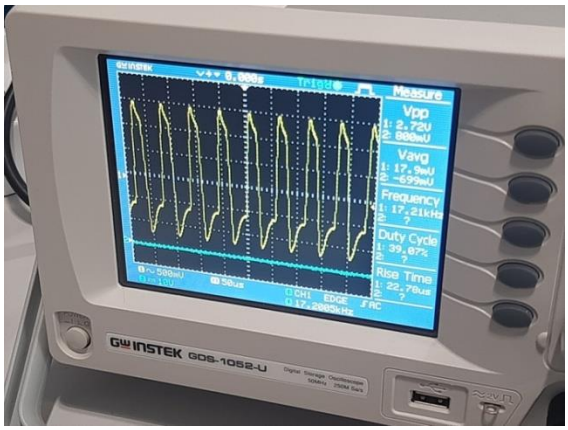

FigureB11: V_2(d=16) for L_1=124µH and L_2=126µH